

University of St Andrews



Full metadata for this thesis is available in
St Andrews Research Repository
at:

<http://research-repository.st-andrews.ac.uk/>

This thesis is protected by original copyright

Eutectic Mixtures and Polyhedral Oligomeric Silsesquioxanes in the Synthesis of Ordered Framework Materials

A thesis submitted in application for the title of Ph.D. by

Ewan Andrew Drylie MChem



University
of
St Andrews



The Edinburgh and St Andrews
Research School of Chemistry

July 2006



TH F395

Declarations

I, Ewan Andrew Drylie, hereby certify that this thesis, which is approximately 34,000 words in length, has been written by me, that it is the record of work carried out by me and that it has not been submitted in any previous application for a higher degree.

date 9/11/06 signature of candidate

I was admitted as a research student in October 2002 and as a candidate for the degree of Ph.D. in October 2003; the higher study for which this is a record was carried out in the University of St Andrews between 2002 and 2005.

date 9/11/06 signature of candidate

I hereby certify that the candidate has fulfilled the conditions of the Resolution and Regulations appropriate for the degree of Ph.D. in the University of St Andrews and that the candidate is qualified to submit this thesis in application for that degree.

date 20/11/06 signature of supervisor

Declaration

In submitting this thesis to the University of St Andrews I understand that I am giving permission for it to be made available for use in accordance with the regulations of the University Library for the time being in force, subject to any copyright vested in the work not being affected thereby. I also understand that the title and abstract will be published, and that a copy of the work may be made and supplied to any bona fide library or research worker.

date 7/11/06 signature of candidate

Courses Attended

The School of Chemistry requires that postgraduate students attend a number of taught courses. The courses attended were:

Crystallography	Dr P. Lightfoot
Electrochemistry	Dr J. A. Crayston
Radical Chemistry	Prof. J. C. Walton

Publications

Synthesis and Crystal Structures of Bromo- and Ester- Functionalised Polyhedral Silsesquioxanes

E. A. Drylie, C. D. Andrews, M. A. Hearshaw, C. Jimenez-Rodriguez, A. Slawin, D. J. Cole-Hamilton and R. E. Morris, *Polyhedron*, **2006**, 25, 853-585

Ionothermal Materials Synthesis Using Unstable Deep-Eutectic Solvents as Template-Delivery Agents

Emily R. Parnham, Ewan A. Drylie, Paul S. Wheatley, Alexandra M. Z. Slawin and Russell E. Morris, *Angew. Chem. Int. Ed.*, **2006**, 45, in press

Abstract

A study has been undertaken with the aim of preparing ordered porous materials by the ionothermal method. Two copper-carboxylate coordination polymer frameworks were prepared using eutectic mixtures as solvent and framework building species and two cobalt/nickel-diphosphonate coordination polymer frameworks were prepared using eutectic mixtures as solvent. All four materials have been prepared previously using different techniques. Three aluminium cobalt phosphate frameworks (a chain, layered and three-dimensional porous structure) were also prepared using eutectic mixtures as solvent. The layered material (termed CoAlPO-1) is novel and is the first example of a zeotype material containing a cobalt-chlorine bond. The template is choline, which is a component of the eutectic mixture solvent. The chain material (CoAlPO-2) is a minor product in the synthesis of CoAlPO-1 and is also novel. The template for CoAlPO-2 is the macrocycle cyclam. The 3-D material (CoAlPO-3) has the previously reported levyne topology. As in CoAlPO-1 choline is the template, which has never previously been reported in the synthesis of levyne topology materials before.

A study has also been undertaken with the aim of preparing ordered porous materials from polyhedral oligomeric silsesquioxanes (POSS) by first appropriately functionalising the POSS for use in polymer synthesis and coordination polymer preparation. An ester functionalised POSS was prepared by the methoxycarbonylation of octavinylsilsesquioxane. It was anticipated that this

material could be converted to a carboxylic acid functionalised POSS to be used in the preparation of POSS coordination polymers. However, the synthesis of a carboxylic acid species was not achieved. Two furyl functionalised POSS have been prepared and their Diels-Alder reaction with maleimide investigated. It was anticipated that the reaction would be efficient and that Diels-Alder reactions with a maleimide functionalised POSS would result in a porous polymer. However, neither furyl POSS underwent sufficient Diels-Alder reaction to proceed with preparation of the polymer.

Table of Contents

Declarations	i
Declaration	ii
Courses Attended	iii
Publications	iv
Abstract	v
1. Introduction	
1.1 Zeolites	1
1.1.1 Background	1
1.1.2 Synthesis	6
1.1.3 Applications	11
1.2 Coordination Polymers	14
1.2.1 Background	14
1.2.2 Synthesis	22
1.2.3 Applications	23
1.3 Ionic Liquids and Eutectic Mixtures	26
1.3.1 Background	26
1.3.2 Synthesis	28

1.3.3 Applications	30
1.4 Polyhedral Oligomeric Silsesquioxanes	31
1.4.1 Background	31
1.4.2 Synthesis	33
1.4.3 Applications	36
1.5 Aims	41
1.6 References	42
2. Experimental and Analytical Techniques	
2.1 Air and Moisture Sensitive Synthetic Chemistry	50
2.2 Ionothermal Synthesis	51
2.3 Nuclear Magnetic Resonance	52
2.4 Mass Spectroscopy and MALDI-TOF	54
2.5 CHN Elemental Analysis	55
2.6 Infra-Red Spectroscopy	56
2.7 X-Ray Diffraction	57
2.7.1 Single Crystal XRD	60
2.7.2 Powder XRD	61
2.7.3 Synchrotron Radiation	64
2.8 Thermal Analysis	66
2.9 References	67

3. Eutectic Mixtures in the Synthesis of Coordination Polymers	
3.1 Introduction	69
3.2 Experimental	72
3.2.1 Preparation of Eutectic Mixtures	72
3.2.2 Preparation of Coordination Polymers from Eutectic Mixture Components	73
3.2.3 Preparation of Diphosphonic Acid Containing Molecules	76
3.2.4 Preparation of Metal-Phosphonate Frameworks	77
3.2.5 Preparation of Metal-Dicarboxylate Framework	79
3.3 Results and Discussion	79
3.3.1 Coordination Polymers from Eutectic Mixture Components	79
3.3.2 Metal-Phosphonate Frameworks	84
3.3.3 Metal-Dicarboxylate Framework	91
3.4 Conclusion	94
3.5 References	95
4. Eutectic Mixtures in the Synthesis of Aluminium Cobalt Phosphate Frameworks	
4.1 Introduction	96
4.2 Experimental	99
4.2.1 Preparation of Eutectic Mixtures	99
4.2.2 Attempted Preparation of AlPO Frameworks	99
4.2.3 Preparation of CoAlPO Frameworks	100

4.3 Results and Discussion	102
4.3.1 Attempted Preparation of AIPO Frameworks	102
4.3.2 CoAIPO-1	103
4.3.3 CoAIPO-2	109
4.3.4 CoAIPO-3	112
4.4 Conclusion	117
4.5 References	119
5. Attempted Synthesis of Carboxylic Acid Functionalised POSS	
5.1 Introduction	121
5.2 Experimental	125
5.2.1 Preparation of Vinyl and Hydride Precursors	125
5.2.2 Attempted Preparation of a Carboxylic Acid	126
POSS <i>via</i> Methoxycarbonylation of Octavinyl POSS	
5.2.3 Attempted Preparation of a Carboxylic Acid POSS	128
<i>via</i> a Tertiary Butyl Ester POSS	
5.3 Results and Discussion	132
5.3.1 Attempted Preparation of Carboxylic Acid	132
POSS <i>via</i> Methoxycarbonylation of Octavinyl POSS	
5.3.2 Attempted Preparation of a Carboxylic Acid POSS	137
<i>via</i> a Tertiary Butyl Ester POSS	
5.4 Conclusion	142
5.5 References	144

6. Synthesis and Use of Furyl Functionalised POSS in Diels-Alder Reactions	
6.1 Introduction	146
6.2 Experimental	151
6.2.1 Preparation of Furyl POSS 1 (FP1) and attempted Diels-Alder Reaction between FP1 and Maleimide	151
6.2.2 Attempted Preparation of Furyl POSS 2 (FP2)	153
6.2.3 Preparation of Furyl POSS 3 (FP3) and attempted Diels-Alder Reaction between FP3 and Maleimide	153
6.3 Results and Discussion	156
6.3.1 Furyl POSS 1 (FP1) and attempted Diels-Alder Reaction between FP1 and Maleimide	156
6.3.2 Attempted Preparation of Furyl POSS 2 (FP2)	159
6.3.3 Furyl POSS 3 (FP3) and attempted Diels-Alder Reaction between FP3 and Maleimide	160
6.4 Conclusion	164
6.5 References	165
7. General Conclusion	
7.1 Eutectic Mixtures in the Synthesis of Porous Materials	167
7.2 POSS Molecules in the Synthesis of Porous Materials	170
7.3 References	172

8. Further Work	
8.1 Eutectic Mixtures in the Synthesis of Porous Materials	173
8.2 POSS Molecules in the Synthesis of Porous Materials	176
8.3 References	179
9. Acknowledgements	180
10. Appendix	
10.1 Crystal Data for CoAlPO-1	181
10.2 Crystal Data for CoAlPO-2	188
10.3 Crystal Data for CoAlPO-3	191
10.4 Crystal Data for octakis[methylpropanoate]octasiloxane	193
10.5 Molecular Structures	196

1. Introduction

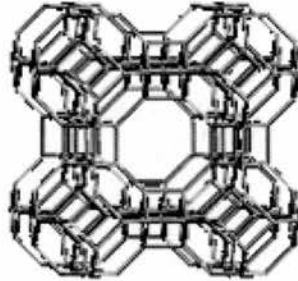
1.1 Zeolitic Materials

1.1.1 Background

Traditional zeolites are crystalline microporous (ca. 3-15 Å) aluminosilicate materials with well-defined pores and channels. Naturally occurring zeolites in the Earth's crust were first discovered in 1756 by Cronstedt when he found a new silicate mineral that lost water on heating [1], a process which was later shown to be reversible by Damour in 1840 [2]. Cronstedt derived the name of this new class of mineral from the Greek words "zeo" (meaning to boil) and "lithos" (stone).

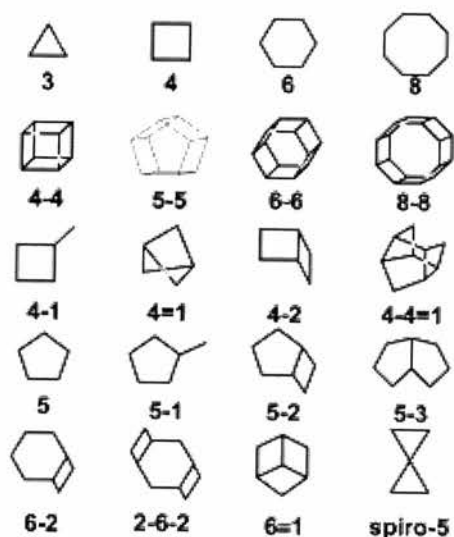
The first non-naturally occurring zeolites were synthesised by Barrer in 1948 by the conversion of known minerals using high temperatures and salt solutions that were perceived to mimic zeolite formation in nature [3]. He prepared a material that displayed the same molecular sieve characteristics as the naturally occurring chabazite zeolite, and was thus able to separate *n*-paraffins from aromatic hydrocarbons. Soon afterwards Milton reported the synthesis of fourteen new zeolites from milder conditions using aluminosilicate gels [4]. There are now over 800 zeolites known, classified by 150 different framework types, each of which is assigned a three-letter code by the International Zeolite Association (IZA) [5].

Figure 1.1.1 Example of a zeolite framework: Zeolite A (LTA). nb: In diagrams of zeolite frameworks often only the T atoms are plotted so each line represents a T-O-T bond [5].



Zeolites are constructed from an open arrangement of corner sharing tetrahedral building blocks [6]. In the centre of the tetrahedra are either silicon or aluminium cations, known as the T atoms. Each of these T atoms is surrounded by four oxygen anions, so are designated TO_4 . The oxygen atoms bridge two adjacent tetrahedra giving a framework ratio of $O/T = 2$ [4]. These TO_4 tetrahedra are known as primary building units (PBUs). Different geometric configurations of PBUs form secondary building units (SBUs) (figure 1.1.2). It is these units that make up the unit cell and are used to describe zeolitic frameworks [7]. All known frameworks can be generated from these arrangements, which can be as simple as 4, 6 and 8 T atom rings, or more complex arrangements containing up to 16 T atoms [8]. A number of different SBUs can be present in a specific zeolite, such as in Zeolite Type A (LTA), which contains the 4, 6 and 8 rings and 4-4 (D4R) SBUs [9].

Figure 1.1.2 Secondary Building Units (T atoms on corners)



Aluminosilicate zeolites are negatively charged due to the AlO_4 tetrahedra (Al^{3+}) having a lower formal charge than the SiO_4 tetrahedra (Si^{4+}). This results in the need to have additional cations in non-framework positions to achieve overall electroneutrality of the material. Originally these cations were first and second column ions such as K^+ , Na^+ and Ca^{2+} ions. A major advance in zeolite chemistry was the introduction of organic molecules (such as quaternary amines and alkylpyridiniums) as the cationic species. This allowed for the synthesis of a greater variety of frameworks than had previously been obtained.

It was postulated that the shape of the organic molecule could be imparted on to the inorganic framework; that the organic molecule would act as a template for the framework to form around. However, it has been found that most zeolites can be formed with a variety of organic ‘templates’ so these molecules are not true templates. Instead the roles they usually fulfil are either as space fillers or as structure directing agents (SDAs).

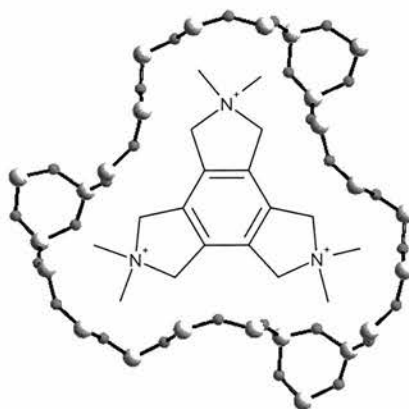
Space filling agents do not offer any control over the pore topologies formed but simply pack into the voids in the framework, making the composite more thermodynamically stable than just the framework alone [6]. Most organic additives in zeolite synthesis fall into this class of role. For example ZSM-5 can be synthesised in the presence of at least twenty-two different organic molecules [10].

Structure directing agents show a closer correspondence between the organic cation and the pore topologies formed. The organic species guides the synthesis of the zeolite to a particular topology that is formed by using no other organic species. However, by changing the other conditions slightly different frameworks can be formed using the same SDA. Examples of true structure directing are rare but one such case is the synthesis of hexagonal faujasite in the presence of 1,4,7,10,13,16-hexaoxacyclooctane (18-crown-6) [11].

There is probably only one reported zeolitic material where true templating of the framework by an organic cation occurs. ZSM-18, an aluminium silicate with the IZA code MEI consisting of channels of twelve-membered rings intersected by seven-membered rings, has been shown to have a very close match between the template and the zeolite walls (figure 1.1.3) [12]. Although the structure can be synthesised within a broad range of conditions it cannot be made without the trispyrrolidinium cation. Computer calculations not only show that the template-structure energetic interactions are favourable but also that there is a relationship between the orientation of the template and the preference of the aluminium to occupy sites in three-membered rings found in the structure. The interactions are sufficiently strong

as to not allow any rotation of the molecule inside the pores, suggesting true templating. This is not usually the case, which implies that it is more often the organic molecule's spatial volume that is more important rather than its geometry [6].

Figure 1.1.3 Encapsulated Template in ZSM-18 [12]



Although the term zeolite is strictly only used for aluminosilicate materials, other ordered inorganic porous frameworks also exist and are referred to as zeotypes. This group of materials includes the aluminophosphates, gallium phosphates, germanates and pure silicates. High silica-containing aluminosilicate zeolites and pure silicate frameworks were first found to be possible to synthesise when organic molecules were added to the reaction gel [13]. The possibilities for forming new high silica frameworks were opened up further when the organic molecules were used in their hydroxide form, meaning that alkali cation hydroxide sources need no longer be used to create the basic conditions required [14].

The aluminophosphates were the first microporous frameworks synthesised without silica and are the most abundant of the non-aluminosilicate microporous materials.

The first examples were synthesised in 1981 by Flannigan *et al* when more than twenty new materials were reported, most of which had novel topologies [15]. Aluminophosphates are built up of strictly alternating AlO_4 (Al^{3+}) and PO_4 (P^{5+}) tetrahedra to form neutral frameworks. Despite their electroneutrality they are similar to aluminosilicates in that they are hydrophilic, rather than exhibiting hydrophobicity like the neutral pure silicates. This can be attributed to the difference in electronegativity between aluminium and phosphorus. Since the frameworks are neutral the only interactions between the framework and organic species are Van der Waals forces. Like the aluminosilicates, the organic molecule can fulfil either the role as space-filler, structure-directing agent or template.

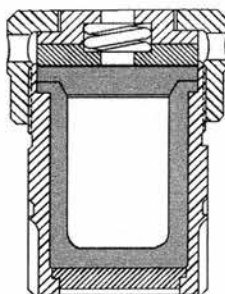
Negatively charged aluminophosphate frameworks are formed if they contain polyhedra such as AlO_5 and $\text{AlO}_4(\text{OH}_2)_2$ or terminal groups such as P-OH or P=O groups [16]. Electronegativity and useful physical and chemical properties can also be obtained by substituting into some of the aluminium or phosphorus positions other metal ions such as Co^{2+} , Zn^{2+} and Mg^{2+} [17]

1.1.2 Synthesis

Generally, aluminosilicate zeolite synthesis is carried out under hydrothermal conditions. First a homogenous gel of the starting materials is formed in an alkaline medium. It is then held at a defined temperature, which is usually between 100 and 250 °C, under autogenous pressure in a sealed autoclave (figure 1.1.4) for the crystallisation period [8]. By varying the reactants (framework precursors, organic

species, mineraliser etc) and the reaction conditions (temperature, time, pH etc), even by slight degrees, a wide variety of frameworks can be formed.

Figure 1.1.4 Cross section of an autoclave showing the steel casing and Teflon liner



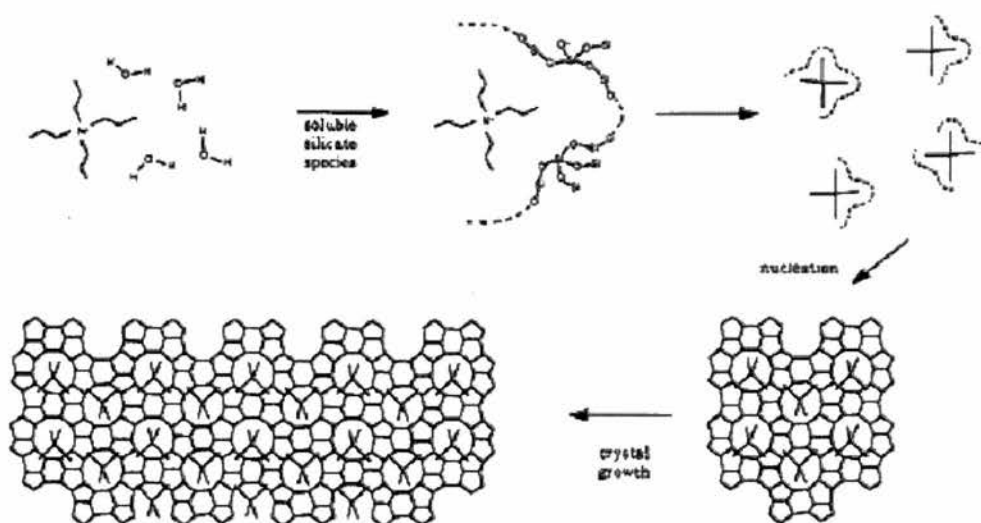
The main difference between aluminosilicate synthesis and aluminophosphate synthesis is that aluminophosphate synthesis is carried out at a slightly acidic pH. However, aluminosilicate synthesis can be performed at a lower pH if fluoride ions are used as mineralisers rather than hydroxide ions. The method can also be used to introduce transition metals into the frameworks as insoluble metal hydroxides do not form at lower pHs. The use of fluoride in aluminophosphate synthesis can catalyse the formation of Al-O-P bonds and its incorporation into the framework results in a negative charge, allowing for interaction with an organic cation. In all types of molecular sieve framework the fluoride can either be occluded in a small cage such as a D4R [18] or incorporated into the framework as a bridging species between two T atoms [19].

The mechanism for zeolite formation proceeds *via* a multiphase reaction-crystallisation process that involves liquid, amorphous solid and crystalline solid phases [20]. The process is complex due to the large number of variables that affect

the crystallisation process, the complicated chemistry of alkaline solutions of aluminium and silicon oxides and the inhomogeneity of the crystallising system [9]. All of these affect the kinetics and reaction pathway in ways that are poorly understood.

It has been postulated that discrete aluminosilicate species known as pre-nucleation building units (PNBUs) that have been identified, or are believed to form, in solution can act as building blocks in the formation of zeolite structures [9]. The crystallisation process would thus involve the formation of these species in solution followed by their ordering and growth to form the final material. Even though ^{29}Si NMR and mass spectrometry studies have shown a number of species that resemble the SBUs in solution there is no direct evidence that these species are involved in the formation of aluminosilicate zeolites [21].

Figure 1.1.5 Simple schematic of zeolite formation (adapted from [22])



There is evidence however, that PNBU's that exist in solution during the synthesis of aluminophosphates are involved in the framework formation mechanism. The PNBU's can be the same as the SBUs or closely related depending on whether they have undergone a rearrangement/isomerisation process before or during condensation into the extended framework. Férey and Taulelle were able to identify the PNBU involved in the synthesis of $\text{AlPO}_4\text{-CJ2}$ using *in situ* NMR techniques [23]. They showed that the PNBU isomerises, implying formation of a bridge within the PNBU, allowing integration to the network. As integration takes place parallel to isomerisation a mixture of different SBUs can be present in the framework. It may be that a similar process occurs in the formation of aluminosilicate zeolites.

It has also been proposed that microporous aluminophosphate frameworks form through first the formation of chain structures, followed by transformation to layered structures and finally the formation of a three-dimensional framework [24]. This mechanism has been suggested as often the first species to crystallise is a chain structure. Depending on the experimental conditions this 'parent' chain, or other chains derived from hydrolysis and condensation reactions of the parent chain, can often be observed in more complex layered or porous frameworks crystallised from the same reaction.

The properties of the solvent and its interaction with the reaction species play a significant role in zeolite synthesis. Water decreases the viscosity of the system, acts as a space filler and can also catalyse T-O-T bond formation [25]. Zeolite synthesis can also be performed in organic solvents (solvothermal synthesis) and mixed

aqueous-organic systems. What is most important is that there is a balance between the framework forming species, the template and the solvent that allows for a molecular sieve to form. This includes ensuring that hydrogen bonding between the framework species and template is neither too high nor too low [26].

Recently, Morris *et al* reported a new method where ionic liquids and eutectic mixtures were used in the formation of aluminophosphates [27]. The attraction of this technique, which is termed ionothermal synthesis, is that the solvent also acts as the ‘template’. This decreases the amount of competing interactions during the reaction and may result in closer templating of zeolite frameworks. As the use of this technique forms a large part of this thesis it will be discussed in more detail later.

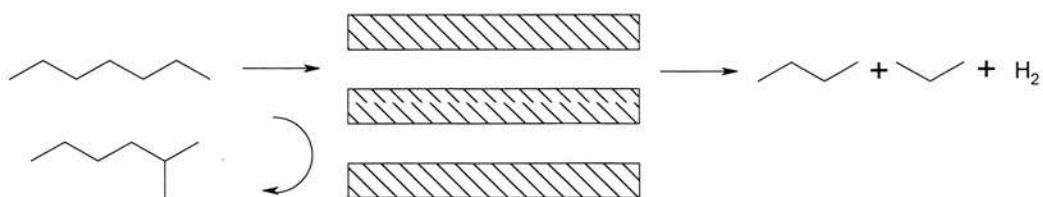
1.1.3 Applications

Zeolites and other microporous materials are used in a great number of applications, which arise from their ability to interact with other molecules and ions at their surface and within their pores. Traditional applications include ion exchange, adsorption and catalysis. Many of these uses benefit from the highly ordered crystalline frameworks allowing the selective separation and adsorption of molecules and ions on the basis of their size and shape [28]. The atoms in the pore walls also have an effect on the molecules that can be adsorbed. For example, aluminosilicate molecular sieves are hydrophilic so can be used to adsorb water from organic solvents, whereas pure silicate porous materials are hydrophobic and adsorb organic

molecules from water. Zeolites can also be used for the purification and separation of gases such as oxygen and nitrogen [7].

An important use of zeolites is in the petrochemical industry, where the world's gasoline production is dependent on zeolites in their 'solid acid' form for the fluidised catalytic cracking of petroleum [20]. In oil refining, zeolites are involved in various processes including hydrocracking, catalytic cracking, oligomerisation and the aromatisation of olefins [7]. Zeolites can also be used as supports for homogeneous catalysts that can form inside the zeolite cages but are then too big to escape through the connecting windows. The smaller substrate molecules can enter the zeolite, react with the complex and leave again after the reaction has taken place (figure 1.1.6). Not only can these 'ship-in-a-bottle' catalysts achieve the same catalytic activity of the same complex under homogeneous conditions but they also have the advantage of heterogeneous catalysts in that they are easily separated from the products [29].

Figure 1.1.6 Schematic of zeolites as shape selective catalysts



As ion exchangers, zeolites have been used in the removal of ammonia from drinking water and also in the removal of heavy metals from industrial wastewater [7]. This ability has also led to their use as replacements for polyphosphates in soap powders for the removal of calcium and magnesium from washing water [30]. This is of great benefit to the environment as even though polyphosphates are very efficient and non-toxic to aquatic life, they result in increased eutrophication in lakes and streams.

Emerging applications of microporous solids include their use in medicine where the reversible and selective adsorption and storage properties of zeolites could be exploited in the design of artificial organs [7]. Zeolites are also utilised in magnetic resonance imaging (MRI) [31]. This technique relies on contrast agents being administered to patients that bind to water and yield much faster proton spin relaxation times. Gadolinium (III) is a very effective contrast agent but is toxic to humans so cannot be administered directly, but on immobilisation inside a zeolite (that is non-toxic) it is hidden from the body so is now being investigated as a contrast agent for the gastrointestinal tract.

Other future uses for zeolites include as replacements for silicon dioxide insulators in microchips. The increase in density of wiring required for higher performance chips cannot be achieved using currently used materials but by using porous materials the required lower dielectric constants are possible [32]. Another use of zeolites is as templates for the construction of porous carbon structures, which are of interest for the storage of natural gas and as electrode materials. It involves packing the space within a zeolite with carbon molecules (e.g. poly(furfuryl alcohol) then removing the

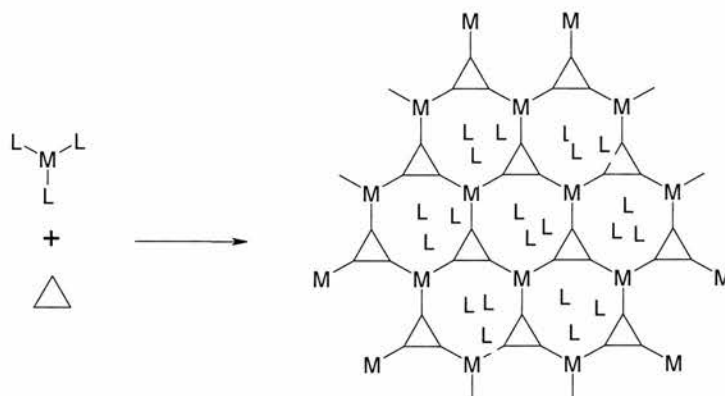
inorganic solid by dissolving it in acid [33]. It has been found that using zeolite Y as a template results in a microporous carbon with regular ordering identical to the supercages of the zeolite [34]. Lastly, the utilisation of zeolites in the drying of organic liquids could be adapted to make them suitable for the adsorption of polar molecules such as ethanol. This could lead to their use in the removal of alcohol from drinks such as wine and beer (which is not thought to influence the taste) to 'soften' the drink [7].

1.2 Coordination Polymers

1.2.1 Background

Although zeolites have made a massive impact on the world's economy, the lack of understanding of their mechanism of formation makes it very difficult to design them to have specific pore sizes and properties and to therefore tailor them to suit specific applications. As an alternative to zeolites there has recently been considerable interest in the area of coordination polymers. These materials are prepared by the assembly of discrete molecules in solution, a technique that has often been termed modular chemistry or the molecular building block approach to porous materials. By appropriately functionalising organic molecules with multiple groups that have the ability to coordinate to a metal or hydrogen bond to each other it is possible for them to self assemble to form a porous material.

Figure 1.2.1 Coordination polymer synthesis schematic showing an ML_3 species reacting with an organic building block (triangle) to form the coordination polymer with the metal ligands filling the pores.



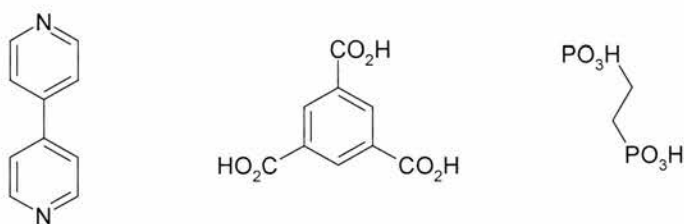
Inorganic-organic hybrid porous materials were first studied during the 1970s by Gravereau *et al* amongst others [35] but the recent interest in the area dates back to the early 1990s and particularly the work of Robson, Hoskins *et al* [36]. They proposed that by deliberate design of the individual components, ordered frameworks might form spontaneously. It was postulated that assembly of the molecules using intermolecular interactions and coordination bonds is an attractive technique as the process is reversible, allowing mistakes in the framework building to be repaired and the ordered growth continued.

Furthermore, from three-dimensional models they observed that even by using only modest length organic molecules the resulting cavity volume of coordination polymers would be relatively large compared to zeolitic materials. Therefore, by increasing the length of organic molecule huge pore sizes previously unattainable in ordered materials would result. Other promising features included easy diffusion of

various species, interesting molecular sieve and ion-exchange properties and possible post-framework formation functionalisation of the organic building blocks.

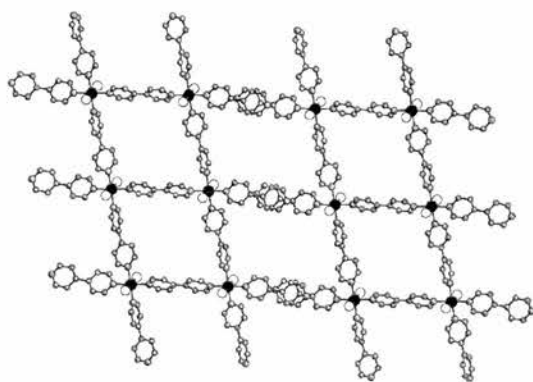
Moreover, the synthesis of coordination polymers offers a more rational design process, which enables more control over the physical and chemical properties of the framework. Careful design of the individual building blocks allows the design of frameworks with desired properties and topologies including direct incorporation of catalytic sites and chirality into the pores [37]. A variety of organic molecules can be used as long as they contain components that allow them to link together in a particular orientation such as pyridyl, carboxylic acid and phosphonic acid groups (figure 1.2.2).

Figure 1.2.2 *Examples of Organic Building Blocks*



The use of pyridyl functionalised molecules as building blocks such as 4,4'-dipyridyl has resulted in a wide variety of framework topologies, including honeycomb [38], adamantoid (also known as the superdiamondoid structure) [39], ladder [40], and railroad [41] architectures (figure 1.2.3). These materials can have large channels and completely different pore shapes and sorption properties compared to zeolites if the anions and molecules that fill the pore space can be removed or exchanged without resulting in the collapse of the framework [42].

Figure 1.2.3 Example of a nickel-dipyridyl framework with railroad topology [41]



Dipyridyl-based materials however suffer from poor thermal stability (generally collapsing below 200 °C), a tendency to collapse when the species filling the pores are removed and a tendency to interpenetrate. Interpenetration is the weaving of one framework through another, occurring when the cavities created would be larger than 50 % of the volume of the structure and without it the crystal lattice would collapse. It was initially thought that this always resulted in the filling of all the available pore space but this has been found not to be the case. For example, a three-dimensional silver dipyridyl structure reported by Yaghi *et al* was found to have void space despite the presence of three interpenetrating frameworks [43].

The use of multi-carboxylic acid functionalised molecules as building blocks results in neutral frameworks capable of shape and size selective ion exchange and other zeolite like applications. These materials suffer from less interpenetration and are much more thermally stable than dipyridyl frameworks (often stable up to between 300 and 400 °C). The multidentate coordination of benzene tricarboxylic acid (BTC) for example results in the formation of a more rigid framework as it allows for the

bridging of two different metal centres by three carboxylates of three separate molecules. BTC molecules can effectively act as hexa-monodentate units linking three metal ions. Furthermore, layers of metal-organic compound made from the condensation of a metal complex and BTC can be held together by mutual π -stacking with a guest molecule such as pyridine [44].

As already stated, coordination polymers can have extremely large pore sizes. In 2005 Férey *et al* reported a thermally stable (up to 275 °C) chromium-benzene-1,4-dicarboxylate structure, termed MIL-101, that has the largest surface area for an ordered material ever recorded at 5900 m²g⁻¹ and with pore sizes between 29 and 34 Å [45]. This by far exceeds the largest surface area of any zeolite, the biggest of which is zeolite Y at 904 m²g⁻¹. Although the crystal structure of coordination polymers can usually be solved from single crystal x-ray data this becomes difficult when the unit cell dimensions are very high. Therefore, MIL-101 was solved by comparison of the experimental powder x-ray diffraction data with computer simulation data from a library of possible coordination frameworks.

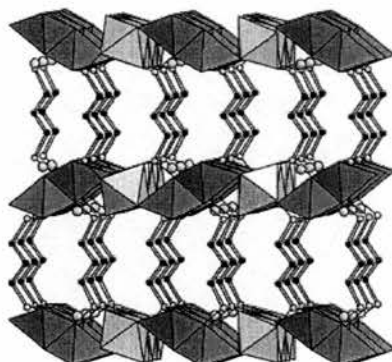
Another advance on zeolite chemistry is that multi-carboxylate containing molecules have been used in the synthesis of homochiral coordination polymers. There are two possible approaches to achieving chirality in coordination polymers: using organic building blocks containing chiral groups or by using chiral solvent molecules that act as template and coordinate to the metal centres to direct the formation of helices. Rosseinsky *et al* demonstrated this latter technique in the preparation of a series of chiral frameworks where the metal centres were not only coordinated by the linking

BTC molecules but also had coordinated chiral solvent alcohol molecules to form helices of uniquely one handedness [46].

The most thermally stable coordination polymers tend to be those synthesised using phosphonic acid-containing molecules as the organic building blocks. Diphosphonic acids were first used in porous material synthesis as a replacement for phosphoric acid in metal-phosphate synthesis [47]. This is because the mechanism of formation of porous materials with phosphate groups shows that they severely limit the pore size that can be obtained. However, if diphosphonic acids are used, the organic part acts as a spacer unit linking the inorganic parts together, so possibly resulting in larger pores. This method is also advantageous because unlike metal-phosphate synthesis it does not require the use of a template, which on removal from phosphate systems often results in their collapse. Initial studies focused on using phosphonic acids with group four metals, but the method was soon extended to other transition metals (Zr, V, Ni etc) and the group fourteen metals [48].

The predominant structure types of metal-diphosphonate frameworks are layered or pillared structures (figure 1.2.4). This is due to the affinities of the hydrophilic metal-oxide octahedra and the hydrophobic organic sections for each other and the solvent [49]. Often this results in the material having no porosity as the organic pillars can take up all the space between the metal-oxide layers, but porous materials can be achieved if the correct reaction conditions are found, often employing solvent molecules or counterions as space fillers between the organic pillars [48, 50].

Figure 1.2.4 Example of a pillared diphosphonate framework prepared using propylene diphosphonic acid [50]

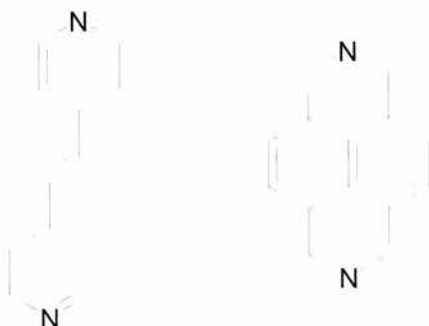


It is also possible to prepare coordination polymers using organic molecules with more than one type of functional group, such as carboxylic acid and phosphonic acid groups. Distler and Sevov reported the first carboxylate-phosphonate framework with a three-dimensional structure, a framework with one-dimensional S-shaped channels, in 1998 [51]. Since then other porous carboxylate-phosphonate structures have been reported [52], including examples that have also incorporated 4,4'-dipyridyl and other molecules into the structure as a secondary metal linkers [53].

Despite the great potential of the molecular building block approach to porous materials there are various challenges to be overcome. Access to the pores is often not possible due to collapse of the framework on guest removal, strong host-guest interactions or interpenetration of the frameworks. However, interpenetration can be prevented by filling the channels with hydrogen bonding guest molecules [41] or by using very large guest molecules such as nitrobenzene [36].

Champness *et al* discovered that altering the size of the organic molecules could also control the degree of interpenetration. It was found that lengthening the dipyriddy building block increased the amount of interpenetration due to the creation of larger cavities needing to be filled [54], whereas decreasing the distance between the two pyridine units such as by using diazapyrene decreased the level of interpenetration (figure 1.2.5) [55]. This result may have been unexpected as increased π - π interactions should have led to more efficient packing and therefore more interpenetrating networks but in general it can be seen that increasing the lateral bulk of the ligand results in fewer voids to be filled, so there is less interpenetration of frameworks.

Figure 1.2.5 Example of differing size of pyridyl building blocks

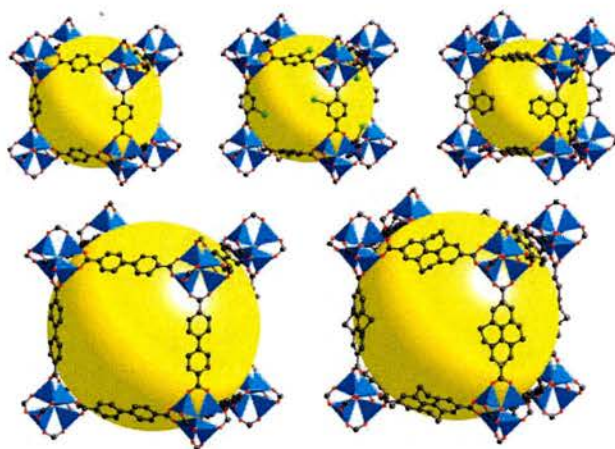


Perhaps more importantly, it is difficult to control the orientation of the molecules to allow them to link together in the desired manner. Although possible framework topologies can be predicted, it is arguable whether true design of coordination polymer frameworks has yet occurred. This is because the labile metal ions favoured in coordination polymer synthesis (Cu^+ , Cu^{2+} , Ag^+ , Cd^{2+} , Zn^{2+} , Co^{2+} and Ni^{2+}) do not have as strong a preference for a given geometry as other ions, leading to a lack of predictability of the framework formed [56]. Lack of predictability also arises from

the flexibility of the organic building blocks although this can be overcome by using rigid molecules.

Once one framework with a certain topology has been prepared however, making subtle changes to the organic building block can result in the formation of a series of closely related structures. Yaghi *et al* demonstrated this with the group of coordination polymers derived from the MOF-5 framework, a benzene dicarboxylic acid (BDC) based structure with a cubic topology [57]. Lengthening the organic unit or adding functional groups to the benzene ring such as an amine group does not change the topology of the structure, only the pore size and functionality of the framework (figure 1.2.6).

Figure 1.2.6 MOF-5 (top left) and some analogous frameworks using different organic linkers. The yellow spheres represent the pore radius [57].



1.2.2 Synthesis

The preparation of coordination polymers is achieved by self-assembly of the individual building blocks into the final material. This can be performed at room temperature by making use of diffusion techniques and evaporation of the solvent to bring the molecules together and form the most thermodynamically stable product. A very successful technique is the diffusion of a base through a metal and carboxylic acid-containing molecule mixture [58]. Hydrothermal [59] and solvothermal [57] techniques, where the high temperatures and pressures allow transition states to be obtained and the most ordered structure to be formed have also proved to be very successful.

Overall the exploitation of the coordination preferences of a transition metal is the predominant controlling factor in the creation of a desired network topology. However, anion control, hydrogen bonding, π - π stacking and other intermolecular interactions also have a profound effect on the framework topology. The metal ligands or counterions that are lost in the reaction or the reaction solvent occupy the pores of the extended solid as either guest molecules or ions, depending on the framework's charge. Access to the pores can be obtained by removal of the guest molecules by heating the material or by ion exchanging with smaller ions, providing that the framework doesn't collapse.

1.2.3 Applications

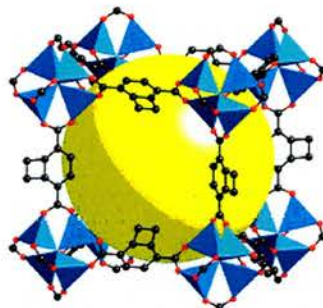
The outlook for coordination polymers is very promising due to their zeolite type properties and the multitude of potential applications of rationally designed porous solids. Unique applications may arise from the ability to exploit the metal component and/or its interaction with guest molecules to create porous materials with unusual properties such as redox potentials, magnetic moments or light absorption properties [33]. What's more, porous solids from distinct molecular entities can be produced in high yields using simple synthetic methods, making them very attractive for large-scale production.

Accessible metal centres in metal-benzene tricarboxylate frameworks offer the possibility of uses in gas separation and liquid purification [60]. Highly selective adsorption of molecules has been observed for neutral frameworks based on BTC, which could also lead to their use in the removal of aromatics and halogenated hydrocarbons from industrial processes. It has been found that frameworks based on dipyriddy building blocks can have selective clathration and catalytic activity. The $\{\text{Cd}(4\text{-}4'\text{-bpy})_2(\text{NO}_3)_2\}_\infty$ framework with a two-dimensional square topology reported by Fujita *et al* reversibly bound the ortho isomers of dibromobenzene and dichlorobenzene but not their meta or para isomers [61]. It was also found to promote the cyanosilylation of aldehydes. Chiral coordination polymers are much easier to prepare than in traditional crystalline materials [62]. This could make a considerable impact on enantioselective sorption and catalysis for reactions that do not require high temperatures.

Recent studies have shown there are potential uses of coordination polymers in gas storage. Hydrogen storage is of particular interest as alternatives are sought for fossil fuels, however there is as of yet no adequate method for its safe storage and transport. One possible solution to this is the use of coordination polymers as they are lightweight, relatively easy to prepare and can be tailored to suit specific requirements [63]. The zinc-benzene dicarboxylate framework termed MOF-5 reported by Yaghi *et al* was found to show a high capacity for hydrogen storage at room temperature (0.5 % by weight), which could be increased by substituting the benzene section for naphthalene (IRMOF-8, 2 % hydrogen uptake by weight) [64]. Although these values are not practical for large-scale use (the target is 6 wt % by 2010 [65]), new materials are continually being prepared that are capable of storing larger amounts of hydrogen. At the time of writing the record was held by the extremely large pored MIL-101 reported by Férey *et al*, which was found to have an initial hydrogen storage measurement of 4.5 % uptake by weight at 77 K and 30 bar [45].

Furthermore, it has been shown by Yaghi *et al* that a derivative of MOF-5 (termed IRMOF-6, figure 1.2.7) was able to absorb amounts of methane exceeding that of other crystalline microporous materials, representing 70% of that stored in a methane cylinder but at much lower pressures [57]. The gas storage properties of this coordination polymer framework, its small volume, low weight and fast kinetics for recharging could lead to its use in methane-fuelled vehicles.

Figure 1.2.7 IRMOF-6. The yellow sphere represents the pore radius [57]



MOF-5 has also attracted interest for applications in surface science and metal organic chemical vapour deposition (CVD) [66]. Catalytically active nanocomposites Pd@MOF-5 and Cu@MOF-5 were prepared by size-selective gas-phase loading of typical OMCVD precursors [67]. These studies could lead to the use of coordination polymers as “crystalline solvent cages” for the analysis of the chemical and physical properties of inorganic nanoparticles.

1.3 Ionic liquids and Eutectic Mixtures

1.3.1 Background

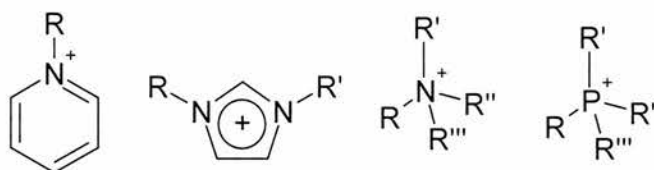
Ionic liquids are salts that are fluids at near ambient temperature (below 100 °C) composed entirely of ions [68]. Although the first ionic liquid was made in 1914 [69], it was not until the 1980s that they were first proposed as solvents for use in organic and inorganic synthesis and are now attracting interest as industrial solvents. This is because whereas most traditional industrial solvents are volatile organic compounds (VOCs), ionic liquids are non-volatile. Therefore, if they are designed to

be environmentally benign, their use results in much less environmental pollution than conventional solvents.

Other useful properties of ionic liquids that may benefit their use over conventional solvents are that they have a high thermal stability, are non-flammable and have excellent solvation properties [68]. Furthermore, there are least a million binary ionic liquids and a further possible 10^{18} ternary ionic liquids, compared to only about 600 molecular solvents being in use today. This means that solvents can be designed and tuned to optimise yields, selectivity, solubility and product separation in a wide range of reactions.

Binary ionic liquids are generally based on four types of organic cations: N,N'-dialkylimidazolium, N-alkylpyridinium, alkylammonium and alkylphosphonium ions (figure 1.3.1). Common anions are halide ions, tetrafluoroborate (BF_4^-) and hexafluorophosphate (PF_6^-). It cannot be predicted reliably which combinations of organic cores, alkyl groups and anions will form near ambient temperature liquids as salts that melt at ambient temperature are unlikely to have greatly differing structures and interionic interactions from those with slightly higher melting points [70]. Therefore, there is an element of chance in ionic liquid synthesis.

Figure 1.3.1 Common Ionic Liquid Cations



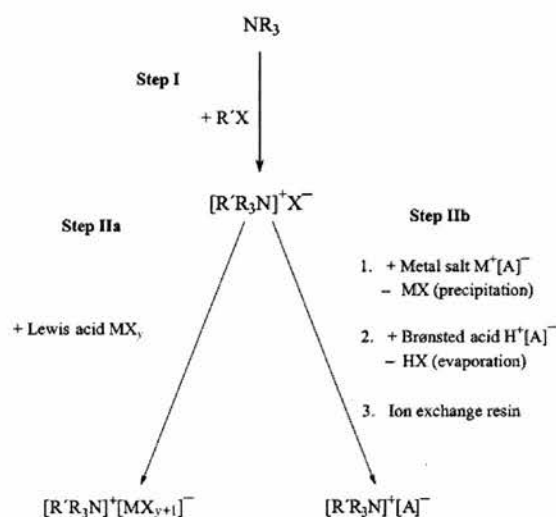
Analogues of ionic liquids can be formed from mixing high melting salts with another compound. The formation of these liquids, termed either eutectic mixtures or deep eutectic solvents, is a result of the hydrogen bonding between the two solids mixed together [71]. These mixtures, like ionic liquids, are not inflammable, have a vanishingly low vapour pressure and exhibit unusual solvent properties influenced by the hydrogen bonding. Generally, compounds that can form hydrogen bonds by donating or accepting electrons or protons are highly soluble in eutectic mixtures.

Abbott *et al* have shown that a number of eutectic mixtures can be formed from mixtures of quaternary ammonium salts and another component. When urea and choline chloride (hydroxyethyltrimethylammonium chloride) are mixed in a 1:2 ratio the resultant product has a melting point of 12 °C, which is much lower than that of urea (133 °C) and choline chloride (302 °C) [71]. Likewise, similar results are obtained by mixing di- and tri-carboxylic acid molecules such as malonic acid (mp 135 °C) with choline chloride to result in a material with a melting point of 25 °C [72]. Near ambient temperature liquids can also result by mixing choline chloride and other ammonium chloride salts with halides of metals such as chromium, tin and zinc [73].

1.3.2 Synthesis

Ionic liquids are generally prepared by either metathesis of a halide salt with for example an ammonium salt of the desired anion [74], by using an acid-base neutralisation reaction [75] or by the quaternisation of an amine or phosphine to form the cation [76]. Different anions can be obtained by changing the alkylation reagent but if it is not possible to obtain the desired anion direct from quaternisation then a further anion exchange step can be employed [77].

Figure 1.3.2 Ionic Liquid Synthesis Schematic (from an amine) [77]



Most ionic liquids and the reagents used to prepare them are air and moisture sensitive so have to be prepared and stored under inert, dry conditions. For example, the imidazolium and ammonium based ionic liquids have a tendency to be hygroscopic and will be hydrated if not stored under dry conditions.

Whereas ionic liquids are often complicated to synthesise or involve a sequence of synthetic steps, the synthesis of eutectic mixtures is very easy. The two separate components are simply mixed together in the correct ratio and, if required, heated to form a liquid. Also in contrast to ionic liquids eutectic mixtures are mostly inexpensive and water and air insensitive (such as those prepared by the combination of ammonium halides with metal halides) so pose no problems for handling or storage [71-73].

1.3.3 Applications

The diversity and tunability of ionic liquids and eutectic mixtures will lead to their uses in a wide range of applications. The first industrial process to use ionic liquids is the BASIL (biphasic acid scavenging using ionic liquids) process and is operated by BASF. It increases productivity of the company's alkoxyphenylphosphine compound, which is an important precursor in the manufacture of printing inks and glass fibre, by a factor of 80,000 compared to the conventional process [78]. In the process an ionic liquid is created *in situ* to remove the reaction by-product hydrogen chloride. The ionic liquid is immiscible with the reaction mixture and so can be easily removed and recycled.

Ionic liquids and eutectic mixtures have also already found uses in scientific laboratories [79]. These include in synthesis, catalysis, batteries and fuel cells. The eutectic mixture formed from zinc chloride and choline chloride has been found to greatly enhance the yield of Diels-Alder reactions [80]. In this system the eutectic

mixture acts as both the solvent and the catalyst and can easily be recovered and recycled. There are also potential uses for ionic liquids and eutectic mixtures as embalming fluids, in ion drives for space travel, for the desulfurisation of fuels, as lubricants and in metal finishing [68].

1.4 Polyhedral Oligomeric Silsesquioxanes

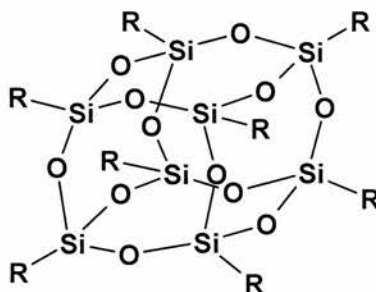
1.4.1 Background

Polyhedral oligomeric silsesquioxanes (POSS) are silicate cage structures of the general formula $[\text{RSiO}_{1.5}]_n$ (where n is any even number greater than four and R is hydrogen or any organic group), derived from the hydrolytic condensation of trihalo- or tri-alkoxy alkylsilanes. They were first discovered in 1946 by Scott when he was studying the thermal rearrangement of branched-chain methylpolysiloxanes [81]. The term silsesquioxane denotes that the silicon atom is connected to three oxygen atoms. The prefix ‘oligo’ is used to indicate a small number of silsesquioxane links or prefixes such as ‘octa’ or ‘deca’ indicate a specific number of links [82].

POSS geometries are often described by the term T_n , where T represents the number of number of $\text{RSiO}_{1.5}$ groups. The T_8 species is the most studied and is particularly interesting as it has an almost cubic shape analogous to the double four ring (D4R) secondary building unit commonly found in zeolites (figure 1.4.1). The first cubic T_8 POSS to be reported was octamethylsilsesquioxane, which was one of the structures isolated by Scott in 1946. He was unable to fully characterise it due to its low

solubility in numerous solvents but its structure was confirmed in 1955 by Sprung [83] and Barry [84].

Figure 1.4.1 Cubic POSS species where *R* is any organic group



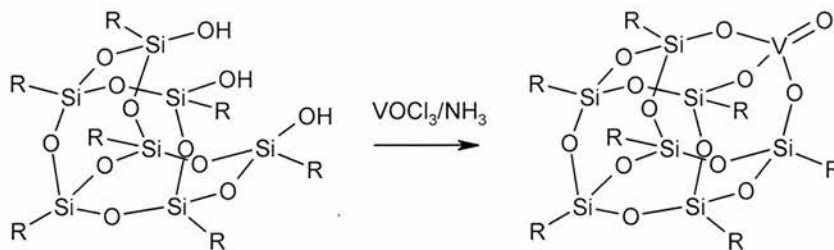
Since then many other cubic POSS species have been prepared from the hydrolytic condensation of appropriately functionalised silanes [85]. All the saturated alkyl functionalised POSS are chemically inert but POSS species with more useful groups have also been prepared. For example, POSS molecules bearing vinyl or hydride functionality offer the possibility of further reactions using the POSS species and further functionalisation of the POSS core with potentially useful groups.

The silicate POSS core is thermally stable, remaining intact at temperatures above 400 °C. The attached organic groups are not as stable, tending to break down at much lower temperatures. The POSS core, however, is susceptible to strong acids, bases and oxidising agents, often making modification of the organic groups without affecting the integrity of the inorganic cage very difficult [86]. Functionalisation is further complicated by the rigid structure of the POSS cage, its strong electron withdrawing properties, (about the same as that of a CF₃ group [87]) and the need for

clean, high yielding reactions to be used. Otherwise undesirable partially or mixed functionalised species result that are extremely difficult to isolate and purify.

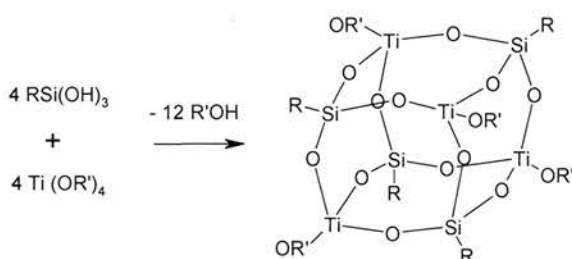
Transition metals can be incorporated into the POSS cage structure in a variety of ways leading to potentially catalytically active POSS species. Partially condensed cubes with one corner missing can be capped with metal species to give either monomeric or dimeric POSS species [88]. A variety of incompletely condensed POSS species have been prepared via hydrolytic condensation reactions from alkyl- and aryl- trichlorosilanes. Capping of these species with a trifunctional metal species such as vanadium, molybdenum or zirconium complexes then gives the desired product (figure 1.4.2). However, the hydrolytic condensation route to partially condensed POSS only results in synthetically useful quantities if trifunctional silanes with relatively bulky organic groups are used.

Figure 1.4.2 Corner capping of a partially condensed POSS



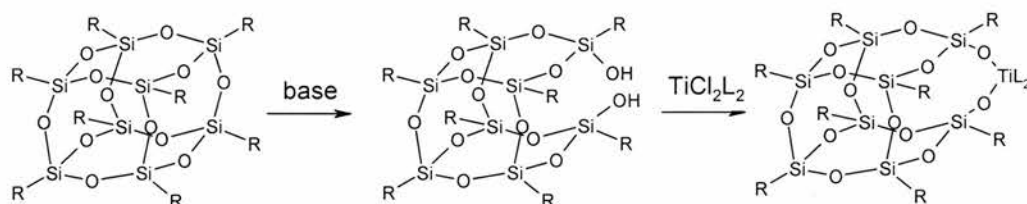
Metals can also be incorporated into the POSS structure whilst the cube is being formed [89]. Hydrolytic condensation of a silicon triol with a metal triol results in a cage structure with alternating silicon and metal corners (figure 1.4.3). The reaction process is the same except the presence of the metal species results in a mixed structure.

Figure 1.4.3 A mixed titanium-silicon POSS species



Feher *et al* have shown that completely condensed POSS cages can be partially broken at one edge or corner using reactions with strong acids or bases, allowing for their derivatisation by the addition of another functional group or by the incorporation of a metal (figure 1.4.4) [90]. The reactions have to be carefully controlled to prevent complete destruction of the POSS cage and cleavage of the organic groups. However, this route appears to be the most practical method to obtaining metal containing POSS on a large scale.

Figure 1.4.4 An example of POSS cleavage followed by metal insertion



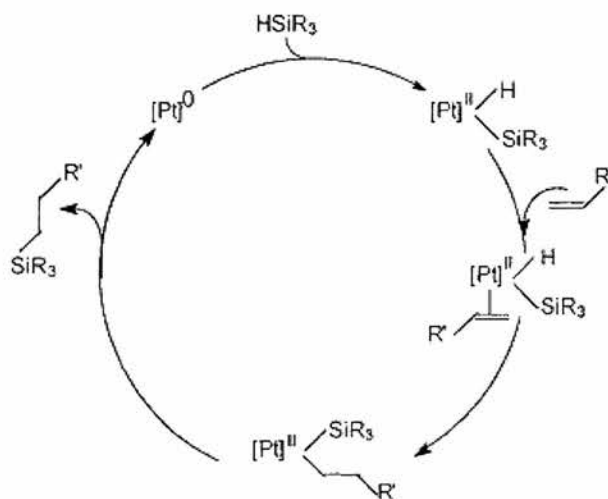
1.4.2 Synthesis

As already stated, POSS cages are prepared by the hydrolytic condensation of a silane consisting of three hydrolysable groups and a non-hydrolysable functional group that remains intact. Typically trihalo- or trialkoxy- organosilanes are used, which on addition to water (which can be generated *in situ* as in the case of

octahydridesilsesquioxane [91]) are hydrolysed to silanols. The silanols then form the POSS core through condensation reactions. The polycondensation process follows a very complicated mechanism, and is dependent on what the functional group is as well as a number of other factors such as temperature, concentration of monomers, quantity of water and the nature of the solvent [82].

Manipulation of the organic groups attached to POSS cores can be carried out using a variety of reaction techniques. A particularly useful reaction is hydrosilation, which involves the addition of a silicon-hydrogen group over a carbon-carbon double bond (figure 1.4.5). The reaction is very high yielding and is selective to addition at the α -carbon of the double bond, resulting in linear alkyl chains. The reaction is generally carried out under mild conditions using platinum, palladium or rhodium containing catalysts [92]. The most successful catalysts have been found to be the platinum complexes Speirs catalyst and Karstedt's catalyst. They have been used with great success in the reaction of hydride POSS species with alkene containing molecules and the reaction of vinyl POSS species with silanes with a silicon-hydrogen bond [93]. This has resulted in the preparation of useful POSS molecules onto which further functionalisation can be achieved using either further hydrosilation reactions or other standard synthetic chemistry techniques.

Figure 1.4.5 Pt catalysed Chalk-Harrod hydrosilation mechanism [94]



Other useful reactions when attempting to functionalise POSS molecules include the cross-metathesis of vinyl groups with other carbon-carbon double bond containing species and the conversion of vinyl groups to epoxides and phosphines [95]. Also of some use is the anti-Markovnikov addition of for example hydrobromic acid to create a linear alkyl halide functionalised POSS [96]. This can then either be used directly in suitable substitution reactions or can be converted to a Grignard reagent for use in further reactions.

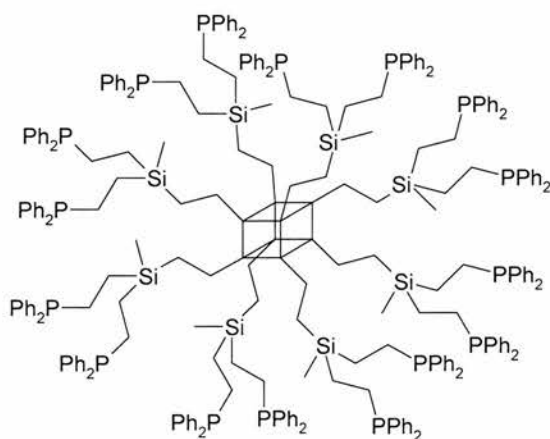
1.4.3 Applications

The unique shape and functionality of POSS molecules lends them to a variety of applications. One particularly interesting use is as the cores of dendrimeric molecules [97]. Dendrimers are globular molecules with branches radiating from a central core that can be used as catalytic supports. They have a large number of active sites and offer an advantage over normal homogeneous catalysts as they can be easily

separated from the substrate using filtration through a membrane due to their large size. Typically dendrimer cores have between three and six reactive sites to which branched organic ‘arms’ are attached to form what is known as a first generation dendrimer. Further arms can then be attached to form a second-generation dendrimer and so on. The arms are then terminated with appropriate functional groups, the steric interactions between which are important to the dendrimer’s properties.

The eight reactive sites of the POSS core makes them particularly suited to dendrimers as a high concentration of branches can be obtained relatively quickly. It has already been shown that a POSS-based dendrimer with arms terminated in phosphine groups (figure 1.4.6) can improve the selectivity of the hydroformylation of oct-1-ene to form the desired linear aldehyde [98]. It has been shown by molecular modelling that this selectivity is due in part to the shape of the POSS core [99].

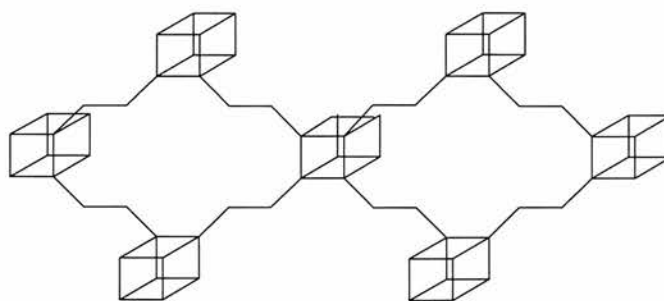
Figure 1.4.6 Phosphine POSS dendrimer. The POSS core is shown as a cube for clarity.



The similarity of cubic silsesquioxanes to the D4R SBU found in zeolites has also lead to their use as building blocks in the synthesis of polymers. By linking cubes through all eight corners it is geometrically difficult to fill all the available space suggesting that these molecules are ideal for the preparation of porous materials. Harrison *et al* and Laine *et al* showed that mesoporous polymers could be prepared through the copolymerisation of POSS molecules using the hydrosilation reaction between octavinyl- and octahydride- functionalised species [100]. By varying the length of the organic linkers between the POSS cubes it is possible to alter the size of the cavities in the polymer.

It was further shown by Morris *et al* that these copolymers can be further derivatised by 'ring-opening' the sides of some of POSS units and incorporating metals such as titanium and molybdenum in a similar way that has been achieved using monomeric POSS species [101]. This can result in the copolymers having possible uses in heterogeneous catalysis. In general, tailoring these porous polymers for specific applications is potentially easier than for zeolitic materials. This is because like coordination polymers they are prepared from pre-formed molecular building blocks that remain intact throughout the reaction process. Therefore, the resultant properties and topology can be predicted to a much greater degree.

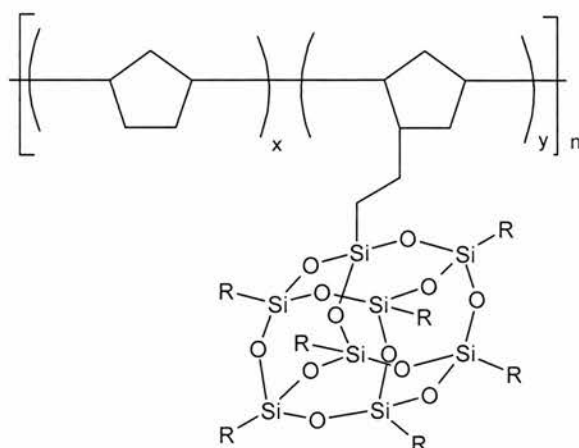
Figure 1.4.7 Simple schematic of a POSS copolymer network



Copolymerisation reactions have also been carried out between POSS molecules and non-POSS molecules to give a variety of potentially useful materials. A successful technique has been the polymerisation of octa-epoxy functionalised POSS with amine-containing molecules [102]. Epoxy polymers are widely studied due to their excellent thermal, mechanical and electrical properties. Incorporation of octa-epoxy functionalised POSS offers the possibility of further improving these polymers' properties such as a reduction in network motion and a higher glass transition temperature, which is obtainable without increasing the cross-linking density [103].

POSS copolymers can also be formed when the POSS additives are tethered to the polymer chain through a linkage on only one corner of the POSS (figure 1.4.8) [104]. These types of polymers have also been found to enhance the physical and thermal properties of plastics as a direct result of the size and shape of the POSS additives, which gives them the ability to control the motions of the chains while still maintaining the processability and mechanical properties of the base resin. Potential uses for polymers with POSS additives include: lightweight polymers; in heat/abrasion resistant paints; and fire retardants [105].

Figure 1.4.8 POSS tethered to a section of a polymer backbone [104]



There is significant interest in polymers containing POSS molecules for uses in space. Standard polymeric materials (such as Teflon) on spacecraft in low Earth orbits are rapidly degraded by atomic oxygen and vacuum ultraviolet radiation. However, if POSS containing polymers are used the POSS core reacts with the atomic oxygen to form a protective SiO_2 layer that can self-heal due to the POSS being uniformly dispersed throughout the matrix [104].

Other uses for POSS molecules are as models for heterogeneous catalysts [106], zeolite defect sites [107] and silica surfaces [108]. Metal containing POSS species can provide new homogeneous catalysts that mimic heterogeneous silica supported catalysts. Also, silsesquioxane derivatives as ligands have been shown to enhance the rate of many reactions including epoxidation and Diels-Alder reactions [109]. There is also potential for the use of POSS molecules in biology and medicine, such as in cardiovascular interventional devices [110].

1.5 Aims and Objectives

The main aim of this project was to prepare microporous materials using the new methodologies of ionothermal synthesis and coordination polymer chemistry. It was hoped that novel framework topologies would be prepared and that a rational design process could be implemented. The synthesis of these materials could then be appropriately adapted to tailor them for specific applications.

The first objective of this project was to prepare crystalline materials using eutectic mixtures as solvent. It was postulated that one component of the eutectic mixture would either form part of the porous framework or act as a template. Without water or any other solvent present the eutectic mixture may have acted as a true template. By altering the eutectic mixture more rationally designed analogues could then be prepared.

The second objective was to prepare crystalline porous materials by appropriately functionalising polyhedral oligomeric silsesquioxane molecules with carboxylic acid groups. It was hoped that by using these almost cubic shaped molecules, which closely resemble the D4R SBU commonly found in zeolites, coordination polymers could be formed with the aluminium cobalt phosphate 1 (ACO) zeolite topology.

A second aim of this project was to prepare a polymeric material where the POSS molecules are linked through Diels-Alder reactions. As the Diels-Alder reaction is thermally reversible the framework building process would be similar to that of

coordination polymer chemistry. Therefore, a highly ordered polymeric material with a topology analogous to the ACO zeolite topology would result.

1.6 References

1. A. F. Cronstedt, *Adak. Handl. Stockholm*, **1756**, 17, 120
2. A. Damour, *Am. Mines.*, **1840**, 17, 191
3. R. M. Barrer, *J. Chem. Soc.*, **1948**, 127
4. D. W. Breck, W. G. Eversole, R. M. Milton, T. B. Reed & T. L. Thomas, *J. Am. Chem. Soc.*, **1956**, 23, 5963
5. International Zeolite Association Website: www.iza-online.org
6. M. E. Davis & R. F. Lobo, *Chem. Mater.*, **1992**, 4, 756
7. H. Ghobarkar, O. Schäf & U. Guth, *Prog. Solid St. Chem.*, **1999**, 27, 29 and references therein
8. R. B. King, *Encyclopaedia of Inorganic Chemistry*, Wiley, Chichester, **1994**
9. R. Szostak, *Molecular Sieves Principals of Synthesis and Identification*, Van Nostrand Reinhold, New York, **1989**
10. K. R. Franklin & B. M. Lowe, *Stud. Surf. Sci. Catal.* **1998**, 49, 174
11. J. P. Arhancet & M. E. Davies, *Chem. Mater.*, **1991**, 3, 567
12. (a) S. T. Lawton and W. J. Rohrbaugh, *Science*, **1990**, 247, 1319 (b) M. J. Sabatar & G. Sastre, *Chem. Mater.*, **2001**, 13, 4520-4526
13. R. M. Barrer & P. J. Denny, *J. Chem. Soc.*, **1961**, 971
14. G. T. Kerr, *Science*, **1963**, 140, 1412

15. S. T. Wilson, B. M. Lok, C. A. Messina, T. R. Cannan & E. M. Flanigen, *J. Am. Chem. Soc.*, **1982**, *104*, 1146-1147
16. S. Feng and R. Xu, *Acc. Chem. Res.*, **2001**, *34*, 239-247
17. (a) B. Feng, X. Bu & G. D. Stucky, *Nature*, **1997**, *388*, 735 (b) G. C. Bond, M. R. Gelsthorpe, K. S. W. Sing & C. R. Theocharis, *Chem. Commun.*, **1985**, 1056 (c) G. W. Noble, P. A. Wright, P. Lightfoot, R. E. Morris, K. J. Hudson, Å. Kvik & H. Graafsma, *Angew. Chem. Int. Ed. Eng.*, **1997**, *36*, 81
18. (a) M. A. Camblor, M.-J. Diaz-Cabañas, J. Perez-Pariente, S. J. Teat, W. Clegg, I. J. Shannon, P. Lightfoot, P. A. Wright & R. E. Morris, *Angew. Chem. Int. Ed. Eng.*, **1998**, *37*, 2122-2126 (b) T. Wessels, L. B. McCusker, Ch. Baerlocher, P. Reinert & J. Patarin, *Micropor., Mesopor. Mater.*, **1998**, *23*, 67-77 (c) D. S. Wragg, G. B. Hix & R. E. Morris, *J. Am. Chem. Soc.*, **1998**, *120*, 6822-6823 (d) I. Bull, L. A. Villaescusa, S. J. Teat, M. A. Camblor, P. A. Wright, P. Lightfoot & R. E. Morris, *J. Am. Chem. Soc.*, **2000**, *122*, 7128-7129 (e) L. A. Villaescusa, I. Bull, P. S. Wheatley, P. Lightfoot & R. E. Morris, *J. Mater. Chem.*, **2003**, *13*, 1978-1982
19. (a) P. S. Wheatley & R. E. Morris, *J. Solid. St. Chem.*, **2002**, *167*, 267-273 (b) T. Loiseau & G. Férey, *J. Mater. Chem.*, **1996**, *6*, 1073-1074
20. C. S. Cundy & P. A. Cox, *Chem. Rev.*, **2003**, *103*, 663-701 and references therein
21. P. Bussian, F. Sobott, B. Brutschy, W. Schrader & F. Schüth, *Angew. Chem. Int. Ed.*, **2000**, *39*, 3901
22. S. L. Burkett & M. E. Davis, *J. Phys. Chem.*, **1994**, *98*, 4647-4653
23. F. Taulelle, M. Pruski, J. P. Amoureux, D. Lang, A. Bailly, C. Huguenard, M. Haouas, C. Gérardin, T. Loiseau & G. Férey, *J. Am. Chem. Soc.*, **1999**, *121*, 12148
24. S. Oliver, A. Kuperman & G. A. Ozin, *Angew. Chem. Int. Ed.*, **1998**, *37*, 46-62

25. S. Y. Yang, A. G. Vlessidis & N. P. Evmiridis, *Microporous Mater.*, **1997**, *9*, 273
26. R. E. Morris & S. J. Weigel, *Chem. Soc. Rev.*, **1997**, *26*, 309
27. (a) E. R. Cooper, C. D. Andrews, P. S. Wheatley, P. B. Webb, P. Wormald and R. E. Morris, *Nature*, **2004**, *430*, 1012-1016 (b) E. R. Parnham, P. S. Wheatley & R. E. Morris, *Chem. Commun.*, **2006**, 380-382 (c) E. R. Parnham & R. E. Morris, *J. Am. Chem. Soc.*, in press
28. S. Mohanty & A. V. McCormick, *Chem. Eng.*, **1994**, *74*, 1
29. M. J. Sabater, A. Corma, A. Domenech, V. Fornés & H. Garcia, *Chem. Commun.*, **1997**, 1285
30. R. Le Van Mao, N. T. Vu, S. Xiao & A. Ramsaran, *J. Mater. Chem.*, **1994**, *4*, 1143
31. M. E. Davis, *Nature*, **2002**, *417*, 813 and references therein
32. R. D. Miller, *Science*, **1999**, *286*, 421
33. T. Kyotani, T. Nagai, S. Inoue & A. Tomita, *Chem. Mater.*, **1997**, *9*, 609
34. Z. Ma, T. Kyotani, Z. Liu, O. Terasaki & A. Tomita, *Chem. Mater.*, **2001**, *13*, 4413
35. P. Gravereau, E. Garnier & A. Hardy, *Acta Crystallographica*, **1979**, *B35*, 2843
36. (a) B. F. Hoskins & R. Robson, *J. Am. Chem. Soc.*, **1990**, *112*, 1546-1554 (b) B. F. Abrahams, B. F. Hoskins, D. M. Michall & R. Robson, *Nature*, **1994**, *369*, 727-729
37. C. J. Kepert & M. J. Rosseinsky, *Chem. Commun.*, **1998**, 31
38. L. R. MacGillivray, S. Subramanian & M. J. Zaworotko, *Chem. Commun.*, **1994**, 1325
39. X. Wang, M. Simard & J. D. Wuest, *J. Am. Chem. Soc.*, **1994**, *116*, 12119-12120

40. P. Losier & M. J. Zaworotko, *Angew. Chem. Int. Ed.*, **1996**, *35*, 2779
41. O. M. Yaghi, H. Li & T. L. Groy, *Inorg. Chem.*, **1997**, *36*, 4292-4293
42. C. J. Kepert & M. J. Rosseinsky, *Chem. Commun.*, **1999**, 375-376
43. O. M. Yaghi & H. Li, *J. Am. Chem. Soc.*, **1996**, *118*, 295-296
44. O. M. Yaghi, G. Li & H. Li, *Nature*, **1995**, *378*, 703-706
45. G. Férey, C. Mellot-Draznieks, C. Sierre, F. Millange, J. Dotour, S. Surblé & I. Margiolaki, *Science*, **2005**, *309*, 2040
46. C. J. Kepert, T. J. Prior & M. J. Rosseinsky, *J. Am. Chem. Soc.*, **2000**, *122*, 5158
47. A. Clearfield, *Curr. Opin. Solid State Mater. Sci.*, **1996**, *1*, 268 and references therein
48. (a) G. Alberti, U. Costantino, F. Marmottini, R. Vivani & P. Zappelli, *Micropor. Mesopor. Mater.*, **1998**, *21*, 297-304 (b) D. Riou & G. Férey, *J. Mater. Chem.*, **1998**, *8*, 2733-2735 (c) Q. Gao, N. Guillou, M. Nogues, A. K. Cheetham & G. Férey, *Chem. Mater.*, **1999**, *11*, 2937-2947 (d) B.-P. Yang, Z.-M. Sun & J.-G. Mao, *Inorganica Chimica Acta*, **2004**, *357*, 1583-1588
49. J.-G. Mao, Z. Wang & A. Clearfield, *Inorg. Chem.*, **2002**, *41*, 2334-2340
50. A. Distler, D. L. Lohse & S. C. Sevov, *J. Chem. Soc. Dalton Trans.*, **1999**, 1805-1812
51. A. Distler & S. C. Sevov, *Chem. Commun.*, **1998**, 959-960
52. (a) N. Stock & T. Bein, *Angew. Chem. Int. Ed. Eng.*, **2004**, *43*, 749-752
53. J.-L. Song, A. V. Prosvirin, H.-H. Zhao & J.-G. Mao, *Eur. J. Inorg. Chem.*, **2004**, 3706-3711
54. A. J. Blake, N. R. Champness, S. S. M. Chung, W.-S. Li & M. Schröder, *Chem. Commun.*, **1997**, 1005

55. A. J. Blake, N. R. Champness, A. N. Khlobstov, D. A. Lemeovskii, W.-S. Li & M. Schröder, *Chem. Commun.*, **1997**, 1339
56. S. L. James, *Chem. Soc. Rev.*, **2003**, 32, 276-288
57. M. Eddaoudi, J. Kim, N. Rosi, D. Vodak, J. Wachter, M. O'Keeffe & O. M. Yaghi, *Science*, **2002**, 295, 469
58. H. Li, M. Eddaoudi, T. L. Groy & O. M. Yaghi, *J. Am. Chem. Soc.*, **1998**, 120, 8571-8572
59. O. M. Yaghi & H. Li, *J. Am. Chem. Soc.*, **1995**, 117, 10401-10402
60. O. M. Yaghi, H. Li, C. Davis, D. Richardson & T. L. Groy, *Acc. Chem. Res.* **1998**, 31, 474-484 and references therein
61. M. Fujita, Y. J. Kwon, S. Washizu & K. Ogura, *J. Am. Chem. Soc.*, **1994**, 116, 1151-1152
62. J. Seo Seo, D. Whang, H. Lee, S. I. Jun, J. Oh, Y. J. Jeon & K. Kim, *Nature*, **2000**, 404, 982
63. M. D. Ward, *Science*, **2003**, 300, 1104-1105
64. N. L. Rosl, J. Eckert, M. Eddaoudi, D. T. Vodak, J. Kim, M. O'Keeffe & O. M. Yaghi, *Science*, **2003**, 300, 1127
65. J. L. C. Rowsell & O. M. Yaghi, *Angew. Chem. Int. Ed. Eng.*, **2005**, 44, 4670-4679
66. S. Hermes, M-K. Schroter, R. Schmid, L. Khodeir, M. Muhler, A. Tissler, R. W. Fischer & R. A. Fischer, *Angew. Chem. Int. Ed.*, **2005**, 44, 6237-6241
67. S. Hermes, F. Schroder, R. Chelmowski, C. Woll & R. A. Fischer, *J. Am. Chem. Soc.*, **2005**, 127, 13744-13745

68. R. D. Rogers & K. R. Seddon, *Science*, **2003**, *302*, 792-793 and references therein
69. P. Walden, *Bull. Acad. Imper. Sci. (St Petersburg)*, **1914**, 1800
70. T. Welton, *Chem. Rev.*, **1999**, *99*, 2071-2083
71. A. P. Abbott, G. Capper, D. L. Davies, R. K. Rasheed & V. Tambyrajah, *Chem. Commun.*, **2003**, 70-71
72. A. P. Abbott, D. Boothby, G. Capper, D. L. Davies and R. K. Rasheed, *J. Am. Chem. Soc.*, **2004**, *126*, 9142-9147
73. (a) A. P. Abbott, G. Capper, D. L. Davies & R. K. Rasheed, *Chem. Eur. J.*, **2004**, *10*, 3769-3774 (b) A. P. Abbott, G. Capper, D. L. Davies, H. L. Munro, R. K. Rasheed & V. Tambyrajah, *Chem. Commun.*, **2001**, 2010-2011 (c) A. P. Abbott, G. Capper, D. L. Davies & R. Rasheed, *Inorg. Chem.*, **2004**, *43*, 3447-3452
74. W. T. Ford, R. J. Haur & D. J. Hart, *J. Org. Chem.*, **1973**, *38*, 3916
75. S. Sugden & H. Wilkins, *J. Chem. Soc.*, **1929**, 1291
76. P. Bonhôte, A.-P. Dias, N. Papageorgiou, K. Kalyanasundaram & M. Grätzel, *Inorg. Chem.*, **1996**, *35*, 1168-1178
77. P. Wasserschied & W. Keim, *Angew. Chem. Int. Ed. Eng.*, **2000**, *39*, 3772-3789 and references therein
78. K. R. Seddon, *Nature Mater.*, **2003**, *2*, 363
79. (a) A. P. Abbott, G. Capper, D. L. Davies, R. K. Rasheed & P. Shikotra, *Inorg. Chem.*, **2005**, *44*, 6497-6499 (b) D. S. Jacob, A. Joseph, S. P. Mallenalli, S. Shanmugam, S. Makhluif, J. Calderon-Moreno, Y. Kolytyn & A. Gedanken, *Angew. Chem. Int. Eng.*, **2005**, *44*, 6560-6563

80. A. P. Abbott, G. Capper, D. L. Davies, R. K. Rasheed & V. Tambyrajah, *Green Chemistry*, **2002**, *4*, 24-26
81. D. W. Scott, *J. Am. Chem. Soc.*, **1946**, *68*, 356
82. P. G. Harrison, *J. Organomet. Chem.*, **1997**, *542*, 141-183
83. M. M. Sprung & F. O. Guenther, *J. Am. Chem. Soc.*, **1955**, *77*, 3990
84. A. J. Barry, W. H. Daudt, J. J. Domicine & J. W. Gilkey, *J. Am. Chem. Soc.*, **1955**, *77*, 4248
85. (a) L. H. Vogt & J. F. Brown, *Inorg. Chem.*, **1963**, *2*, 189 (b) M. M. Sprung & F. O. Guenther, *J. Am. Chem. Soc.*, **1955**, *77*, 3996 (c) J. F. Brown, *J. Am. Chem. Soc.*, **1965**, *87*, 4317 (d) J. F. Brown, L. H. Vogt & P. I. Prescott, *J. Am. Chem. Soc.*, **1964**, *86*, 1120 (e) C. I. Frye & W. T. Collins, *J. Am. Chem. Soc.*, **1970**, *92*, 5586 (f) M. G. Voronkov, T. N. Martynova, R. G. Mirskov & V. L. Belyi, *Zh. Obshch. Khim.*, **1979**, *49*, 1522-1525 (g) T. N. Martynova, V. P. Korchkov & P. P. Semyannikov, *J. Organomet. Chem.*, **1983**, *258*, 277-282
86. H. C. Marsmann & E. Rikowski, *Polyhedron*, **1997**, *16*, 3357
87. F. J. Feher & T. A. Budzichowski, *J. Organomet. Chem.*, **1989**, *379*, 33-40
88. (a) F. J. Feher & J. F. Waltzer, *Inorg. Chem.*, **1991**, *30*, 1689-1694 (b) F. J. Feher, *J. Am. Chem. Soc.*, **1986**, *108*, 3850-3852 (c) F. J. Feher & T. L. Tajima, *J. Am. Chem. Soc.*, **1994**, *116*, 2145-2146
89. A. Voigt, R. Murugavel, V. Chandrasekhar, N. Winkhofer, H. W. Roesky, H.-G. Schmidt & I. Uson, *Organomet.*, **1996**, *15*, 1610-1613
90. (a) F. J. Feher, R. Terroba & J. W. Ziller, *Chem. Commun.*, **1999**, 2309-2310 (b) F. J. Feher, D. Soulivong & A. G. Eklund, *Chem. Commun.*, **1998**, 399-400
91. P. A. Agaskar, *Inorg. Chem.*, **1991**, *30*, 2707

92. (a) P. N. Rylander, *Organic Syntheses with Nobel Metal Catalysts*, Academic Press, New York & London, **1973**, chapter 9 and references therein (b) J. L. Speier, J. A. Webster & G. H. Barnes, *J. Am. Chem. Soc.*, **1956**, *79*, 974 (c) C. N. Stengone & R. A. Widenhoefer, *Tet. Lett.*, **1999**, *40*, 1451
93. (a) A. Provatas, M. Luft, J. C. Mu, A. H. White, J. G. Matison & B. W. Skelton, *J. Organomet. Chem.*, **1998**, *565*, 159-164 (b) M. S. Said, H. W. Roesky, C. Rennekamp, M. Andruh, H.-G. Schmidt & M. Noltemeyer, *Angew. Chem. Int. Ed. Eng.*, **1999**, *38*, 661 (c) B. W. Manson, J. J. Morrison, P. I. Couper, P.-A. Jaffrès & R. E. Morris, *J. Chem. Soc. Dalton Trans.*, **2001**, 1123-1127
94. B. Marciniec, *Silicon Chemistry 1*, **2002**, 155-175
95. (a) F. J. Feher, D. Soulivong, A. G. Eklund & K. D. Wyndham, *Chem. Commun.*, **1997**, 1185 (b) Y. Itami, B. Marciniec & M. Kubicki, *Chem. Eur. J.*, **2004**, *10*, 1239-1248 (c) L.-H. Lee & W.-C. Chen, *Polymer*, **2005**, *46*, 2163-2174 (d) S. Lucke, K. Stoppek-Langner, J. Kuchinke & B. Krebs, *J. Organomet. Chem.*, **1999**, *584*, 11-15
96. E. A. Drylie, C. D. Andrews, M. A. Hearshaw, C. Jimenez-Rodriguez, A. Slawin, D. J. Cole-Hamilton & R. E. Morris, *Polyhedron*, **2006**, *25*, 853-858
97. (a) P. I. Coupar, P.-A. Jaffrès & R. E. Morris, *J. Chem. Soc. Dalton Trans.*, **1999**, 2183-2187 (b) B. Hong, T. P. S. Thoms, H. J. Murfee & M. J. Lebrun, *Inorg. Chem.*, **1997**, *36*, 6146-6147
98. L. Ropartz, R. E. Morris, D. F. Foster & D. J. Cole-Hamilton, *Chem. Commun.*, **2001**, 361-362
99. K. J. Haxton, D. J. Cole-Hamilton & R. E. Morris, *J. Chem. Soc. Dalton Trans.*, **2004**, 1665-169

100. (a) P. G. Harrison, *J. Organomet. Chem.*, **1997**, *542*, 141-183 and references therein (b) C. Zhang, F. Babonneau, C. Bonhomme, R. M. Laine, C. L. Soles, H. A. Hristov & A. F. Yee, *J. Am. Chem. Soc.*, **1998**, *11*, 8380-8391
101. J. J. Morrison, C. J. Love, B. W. Manson, I. J. Shannon & R. E. Morris, *J. Mater. Chem.*, **2002**, *12*, 3208-3212
102. C. Ramirez, M. Rico, J. M. L. Vilariño, L. Barral, M. Ladra & B. Montero, *J. Therm. Anal. Cal.*, **2005**, *80*, 153-157
103. A. Lee & J. D. Lichtenhan, *Macromolecules*, **1998**, *31*, 4970-4974
104. S. H. Phillips, T. S. Haddad & S. J. Tomczak, *Curr. Opin. Solid State Mater. Sci.*, **2004**, *8*, 21-29 and references therein
105. (a) Zyn POSS Website: www.zyn.com/flcfw/fwtproj/Poss.htm (b) Hybrid Plastics Website: www.hybridplastics.com
106. H. C. L. Abbenhuis, S. Krijnen & R. A. van Santen, *Chem. Commun.*, **1997**, 331
107. S. Krijnen, R. J. Harmsen, H. C. L. Abbenhuis, J. H. C. van Hooff & R. A. van Santen, *Chem. Commun.*, **1999**, 501-502
108. F. J. Feher, D. A. Newman & J. F. Walzer, *J. Am. Chem. Soc.*, **1999**, *111*, 1741-1748
109. H. C. L. Abbenhuis, H. W. G. van Herwijnen & R. A. van Santen, *Chem. Commun.*, **1996**, 1941
110. R. Y. Kannan, H. J. Salacinski, P. E. Butler & A. M. Seifalian, *Acc. Chem. Res.*, **2005**, *38*, 879-884

2. Experimental and Analytical Techniques

2.1 Air and Moisture Sensitive Synthetic Chemistry

For air and moisture sensitive chemistry standard Schlenk techniques were used. All reaction vessels and syringes were oven dried before use and all solvents and liquid reactants were either obtained dry or were dried using established procedures [1].

For all reactions a Schlenk line was used fitted with a Drierite (anhydrous calcium sulfate) column through which argon passed through before entering the line. A magnetic stirrer was placed in the Schlenk glassware to be used, which was then fitted with a rubber seal and evacuated of air then refilled with argon. This filling/evacuation procedure was repeated twice before any reagents were added to ensure an inert atmosphere was obtained. Solvents were added *via* a syringe from storage under a dry, inert atmosphere. Before filling the syringes with liquid they were filled with argon then evacuated three times as for the reaction vessel. All solid reagents were added to the reaction flask under a steady stream of argon.

For reactions performed at reflux a condenser was fitted under a steady stream of argon. Argon was passed over the reaction and through an oil bubbler to ensure an inert atmosphere was maintained.

2.2 Ionothermal Synthesis

The usual route of zeotype synthesis (hydrothermal synthesis) is crystallisation from a reactant solution/slurry at high temperature and autogenous pressure in a sealed autoclave [2]. The reactants include the framework building species, the structure directing agent/template, the solvent and if required a mineraliser such as hydrofluoric acid. Ionothermal synthesis is similar to hydrothermal synthesis except that the solvent (the ionic liquid or eutectic mixture) is also the template. Also, ionothermal zeotype synthesis can sometimes be performed in an open vessel such as a round-bottomed flask.

Typically an ionothermal procedure involves partially filling a Teflon lined autoclave with the solvent and then adding the other reactants before sealing the autoclave and heating for a few days in an oven. Many variables can be investigated such as framework cations, solvent, time and temperature. The product is recovered by vacuum filtration, washed and if required sonicated to separate the larger particles. Finally the product is dried.

Ionothermal synthesis has mostly been used for aluminophosphate synthesis, for which an aluminium source (eg aluminium isopropoxide) and a phosphate source (eg phosphoric acid) are required plus any other desired additives such as a source of transition metals. For coordination polymers organic molecules functionalised with, for example, carboxylic acids or phosphonic acids and a metal source (eg cobalt acetate) are necessary, plus any other additives required such as a base.

2.3 Nuclear Magnetic Resonance

Nuclear magnetic resonance (NMR) spectroscopy is a valuable tool for the organic and inorganic synthetic chemist, allowing the analysis of nuclei with non-zero magnetic moments, resulting in structural information on the material [3].

Atomic nuclei with an intrinsic angular momentum known as a nuclear spin (I) adopt $2I + 1$ orientations in the presence of a magnetic field (B_0). Nuclei with an odd mass number have nuclei spins of $1/2$, $3/2$, $5/2$ etc. In solution state NMR ^1H and ^{13}C are the most important nuclei and both have spins of a $1/2$. For these nuclei only two orientations are possible: a low energy orientation aligned with the magnetic field and a high energy orientation opposed to the magnetic field. When a radio frequency signal that matches the energy difference between the two levels (equation 2.1) is applied to the system some of the low energy nuclei are promoted to the high energy level. A small portion of the radio signal is absorbed and the signal is measured from the re-emission of the radiation as the nuclei relax to the ground state again.

Equation 2.1 $\mathbf{E} = \mathbf{h}\cdot\nu$ $\nu = \gamma B_0/2\pi$

Commonly the method used to obtain NMR spectra is FT (Fourier Transform) NMR spectroscopy. The FT NMR spectrum is measured by applying the radio frequency signal as a single pulse that generates an oscillating magnetic field at a right angle to the applied magnetic field. The sample being analysed has a net magnetisation initially aligned in the direction of the applied field, which on application of the pulse

is disturbed and its oscillation is detected. The frequency of the oscillation is the difference between the NMR resonance frequency and the excitation frequency. As the magnetisation oscillates it decays as relaxation allows it to return back to equilibrium. This oscillation signal from the sample's nuclei is known as the free induction decay (FID), which after Fourier transformation (FT) shows the nuclei's frequency or chemical shift spectrum.

The precise frequency at which a nucleus comes into resonance depends on the applied magnetic field and also the differences in magnetic environment experienced by each nucleus. These differences are mainly caused by variations in electron density and their movement, which creates a magnetic field, resulting in each chemically distinct atom coming into resonance at a slightly different frequency from the others. The signals obtained are described as having a chemical shift (δ) from a standard frequency and are measured in parts per million (ppm). The common standard for ^1H , ^{13}C and ^{29}Si NMR is tetramethylsilane, which is chosen because it only has one signal (which appears at one extreme of the spectrum), is inert, volatile, non-toxic and cheap.

With ^1H NMR spectra the absorption of the signal is generally proportional to the number of protons coming into resonance at that frequency. Therefore, the area under the peaks can be used to calculate how many protons are in a specific environment. Furthermore, these peaks are also split into a fine structure due to the interactions (coupling) between neighbouring or nearby magnetic nuclei. With first order ^1H - ^1H coupling if a carbon is connected to another carbon with n identical

hydrogens its signal will be split into $n + 1$ peaks, the intensities of which are given by the coefficients of the terms in the expansion of $(x + 1)^n$. For example if a methyl group is connected to a methylene group with identical hydrogens its signal will be split into a triplet with intensities of the peaks being 1:2:1. This allows for the connectivity between the atoms in the molecule to be established.

All solution NMR spectra (^1H , ^{13}C and ^{29}Si) were recorded on a Varian 300 or a Bruker 300 spectrometer operating at the appropriate frequency.

2.4 Mass Spectroscopy and MALDI-TOF

Mass spectroscopy involves the vaporisation of compounds and the production of ions from the resultant gas phase molecules [3]. The ions are then separated according to their mass to charge ratio (m/z), detected and recorded. Usually only singly charged ions are produced so the abundance of the ions is generally plotted against m/z . The types of ions produced can be predicted so the output provides valuable evidence of a compound's structure and mass. Electrospray ionisation (ESI) mass spectroscopy produces a single peak allowing for straightforward confirmation of a sample's mass.

Matrix-assisted laser desorption – time of flight (MALDI-TOF) spectra is a powerful tool for the determination of molecular weights of very large molecules such as proteins and dendrimers, which are outside the range of conventional mass spectrometers [4]. For MALDI, the sample to be analysed is mixed with an excess of

an ultraviolet absorbing matrix, which is usually a low molecular weight aromatic acid. On irradiation with a focused beam at the appropriate wavelength, the excess matrix sublimates and transfers the embedded analyte molecules into the gas phase. Singly protonated ions are formed from the numerous ion-atom collisions, which are then accelerated into the spectrometer.

Mass spectroscopy was carried out by the University of St Andrews Mass Spectrometry Service on a Micromass GCT spectrometer and a Micromass LCT spectrometer. MALDI-TOF spectroscopy was carried out by the University of St Andrews Biomolecular Mass Spectrometry and Proteomics Service on a Micromass, ToFSpec 2E, MALDI-TOF mass spectrometer.

2.5 CHN Elemental Analysis

CHN (carbon, hydrogen, nitrogen) elemental analysis provides information on the ratios of these three elements in a material. From comparison with the calculated values it is possible to verify the composition and purity of a material. Elemental analysis was carried out by the St Andrews Microanalysis Service on a Carlo Erba 1106 CHN Elemental Analyser.

2.6 Infra-Red Spectroscopy

Most molecular vibrations can be detected and measured in the infra-red region of the electromagnetic spectrum. The most useful range of the spectrum is between 4000 cm^{-1} and 625 cm^{-1} (cm^{-1} is the scale in which the reciprocal of the wavelength is measured). Vibrations of individual types of bonds and functional groups occur in well-defined areas, providing useful structural information on a material [3].

Liquids for analysis are prepared by squeezing a drop of the liquid between flat plates of sodium chloride (which are transparent through the $4000\text{-}625\text{ cm}^{-1}$ region) before the infra-red beam is passed through the sample. Solid samples are mixed with a hydrocarbon (usually nujol) to form a thick paste or mull before pressing between the plates. Alternatively the sample is ground with potassium bromide and pressed into a disc using a special mould and hydraulic press. This method eliminates the problems of bands due to the mulling agent in the spectrum, although this is not usually a problem.

All FTIR spectra were recorded on a Perkin-Elmer 1710 spectrometer or a Perkin-Elmer Spectrum GX IR spectrometer.

2.7 X-Ray Diffraction

X-ray diffraction is the main method for the structural characterisation of crystalline inorganic solids. It is used to determine the average atomic positions in a solid and from them the distances and bond angles between the atoms.

X-rays are typically generated by bombarding a metal (usually copper or molybdenum) with high-energy electrons. The electrons slow down as they enter the metal and generate radiation with a continuous range of wavelengths called Bremsstrahlung [5]. Superimposed on this are sharp peaks resulting from collisions between the incoming electrons and the electrons in the inner shells of the metal atoms. This leads to the ejection of the inner shell electrons. The vacancies are then filled by electrons dropping from higher energy shells and the excess energy is emitted as x-ray photons.

A crystalline solid is made up of a large number of units that are regularly repeated in all directions, resulting in an ordered structure [6]. These units can be atoms, molecules or segments of molecules. The smallest repeating unit is known as the unit cell, which has three sides (conventionally denoted a , b and c) and three angles (α , β and γ). However, symmetry (other than translation symmetry, i.e. moving from one point in the unit cell to another) within a unit cell relates the atoms and molecules within the cell to each other, thus the unique, independent part of the structure is usually only a fraction of the unit cell and is known as the asymmetric unit. Restrictions are imposed on the unit cell parameters by rotational and reflection

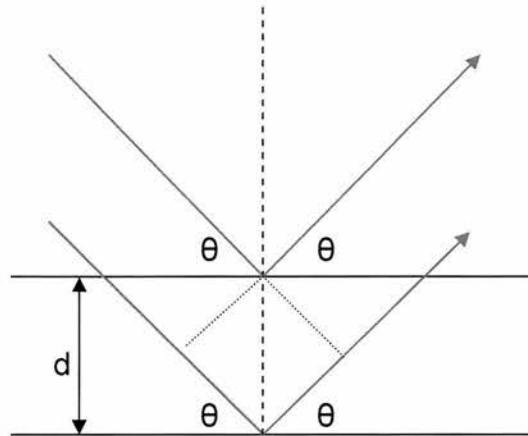
symmetry, leading to seven types of crystal symmetry known as crystal systems (table 2.1). Symmetry elements allow these crystal systems to be subdivided into thirty-two point groups that are then subdivided into two hundred and thirty space groups due to translational symmetry [7].

Table 2.1 *Crystal systems*

Crystal system	Essential symmetry	Restrictions on unit cell
Triclinic	None	None
Monoclinic	one 2-fold rotation and/or mirror	$\alpha = \gamma = 90^\circ$
Orthorhombic	three 2-fold rotations and/or mirrors	$\alpha = \beta = \gamma = 90^\circ$
Tetragonal	one 4-fold rotation	$a = b; \alpha = \beta = \gamma = 90^\circ$
Rhombohedral	one 3-fold rotation	$a = b = c; \alpha = \beta = \gamma (\neq 90^\circ)$
Hexagonal	one 6-fold rotation	$a = b; \alpha = \beta = 90^\circ; \gamma = 120^\circ$
Cubic	four 3-fold rotation axes	$a = b = c; \alpha = \beta = \gamma = 90^\circ$

The three dimensional symmetry of a crystalline material is conventionally described as the crystal lattice. The lattice defines points in space that have the same environment (symmetry). These lattice points can lie either on the atoms or on symmetry elements (for example an inversion centre or a rotational axis) and are connected to each other by equally spaced parallel lines that cut through the unit cells called Miller planes, which are described by Miller indices (h, k and l). The distance between the Miller Planes is referred to as the d spacing.

Figure 2.1 Reflection of x-rays from two lattice planes



The crystal lattice acts as a diffraction grating for x-rays. A diffraction pattern occurs when an x-ray beam is scattered by the electrons surrounding the atoms or ions and there is constructive interference between all the beams diffracted in the crystal lattice. For constructive interference to occur Bragg's law must be satisfied. The path length difference ($2d\sin\theta$) between scattering from successive planes must be an integer number of wavelengths. θ (theta) is the angle between the incident beam and the lattice planes.

Equation 2.2 Bragg's Law

$$\mathbf{n\lambda = 2d\sin\theta}$$

The complete pattern of scattered x-rays produced by a crystal is obtained by rotating the crystal in the x-ray beam, which allows diffraction to be measured at different values of θ . The result is a regular pattern of spots (known as the reciprocal lattice),

which has three points of interest that correspond to the structure [6]. Firstly, the geometry of the pattern is related to the lattice and unit cell geometry so gives information on the repeat distances between the repeating units. Secondly, the symmetry of the pattern is related to the symmetry of the unit cell so allows determination of the crystal system and space group. Thirdly, the different intensities of the spots hold information on the actual positions of the atoms within the unit cell of the material.

2.7.1 Single crystal XRD

Single crystal x-ray diffraction is the most straightforward method for obtaining structural information on a crystalline solid and is the method of choice if suitable crystals are obtained. For single crystals each set of Miller planes can be brought into the reflecting position using three degrees of freedom (ϕ , χ and ω) of a four circle diffractometer. The remaining degree of freedom (2θ) is then scanned so that data is collected in a range of orientations and obtained for the full three-dimensional lattice.

X-ray reflections (positions and intensities) used to have to be observed one at a time but nowadays diffraction experiments routinely use area detectors, which can record a number of incident beams at the same time. The most common of these is the charge-coupled device (CCD) detector. Due to the size of these detectors it is possible to reduce the number of rotation axes for the crystal so it is now no longer necessary to bring all the reflections into the horizontal plane to record them, allowing for faster data collection and a complete diffraction pattern to be collected.

Single crystal data collected at the University of St Andrews was collected at 293 K using a Bruker SMART diffractometer with graphite-monochromated Mo K_{α} radiation ($\lambda = 0.71074$) or Cu K_{α} radiation ($\lambda = 1.54180$). The crystal structures were solved using the direct methods program SHELXS-97 and refined with a full matrix least-squares technique using the program SHELXL-97.

2.7.2 Powder XRD

When suitable crystals for single crystal x-ray diffraction cannot be obtained powder x-ray diffraction can be used to solve a sample's structure. However, the orientations of the particles (crystallites) in a crystalline powder are generally random, causing the observed pattern to be an average of the particle orientations so it appears as a pattern of concentric rings. The diffractometer therefore only has two variables (2θ and ω) and the three-dimensional pattern is observed as a two-dimensional pattern. Therefore there is a loss of data through peak overlap and it is much more difficult to index the sample, assign the correct space group and solve the structure than by using single crystal XRD.

Although it is possible to solve the structures of microporous materials using powder XRD it was not necessary during this project. Instead it was used for the identification of known phases and confirmation of structures prepared. Reitveld refinement of a sample's observed powder pattern against a structural model (equation 2.3) minimises the residual (S) by a least squares process, where y_{io} and y_{ic}

are the observed and calculated intensities and w_i is a suitable weight at the i th step [8].

$$\text{Equation 2.3} \quad S = \sum w_i |y_{io} - y_{ic}|^2$$

This is achieved by first refining several profile parameters involving the diffractometer zero point, background and peak shape. When a close fitting model is obtained the atomic positions, thermal parameters and site occupancies are then refined to give the final structure solution.

As with least squares refinement of single crystal data, the progress of powder refinements are monitored by R-factors, normally the profile R_p and the weighted profile R_{wp} , the more meaningful of the two being the weighted R-factor. However, R_{wp} is heavily dependent on the treatment of the background so is not ideal for comparing refinements between different samples.

$$\text{Equation 2.4} \quad R_p = \frac{\sum |y_{io} - y_{ic}|}{\sum y_{io}}$$

$$\text{Equation 2.5} \quad R_{wp} = \sqrt{\frac{\sum w_i (y_{io} - y_{ic})^2}{\sum w_i y_{io}^2}}$$

The quality of the data is expressed by equation 2.6, where N is the number of profile points and P is the refined parameters. In theory the value of R_{wp} should approach that of R_{exp} . A measure of this is the goodness of fit function, χ , which shows how well the structural model fits the data. This value should converge to unity for a well-refined structure.

Equation 2.6
$$R_{exp} = \sqrt{\frac{(N - P)}{\sum w_i y_{io}^2}}$$

Equation 2.7
$$\chi = \sqrt{\frac{R_{wp}}{R_{exp}}}$$

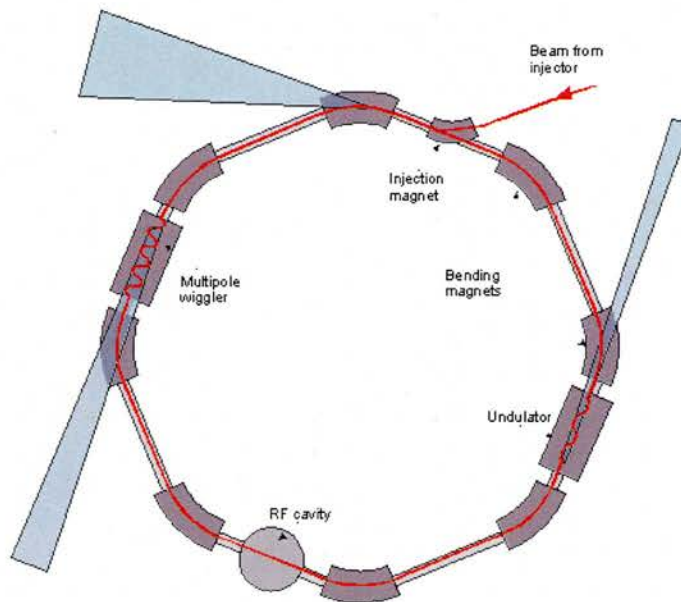
When refining a structure it is also helpful to look at the plot of the observed and calculated profiles and the difference between them. In a well refined structure the two sets of values should fit exactly. Also, the highest possible resolution data should be collected to minimise peak overlap and background noise.

Data for phase identification purposes were collected on a STOE STADIP diffractometer using monochromated Cu $K_{\alpha 1}$ radiation in flat plate geometry. Data for refinement was collected on a STOE STADIP diffractometer using monochromated Cu $K_{\alpha 1}$ radiation collected in Debye-Scherrer geometry using 0.7 mm quartz capillaries over 12 hours.

2.7.3 Synchrotron Radiation

Synchrotron radiation is a highly intense, concentrated in a narrow angular range, polarised, tuneable beam of x-rays delivered in a series of short pulses of less than a nanosecond in length [9]. It is created by accelerating electrons to relativistic speeds, injecting them into a storage ring (operated at high vacuum) and holding them at a fixed energy using a constant magnetic field. Synchrotron radiation is emitted tangentially from the ring and has a continuous spectrum ranging from infra-red to x-rays, of which any wavelength can be selected by the use of a monochromator [6]. The electron current of the storage ring decays exponentially due to electrons being scattered out of the beam from electron-electron interactions and scattering from gaseous molecules. It therefore has to be refilled every 24 hours.

Figure 2.2 Schematic illustration of a synchrotron radiation storage ring [10]



Synchrotron radiation allows diffraction experiments on very small crystals or weakly scattering crystals because of the high intensity and low divergence of the beam [11]. The ultrafast high-resolution data obtainable using synchrotron radiation has led to improved structure solutions of zeolitic materials, which are often only obtained as microcrystals. It can also be used for other applications such as collection of high resolution powder data, time-resolved crystallography and high-pressure studies.

Single-crystal x-ray diffraction was carried out at either station 9.8 or 16.2smx at the CCLRC Daresbury Laboratory Synchrotron Radiation Source, Cheshire, UK [12]. Station 9.8 is a high flux, tuneable, monochromatic, single crystal diffraction facility, which utilises a Bruker-Nonius APEXII CCD area detector and D8 diffractometer at X-ray wavelength between 1.45 Å and 0.30 Å. The station is placed 10.7 m from the 5T wiggler and can receive up to 3.8 mrad of beam. This is focussed in the horizontal plane by a cylindrically bent asymmetrically cut triangular silicon monochromator, cooled by GaInSn alloy. There is a choice of either a (111) or (220) monochromator crystal. The (111) crystal has an asymmetric cut of 2.01°, which gives in an optimum focus at the sample for a wavelength of 0.7 Å. At this wavelength the $\Delta\lambda/\lambda = 0.1\%$. The operational range of this crystal is from 1.45 Å to 0.45 Å. The (220) crystal has an asymmetric cut of 1.03°, which gives in an optimum focus at the sample for a wavelength of 0.3 Å. At this wavelength the $\Delta\lambda/\lambda = 0.1\%$. The operational range of this crystal is from 0.8 Å to 0.30 Å. The monochromator is mounted on a Huber rotatory table and can be positioned to a precision of 0.001°. For normal use (and for our requirements) the station is set to approximately 0.68 Å. The second optical

component is a flat 1.2 m palladium coated (300 mm) zerodur glass mirror. This is mounted to allow it to be cylindrically bent to provide vertical focussing of the monochromatic beam. Its second purpose is to act as a harmonic rejecter. At 0.68 Å the mirror operates at 6 mrad to the incident beam. The mirror has been successfully used between 0.48 Å and 1.45 Å. The station operates a Bruker-Nonius APEXII CCD area detector and D8 diffractometer. The APEXII has a choice of four standard collimators (0.8, 0.5, 0.3, 0.2 mm) plus two for microcrystal work (0.1, 0.05 mm under testing). The uncollimated beam is 2.5 mm in width by 1.0 mm high.

Station 16.2smx is used as an overflow for station 9.8. It is a high flux, fixed wavelength, monochromatic, single crystal diffraction facility. It utilises a Bruker-Nonius APEXII CCD area detector and D8 diffractometer at an X-ray wavelength of 0.846 Å. The APEXII has a choice of four standard collimators (0.8, 0.5, 0.3, 0.2 mm) plus two for microcrystal work (0.1, 0.05 mm under testing).

2.8 Thermal Analysis

Thermogravimetric analysis (TGA) is used to study the loss of mass in porous materials. The technique involves weighing a sample whilst it is being heated in a controlled manner, usually under oxygen or an inert gas. The observed changes in mass provide information on the stability and molecular formula of the material. Combining TGA with mass spectroscopy (TG-MS) provides further information on what masses are being lost from the material, allowing assignment of molecules or molecular fragments lost on heating.

TG-MS analysis was carried out by the St Andrews Microanalysis Service on a Netzsch STA 449C analysis coupled to a Pfeiffer mass spectrometer (200 amu). Samples were heated at 5 °C min⁻¹ to a maximum of 600 °C under an atmosphere of argon at a rate of 50 ml min⁻¹.

2.9 References

1. D. D. Perrin & W. L. F. Armarego, *Purification of Laboratory Chemicals*, Pergamon Press, Oxford, **1986**, 3rd edition
2. M. E. Davis & R. F. Lobo, *Chem. Mater.*, **1992**, 4, 756-768 and references therein.
3. D. H. Williams & I. Fleming, *Spectroscopic Methods in Organic Chemistry*, McGraw Hill, Cambridge, **1997**, 5th Edition
4. H. Steen & M. Mann, *Nature Reviews; Molecular Cell Biology*, **2004**, 5, 699-711
5. P. W. Atkins, *Physical Chemistry*, Oxford University Press, Sussex, **1987**, 3rd Edition
6. W. Clegg, *Crystal Structure Determination*, Oxford University Press, New York, **1998**
7. P. Lightfoot, *Characterisation of Materials*, University of St Andrews, **2001**
8. (a) H. M Reitveld, *J. Appl. Chem.*, **1969**, 2, 65 (b) A. Le Bail, *J. Solid St. Chem.*, **1989**, 83, 267-271
9. P. Coppens, *Synchrotron Radiation Crystallography*, Academic Press, London, **1992**
10. P. S. Wheatley, *The Synthesis of Microporous Materials using Aza Macrocycles as Structure Directing Agents*, University of St Andrews, **2003**

11. R. Bachmann, H. Kohler, H. Schulz & H.-P. Weber, *Acta. Cryst.*, **1985**, *A41*, 35-40
12. CCLRC Daresbury Synchrotron Radiation Source website: www.srs.ac.uk/src

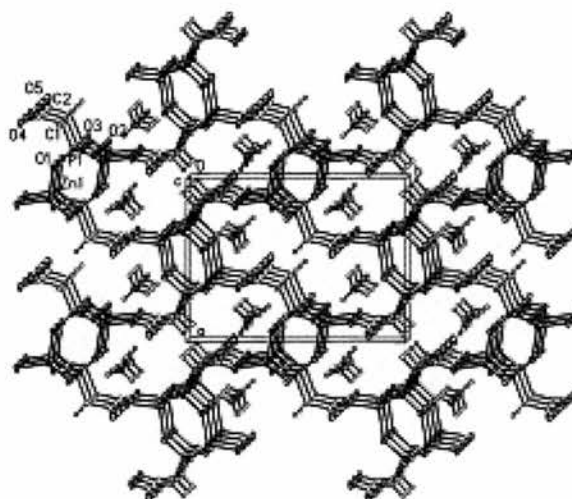
3. Eutectic Mixtures in the Synthesis of Coordination Polymers

3.1 Introduction

Conventionally porous coordination polymers are prepared using either hydrothermal, solvothermal or room temperature diffusion techniques. Finding new methodologies to form these materials may result in the formation of novel framework topologies. Furthermore, it may be possible to impart more rational design into the process of making new materials. Ionothermal synthesis, a novel method of making porous materials by using ionic liquids and eutectic mixtures as solvent and template, is an attractive route to these goals. Since there are fewer interactions between the framework building species and water, the interactions with the other species in the reaction mixture are more important.

At the time of writing the only reported use of ionothermal synthesis to prepare a porous coordination polymer was in the synthesis of $Zn(O_3PCH_2CO_2)NH_4$ (figure 3.1.1) by Liao *et al* [1]. The eutectic mixture prepared by mixing urea and choline chloride was used as the solvent and partial decomposition of the urea to ammonium cations during the synthesis provided the template for the framework. No framework was formed at ambient temperature suggesting that the conditions in the autoclave during ionothermal synthesis were responsible for the break-up of the urea.

Figure 3.1.1 $Zn(O_3PH_2CO_2) \cdot NH_4$ framework [1]

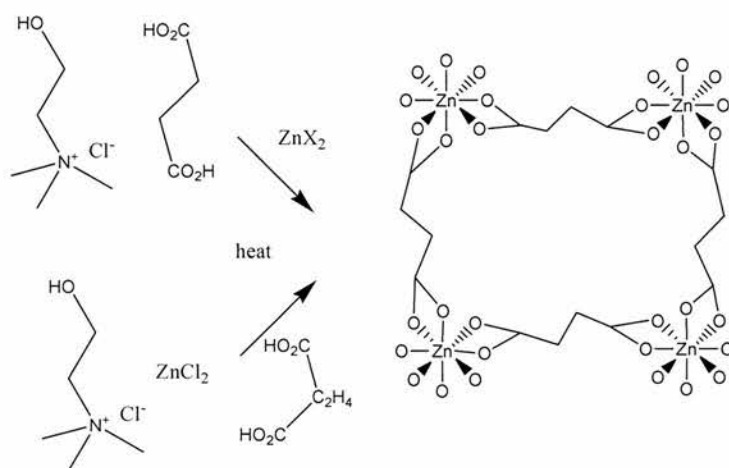


This chapter is concerned with the use of eutectic mixtures to prepare porous coordination polymers through two different methodologies. The first uses one of the components of the eutectic mixture itself to form part of the coordination polymer framework. The second method uses a eutectic mixture in the preparation of metal-phosphonate and metal-carboxylate frameworks where the eutectic mixture either remains intact throughout the reaction or decomposes to contribute to the formation of a porous framework.

The most commonly studied coordination polymers consist of an organic molecule functionalised with carboxylic acid groups that coordinate to transition metal clusters. Eutectic mixtures can be prepared from di- and tri-carboxylic acid containing molecules and choline chloride [2]. The reaction of these solvents with a transition metal salt was studied to see if this would result in the carboxylic acid containing molecule coming out of solution to form the organic part of a metal-organic framework (figure 3.1.2).

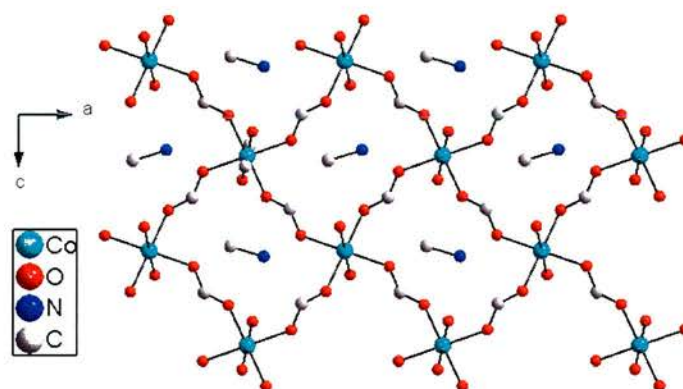
Similarly, the zinc chloride/choline chloride eutectic mixture was studied in the same way [3]. This time, however, an organic molecule with groups that could coordinate to a metal was added in an attempt to form a coordination polymer with organic molecules linked by zinc clusters (figure 3.1.2).

Figure 3.1.2 *Coordination Polymer Synthesis from Eutectic Mixtures Schematic*



The decomposition of urea in coordination polymer synthesis using eutectic mixtures was previously utilised to form a template. Here it was investigated whether it could be used to form part of the actual framework. A very similar break-up of N-methylformamide (NMF) has been observed in the formation of a porous cobalt-formate framework templated by methyl ammonium prepared by Mike Friel in St Andrews in 2004 (figure 3.1.3). In this case the NMF supplies both the formate and the methyl ammonium ions, so it was thought that a similar thing might happen with urea [4].

Figure 3.1.3 Crystal Structure of cobalt-formate framework templated by methyl ammonium [4]



Also in this chapter the use of eutectic mixtures as solvent in the synthesis of metal-phosphonate frameworks and metal-carboxylate frameworks is studied. Diphosphonic acids containing benzene rings and benzene dicarboxylic acid were chosen as building blocks as the benzene rings impart rigidity and a precisely defined shape into the structure. Interactions between aromatic rings and guest molecules can also give these materials potentially useful properties.

3.2 Experimental

3.2.1 Preparation of Eutectic Mixtures

Eutectic mixtures were prepared by mixing choline chloride with either succinic acid, urea or zinc chloride (x) in the correct ratio.

Eutectic mixture	x	ratio x: choline chloride
EM1	succinic acid	1:1
EM2	succinic acid	2:1
EM3	urea	2:1
EM4	zinc chloride	1:2

3.2.2 Preparation of Coordination Polymers from Eutectic Mixture Components

General method for unsuccessful preparations of metal-succinate frameworks.

Into a Teflon lined autoclave was placed the succinic acid/choline chloride mixture (EM1 or EM2), the transition metal source and in some reactions a base. The autoclave was heated in an oven for a period of days. If a solid product formed it was recovered by dissolving the eutectic mixture in distilled water followed by filtration. It was then washed with distilled water and acetone then air dried. All solid samples were submitted for powder XRD and checked for single crystals.

EM (g)	$\text{MX}_2 \cdot x\text{H}_2\text{O}$ (g, mmol)	T ($^{\circ}\text{C}$)	Time (days)	Result
EM1 (5.04)	$\text{Zn}(\text{OAc})_2 \cdot 2\text{H}_2\text{O}$ (0.25, 1.14)	150	3	no product
EM1 (5.00)	$\text{Zn}(\text{OAc})_2 \cdot 2\text{H}_2\text{O}$ (0.25, 1.14)	200	3	no product
EM1 (5.04)	$\text{Zn}(\text{OAc})_2 \cdot 2\text{H}_2\text{O}$ (2.00, 9.11)	150	3	no product
EM1 (5.09)	$\text{Ni}(\text{OAc})_2 \cdot 4\text{H}_2\text{O}$ (0.26, 1.04)	150	3	no product
EM1 (5.01)	$\text{Ni}(\text{OAc})_2 \cdot 4\text{H}_2\text{O}$ (0.99, 3.98)	150	3	no product
EM1 (5.06)	$\text{Ni}(\text{OAc})_2 \cdot 4\text{H}_2\text{O}$ (2.09, 8.40)	150	3	no product
EM1 (2.48)	$\text{Ni}(\text{OAc})_2 \cdot 4\text{H}_2\text{O}$ (0.75, 3.01)	150	3	no product
EM1 (3.20)	$\text{Ni}(\text{OAc})_2 \cdot 4\text{H}_2\text{O}$ (0.26, 1.04)	110	3	no product
EM1 (3.63)	$\text{Co}(\text{OAc})_2 \cdot 4\text{H}_2\text{O}$ (0.25, 1.00)	110	3	no product
EM1 (3.63)	$\text{Co}(\text{OAc})_2 \cdot 4\text{H}_2\text{O}$ (0.25, 1.00)	110	3	no product
EM1 (2.03)	$\text{Co}(\text{NO}_3)_2 \cdot 6\text{H}_2\text{O}$ (0.20, 0.68)	180	14	no product
EM1 (2.52)	$\text{Mn}(\text{OAc})_2 \cdot 4\text{H}_2\text{O}$ (0.77, 3.14)	150	3	no product
EM1 (5.09)	$\text{Cu}(\text{OAc})_2 \cdot \text{H}_2\text{O}$ (1.47, 7.36)	150	3	no product
EM1 (4.09)	$\text{Cu}(\text{NO}_3)_2 \cdot 6\text{H}_2\text{O}$ (1.47, 6.32)	150	3	no product
EM2 (4.00)	$\text{Cu}(\text{OAc})_2 \cdot \text{H}_2\text{O}$ (0.24, 1.20)	150	3	no product
EM2 (4.02)	$\text{Co}(\text{OAc})_2 \cdot 4\text{H}_2\text{O}$ (0.24, 0.96)	150	3	no product

EM (g)	MX ₂ .xH ₂ O (g, mmol)	Base	T (°C)	Time (days)	Result
EM1 (3.96)	Ni(OAc) ₂ .4H ₂ O (0.25, 1.00)	Pyridine 4 drops	150	3	Green amorphous solid
EM1 (4.09)	Cu(OAc) ₂ . H ₂ O (0.25, 1.25)	Pyridine 4 drops	150	3	no product
EM1 (2.56)	Cu(OAc) ₂ . H ₂ O (0.25, 1.25)	Et ₃ N (0.1 ml)	110	3	no product
EM2 (4.06)	Cu(OAc) ₂ . H ₂ O (0.25, 1.25)	NaOH 3M 0.26 ml	150	3	no product
EM2 (4.02)	Co(OAc) ₂ .xH ₂ O (0.25, 1.00)	NaOH 3M 0.25 ml	150	3	no product

Copper-succinate framework. Into a Teflon lined autoclave was placed the succinic acid/choline chloride eutectic mixture (2.5 g, 9.62×10^{-3} mol), copper acetate monohydrate (0.25 g, 1.25×10^{-3} mol), sodium hydroxide (0.20 g, 5.00×10^{-3} mol) and water (0.11 g, 6.11×10^{-3} mol). The autoclave was heated at 110 °C for 2 days. The green crystalline product was recovered by dissolving the eutectic mixture in water followed by filtration. It was then washed with distilled water and acetone then air dried.

General method for unsuccessful preparations of a cobalt-formate framework. Into a Teflon lined autoclave was placed the urea/choline chloride eutectic mixture, the cobalt source and in some cases an acid. The autoclave was heated in an oven for a period of days. If a solid product formed it was recovered by dissolving the eutectic mixture in distilled water followed by filtration. It was then washed with distilled water and acetone then air dried. All solid samples were submitted for powder XRD and checked for single crystals.

EM (g)	MX ₂ .xH ₂ O (g, mmol)	Acid (g)	T (°C)	Time (days)	Result
EM3 (3.00)	Cu(OAc) ₂ .H ₂ O (0.52, 2.60)	none	150	3	Brown amorphous solid
EM3 (3.09)	CoCl ₂ .xH ₂ O (0.50, 3.85)	none	150	3	blue solid
EM3 (2.59)	Co(OAc) ₂ .4H ₂ O (0.25, 1.00)	none	170	3	Green amorphous solid
EM3 (2.44)	Cu(OAc) ₂ .H ₂ O (0.25, 1.25)	none	170	3	No product
EM3 (4.28)	Co(OAc) ₂ .4H ₂ O (0.15, 0.60)	BDC (0.11)	150	3	Grey amorphous solid
EM3 (4.02)	Co(OAc) ₂ .4H ₂ O (0.25, 1.00)	H ₃ PO ₄ (0.18)	150	3	Blue solid
EM3 (4.21)	CoCl ₂ .xH ₂ O (0.25, 3.85)	H ₃ PO ₄ (~0.18)	150	3	Blue amorphous solid
EM3 (3.82)	Co(OAc) ₂ .4H ₂ O (0.21, 0.84)	1M HCl (~0.1)	150	3	green amorphous solid

Unsuccessful preparation of a zinc-bipyridine framework. Into a Teflon lined autoclave was placed the zinc chloride/choline chloride eutectic mixture (EM3) (4.00 g) and bipyridine (0.23 g, 1.47×10^{-3} mol). The autoclave was heated at 150 °C for 3 days. The product was recovered by dissolving the eutectic mixture in distilled water followed by filtration. It was then washed with distilled water and acetone then air dried.

3.2.3 Preparation of Diphosphonic Acid Containing Molecules

(4,4'-Diphenylene-dimethylene)diphosphonic acid was synthesised and supplied by Dr Paul Wheatley.

p-Xylylene di-isopropylphosphonate. p-Xylylene dibromide (4.95 g, 1.90×10^{-2} mol) was refluxed in tri-isopropyl phosphite (50 ml) for 6 hours. The reaction was cooled and petroleum ether was added to form the product as a white precipitate (6.39 g, 78 %). ^1H NMR (CDCl_3 , 300 MHz): δ_{H} 1.16 (12H, d, J_{H} 6.144, CH_3), 1.26 (12H, d, J_{H} 6.144, CH_3), 3.07 (4H, d, J_{H} 19.970, CH_2), 4.59 (4H, m, CH) and 7.23 (4H, m, ArH). ^{13}C NMR (CDCl_3 , 75 MHz) δ_{C} 23.83 (2C, CH_3), 24.03 (2C, CH_3), 35.35 (2C, CH_2), 70.46 (2C, CH), 129.86 (4C, aryl-CH) and 130.40 (2C, aryl-C). ^{31}P NMR (CDCl_3 , 121 MHz) δ_{P} 25.75 (2P, m, CH_2P). CHN (calc): 55.23 (55.29) C, 8.32 (8.35) H.

p-Xylylene diphosphonic acid. p-xylylene di-isopropylphosphonate (2.80 g, 6.45×10^{-3} mol) was refluxed in concentrated hydrochloric acid (20 ml) for 4 hours. The product, which had formed as a white precipitate was recovered by filtration, washed with cold water and air dried (1.45 g, 85 %). ^1H NMR (DMSO, 300 MHz): δ_{H} 2.90 (4H, d, J_{H} 19.97, CH_2) and 7.14 (4H, s, ArH). ^{31}P NMR (DMSO, 121 MHz) δ_{P} 22.30 (2P, t, J_{P} 18.93, CH_2P). CHN (calc): 36.25 (36.11) C, 4.47 (4.54) H.

3.2.4 Preparation of Metal-Phosphonate Frameworks

Cobalt-dibenzyldiphosphonate framework. Into a Teflon lined autoclave was placed the urea/choline chloride eutectic mixture (5 g), (4,4'-diphenylylene-dimethylene)diphosphonic acid (0.12 g, 4.44×10^{-4} mol) and cobalt acetate tetrahydrate (0.25 g, 1.00×10^{-3} mol). The autoclave was heated at 150 °C for 3 days. The purple solid product was recovered by dissolving the eutectic mixture in distilled water followed by filtration. It was then washed with distilled water and acetone and finally air dried.

Nickel-dibenzyldiphosphonate framework. Into a Teflon lined autoclave was placed the succinic acid/choline chloride eutectic mixture (5 g), (4,4'-diphenylylene-dimethylene)diphosphonic acid (0.13 g, 4.81×10^{-4} mol) and nickel acetate tetrahydrate (0.23 g, 9.24×10^{-4} mol). The autoclave was heated at 150 °C for 3 days. The yellow solid product was recovered by dissolving the eutectic mixture in distilled water followed by filtration. It was then washed with distilled water and acetone and finally air dried.

Nickel-benzyldiphosphonate framework. Into a Teflon lined autoclave was placed the succinic acid/choline chloride eutectic mixture (4 g), p-xylylene diphosphonic acid (0.11 g, 6.47×10^{-4} mol) and nickel acetate tetrahydrate (0.16 g, 6.43×10^{-4} mol). The autoclave was heated at 180 °C for 3 days. The yellow solid product was recovered by dissolving the eutectic mixture in distilled water followed by filtration. It was then washed with distilled water and acetone and finally air dried.

To confirm that the p-xylylenediphosphonate was still intact the framework was destroyed in 6M hydrochloric acid. The white residual solid was then submitted for ^1H NMR. ^1H NMR (DMSO, 300 MHz): δ_{H} 2.90 (4H, d, J_{H} 19.97, CH_2) and 7.14 (4H, s, aryl-H).

Cobalt-benzylidiphosphonate framework. Into a Teflon lined autoclave was placed the urea/choline chloride eutectic mixture (4 g), p-xylylene diphosphonic acid (0.11 g, 6.47×10^{-4} mol) and cobalt acetate tetrahydrate (0.14 g, 5.62×10^{-4} mol). The autoclave was heated at 180 °C for 3 days. The purple solid product was recovered by dissolving the eutectic mixture in distilled water followed by filtration. It was then washed with distilled water and acetone and finally air dried.

General method for unsuccessful preparations of a porous cobalt-benzylidiphosphonate framework. Into a Teflon lined autoclave was placed the urea/choline chloride eutectic mixture (EM3), p-xylylene diphosphonic acid (P2) and cobalt source. The autoclave was heated in the oven for a period of days. The purple solid product was recovered as before.

E. M. (g)	P2 (g, mmol)	$\text{MX}_2 \cdot x\text{H}_2\text{O}$ (g, mol)	T (°C)	time (days)	Result
EM3 (4.41)	0.10, 0.59	$\text{Cu}(\text{NO}_3)_2 \cdot x\text{H}_2\text{O}$ (0.15, 0.64)	110	3	blue solid
EM3 (4.02)	0.10, 0.59	$\text{Co}(\text{OAc})_2 \cdot 4\text{H}_2\text{O}$ (0.14, 0.56)	150	14	purple solid
EM3 (4.01)	0.01, 0.59	$\text{Co}(\text{OAc})_2 \cdot 4\text{H}_2\text{O}$ (0.14, 0.56)	150	28	purple solid
EM3 (1.00)	0.08, 0.47	$\text{Co}(\text{NO}_3)_2 \cdot 6\text{H}_2\text{O}$ (0.09, 0.31)	110	3	purple solid
EM3 (1.00)	0.10, 0.59	$\text{Co}(\text{NO}_3)_2 \cdot 6\text{H}_2\text{O}$ (0.15, 0.52)	110	15	purple solid

3.2.5 Preparation of Metal-Dicarboxylate Framework

Chain Cu-BDC framework. Into a Teflon lined autoclave was placed the urea/choline chloride eutectic mixture (4 g), benzene-1,4-dicarboxylic acid (0.10 g, 6.02×10^{-4} mol) and copper nitrate hydrate (0.23 g, 9.89×10^{-4} mol). The autoclave was heated at 110 °C for 3 days. The blue/purple crystalline product was recovered as before.

Attempted preparation of a porous Cu-BDC framework (general procedure as above):

E. M. (g)	BDC (g, mmol)	Cu(NO ₃) ₂ .xH ₂ O (g, mmol)	T (°C)	Time (days)	Result
EM3 (4.32)	0.20, 1.20	0.22, 0.95	110	3	Cu-BDC chain framework
EM3 (4.17)	0.10, 0.60	0.23, 0.99	150	3	no solid

3.3 Results and Discussion

3.3.1 Coordination Polymers from Eutectic Mixture Components

It was expected that simply heating a dicarboxylic acid/choline chloride eutectic mixture in an autoclave with a transition metal salt would result in the formation of a coordination polymer. However, despite trying a variety of metal salts and conditions this did not prove to be the case, with either nothing or amorphous materials being formed. This may be because the interactions between the two components of the

eutectic mixture are too strong to allow for one of them to leave the mixture and form a coordination polymer. Alternatively, the lack of coordination polymer formation may have been due to the carboxylic acid protons not being removed to form carboxylate groups, essential for coordination polymer synthesis.

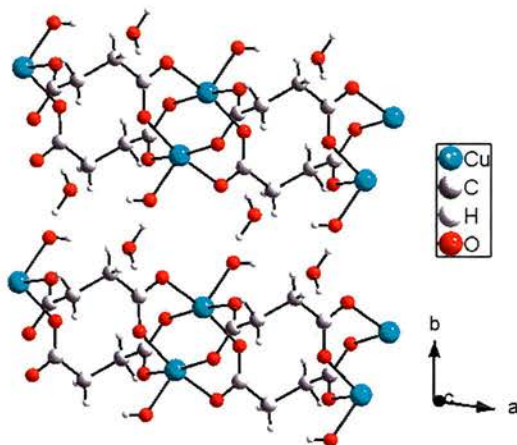
It was therefore thought that an additional reactant would have to be added to form a coordination polymer. It was anticipated that addition of a base would disrupt the hydrogen bonding in the eutectic mixture as some of the carboxylic acids would be deprotonated. This would result in re-equilibration and a metal-organic framework to be formed. Deprotonation of some of the carboxylic acids would also aid in their coordination to the metal centre.

The addition of triethylamine or pyridine, which are common basic additives in coordination polymer synthesis, did not produce any favourable results. However, the addition of sodium hydroxide solution when copper acetate hydrate was used as the metal source and heating at 110 °C for three days resulted in the formation of a green crystalline material. The unit cell of this material was obtained from single crystal data at the synchrotron radiation source at Daresbury [5] and was found to be the same as a material reported by Ang *et al* ($a = 6.4370 \text{ \AA}$, $b = 7.6230 \text{ \AA}$, $c = 8.0810 \text{ \AA}$, $\alpha = 103.90^\circ$, $\beta = 73.50^\circ$, $\gamma = 98.62^\circ$; space group: P-1; crystal system: triclinic) [6].

The structure consists of chains where slightly distorted square pyramidal copper centres are bridged by two succinate ligands, coordinated in the equatorial environments (figure 3.3.1). A water molecule occupies the axial position. Hydrogen

bonding between coordinated and guest water molecules and the oxygen atoms of the carboxylates hold the chains together.

Figure 3.3.1 Crystal Structure of the known Cu-succinate framework [6] prepared using a eutectic mixture



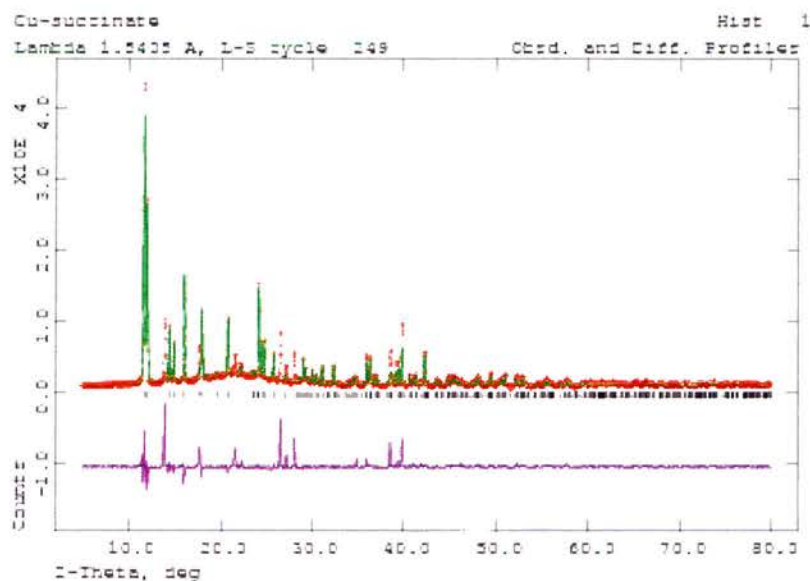
The method reported by Ang *et al* involved dissolving succinic acid in a sodium hydroxide solution then adding copper acetate dihydrate and 2-pyridinemethanol. A precipitate was formed, which was removed by filtration and the crystals were obtained by slow evaporation of the filtrate at room temperature. Doubling the amount of 2-pyridinemethanol resulted in the formation of another framework where the 2-pyridinemethanol was part of the structure. Ang states that the 2-pyridinemethanol acts as a buffer in the structure where it is not coordinated, so it may be that eutectic mixture conditions give a similar pH.

The structure contains a lot of water, which may have come from the water in the copper source or from the sodium hydroxide solution. The molar ratio of eutectic mixture to water in the reaction mixture is not that high (1.57:1) so the product has

not formed under true ionothermal conditions. There is also the possibility that the structure is not formed during heating in the autoclave but is formed when the eutectic mixture is dissolved in water prior to filtration. To test for this the reaction was carried out as normal but the eutectic mixture was dissolved in ethanol. The resultant product was not the same material so it seems likely that this copper succinate framework was not formed ionothermally.

To check if the sample was phase pure a powder x-ray pattern was collected from 5 to 80 °C on a STOE stadip diffractometer using Cu K_{α1} radiation. Le Bail fitting of the pattern in triclinic P-1 did not satisfactorily model all the observed peaks, implying that even though the majority of the product was the Cu-succinate chain framework there was another crystalline material in the sample (wRp = 17.47 %, $\chi^2 = 56.70$). This was expected as the sample could be seen to not be a homogeneous green colour.

Figure 3.3.2 Plot of the Reitveld refinement of the PXRD Pattern of the Cu-succinate framework. The red crosses are of the observed powder pattern and the green line is the calculated powder pattern. The purple line shows the difference between the observed and calculated patterns.



Simply heating the urea/choline chloride eutectic mixture with a metal salt was unsuccessful in forming a coordination polymer. It may be that adding an extra reagent would help achieve the desired result but reactions performed with the addition of acids did not result in any crystalline materials. Substituting the urea for a urea derivative such as methylurea, which would break-up to form methylamine, and make the system closer to that which resulted in the cobalt-formate framework described earlier may also produce better results.

Only one reaction was performed with the zinc chloride/choline chloride eutectic mixture. Bipyridine was chosen as the organic building block as it was thought that a carboxylic acid containing molecule may prefer to form a eutectic mixture with the choline chloride rather than a coordination polymer with the zinc chloride. A

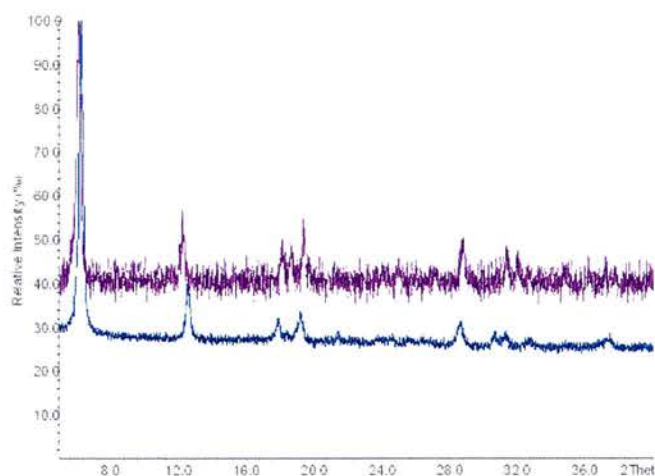
crystalline material was not formed but further studies into this system may result in the formation of a coordination polymer.

3.3.2 Metal-Phosphonate Frameworks

The zinc phosphonate/carboxylate prepared by Liao *et al* in urea/choline chloride showed that eutectic mixtures could be used as the solvent in coordination polymer synthesis. Therefore it was expected that the technique could be used to prepare porous metal-phosphonates containing aromatic rings. (4,4'-Diphenylene-dimethylene)diphosphonic acid had been used by Dr Paul Wheatley to prepare a cobalt-dibenzoyldiphosphonate structure (figure 3.3.4). The reaction was carried out in an autoclave in a water/methanol mixture with cobalt acetate tetrahydrate as the cobalt source. This resulted in a purple powder containing small needle single crystals (unit cell: $a = 5.1715 \text{ \AA}$, $b = 9.3854 \text{ \AA}$, $c = 15.6294 \text{ \AA}$, $\alpha = 103.36^\circ$, $\beta = 93.02^\circ$, $\gamma = 98.68^\circ$; space group: P-1; crystal system: triclinic).

By changing the solvent to urea/choline chloride it was possible to prepare the same material. However, the purple powder was not highly crystalline and did not contain any single crystals. Comparison of each of the two materials' powder x-ray diffraction patterns by eye confirmed they were the same material but this could not be proved satisfactorily by Reitveld refinement due to the poor quality of the PXRD data (figure 3.3.3). Furthermore, the peaks are not in exactly the same positions. This may be due to some residual solvent distorting the structure.

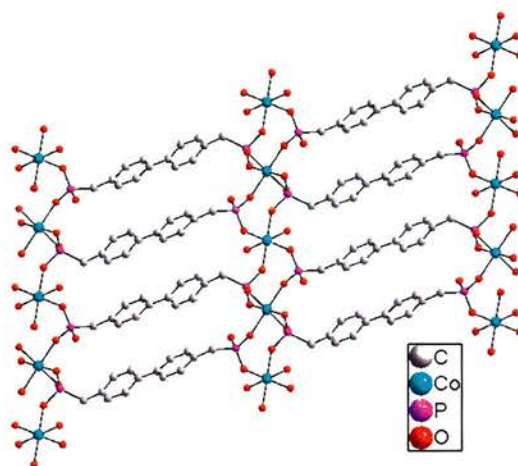
Figure 3.3.3 PXRD Patterns of Co-dibenzoyldiphosphonate prepared solvothermally (purple) and ionothermally (blue).



The structure consists of layers of cobalt oxide octahedra pillared by layers of the dibenzoyldiphosphonate (figure 3.3.4). Each cobalt atom is coordinated to six oxygens belonging to phosphate groups. From the single crystal data it can be seen that the benzene rings may be able to rotate.

Further characterisation of this material was not possible as a highly crystalline, phase pure sample was not obtained. Although the layered structure was the only crystalline phase present much of the sample was amorphous powder.

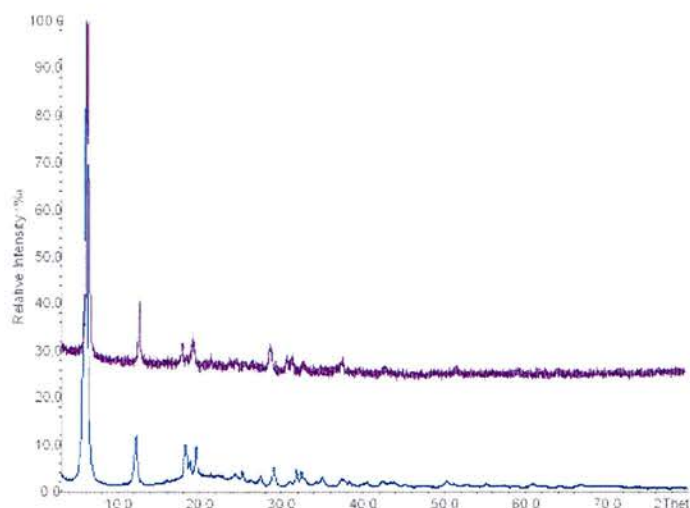
Figure 3.3.4 Crystal Structure of Co-dibenzoyldiphosphonate framework



There was no ammonia like smell from the cooling autoclaves (characteristic of the break-up of urea), suggesting that the eutectic mixture remained intact throughout the reaction. If it had broken up it may have acted as a space filler between the phosphonate molecules, resulting in the formation of a porous solid. It may be that the π - π interactions between the benzene rings are too strong for it to make a difference, although there are many examples of porous metal-organic frameworks containing aromatic rings suggesting this is not the case [7].

By changing the solvent to succinic acid/choline chloride it was possible to prepare a nickel analogue of this material. Even though this material also contained no single crystals it was much more crystalline than the cobalt version, however a Reitveld refinement was still not possible.

Figure 3.3.5 PXRD Patterns of Co-dibenzylidiphosphonate (purple) and Ni-dibenzylidiphosphonate (blue)

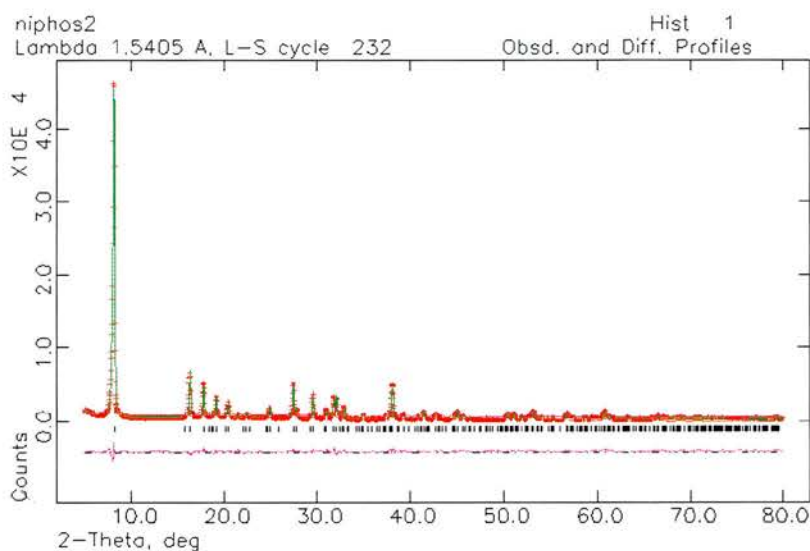


A p-xylylene diphosphonic acid was prepared by first refluxing p-xylylene dibromide in triisopropylphosphite (Arbusov reaction) and then hydrolysing the resulting ester in refluxing concentrated hydrochloric acid. Using this compound nickel- and cobalt- phosphonate structures could be made in the same way as with (4,4'-diphenylenedimethylene)diphosphonic acid. It was expected that an analogue of the dibenzyl structure would be formed except with the organic molecule containing only one benzene ring. Again no single crystals were formed and although the powder XRD patterns of the cobalt and nickel versions showed the same peaks, the nickel containing material was again much more crystalline.

No single crystals were obtained but the sample of the nickel analogue was very crystalline and was suitable for Reitveld refinement. The powder pattern was collected from 5-80° 2 θ on a STOE stadip diffractometer using Cu K α_1 radiation. Le Bail fitting of the pattern in space group Pca2 $_1$ and orthorhombic crystal system, with

a unit cell of $a = 9.4964 \text{ \AA}$, $b = 5.6211 \text{ \AA}$, $c = 21.7589 \text{ \AA}$ gave a reasonable fit ($wRp = 8.02 \%$, $\chi^2 = 4.78$), showing the sample was phase pure and exactly the same as a material synthesised hydrothermally by Stock and Bein in 2002 [8].

Figure 3.3.6 Plot of the Reitveld refinement of the PXRD Pattern of the Ni-benzoyldiphosphonate framework. The red crosses are of the observed powder pattern and the green line is the calculated powder pattern. The purple line shows the difference between the observed and calculated patterns.



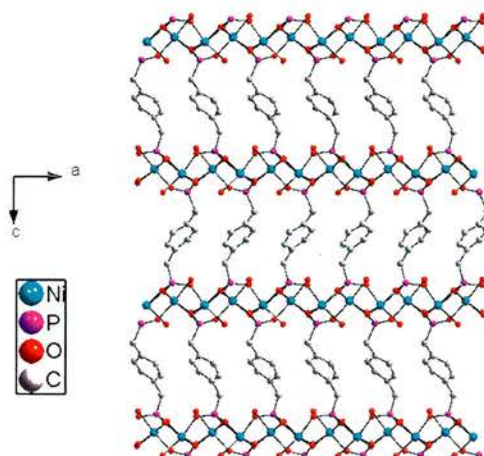
Similar frameworks have also been reported containing lead and copper instead of nickel [9]. The structure is similar to the dibenzoyldiphosphonate framework described above as it consists of layers of metal oxide octahedra pillared by the diphosphonate molecule. However, there are a few significant differences. Firstly, although the metals are also in an octahedral environment one of the ligands is water. A second difference in the metal oxide sheets is their shape: the layers of the dibenzoyldiphosphonate structure are flat whereas the layers of the benzoyldiphosphonate framework have a ‘zig-zag’ topology.

Table 3.3.1 Crystal data and structure refinement for Ni-benzyldiphosphonate framework [8]

Identification code	Ni-benzyldiphosphonate
Empirical formula	(NiPO ₃) ₂ C ₈ H ₈ 2H ₂ O
Temperature	298 K
Wavelength	1.54051 Å
Crystal system, Space Group	Orthorhombic, Pca2 ₁
Unit cell dimensions	A = 9.4964 Å α = 90°.
	B = 5.6211 Å β = 90°.
	C = 21.7589 Å γ = 90°.
Volume	1161.5 Å ³
Z	4
P _{calc} (g cm ⁻³)	2.369
Profile range	5 ≤ 2θ ≤ 80
No. of data points	3749
Obs. Reflections	431
Atomic Parameters	60
Profile Parameters	8
R values	wR _p = 0.0802
	R _p = 0.595
	R _F = 0.1290

Another significant difference between the two frameworks is the directions that the organic pillars are facing. The dibenzyldiphosphonates are all at the same angle from the metal-oxide layer whereas the layers of benzyldiphosphonates alternate between two different directions.

Figure 3.3.7 Crystal structure of Ni-benzylidiphosphonate framework



To further confirm that the two structures were the same the nickel product was added to 6M hydrochloric acid to dissolve the metal and leave the p-xylylene diphosphonic intact for solution NMR. This would prove that the diphosphonic acid was still intact in the framework. This procedure resulted in the hydrochloric acid turning green and the formation of a residual white solid. The ^1H NMR of this solid confirmed it was the p-xylylene diphosphonic acid. Furthermore, to verify that water was coordinated to the nickel and cobalt FTIR spectra were obtained. Both the cobalt and nickel analogues showed spectra similar to that of the frameworks reported and the expected signal of the $\delta\text{M-O-H}$ vibration ($\sim 605\text{ cm}^{-1}$).

Further attempts to produce a porous material were made using this diphosphonic acid, a cobalt source, the urea/choline chloride eutectic mixture and by changing the reaction conditions. It was expected that by making the reaction conditions closer to those of Liao *et al* that the urea would break-up and form a spacer between the benzene rings and a porous material would result. The quantity of solvent was reduced from four grams to one gram and cobalt nitrate was substituted for cobalt

acetate. However, despite an ammonia-like smell being produced on cooling of the autoclaves, the resulting framework was found to be the same as before.

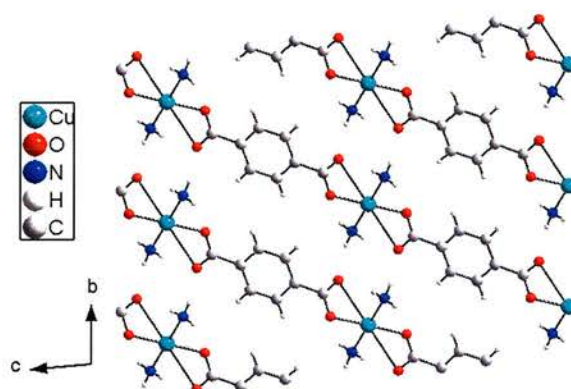
It was also anticipated that a longer reaction time could result in the formation of a porous solid. It was thought that longer reaction times might have resulted in more urea break-up and therefore more chance of the decomposition product acting as a template or spacer between the benzyldiphosphonates. It was also postulated that the general topology might change from the hydrophobic areas and hydrophilic areas being separated into layers into another type of framework. Unfortunately, all attempts resulted in the same non-porous, layered structure being formed.

3.3.3 Metal-Dicarboxylate Framework

In addition to phosphonic acid building blocks, reactions were also performed using benzene-1,4-dicarboxylic acid (BDC). By reacting with copper nitrate in the urea/choline chloride eutectic mixture at 110 °C a dark blue/purple crystalline material was formed. The unit cell ($a = 4.0900 \text{ \AA}$, $b = 6.0370 \text{ \AA}$, $c = 9.8200 \text{ \AA}$, $\alpha = 93.57^\circ$, $\beta = 99.19^\circ$, $\gamma = 100.16^\circ$; space group: P-1; crystal system: triclinic) was determined from a single crystal at the synchrotron radiation source at Daresbury [5] and was found to be the same as that of a material already reported by Zimmermann *et al* [10].

The structure consists of chains of BDC molecules linked through the equatorial sites of octahedral copper ions (figure 3.3.8). The axial sites are occupied by ammonia ligands. The chains are held in place by hydrogen bonding between the N-H of the ammonia molecules and an oxygen of the benzenedicarboxylate ligand.

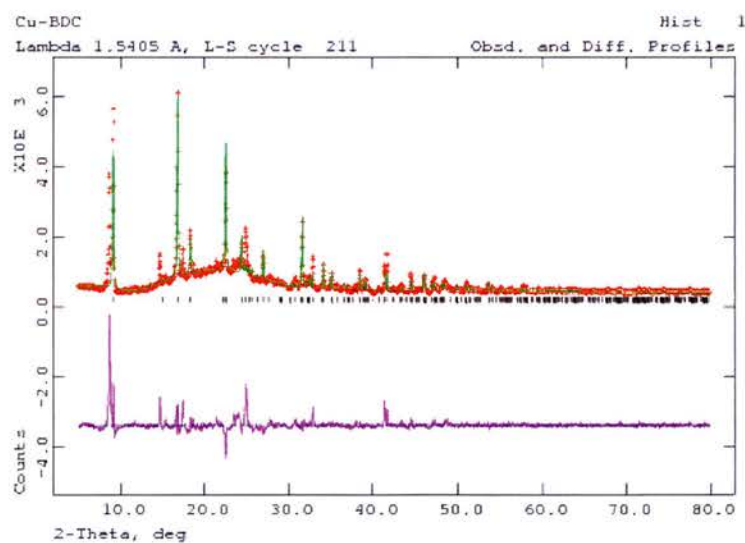
Figure 3.3.8 Crystal Structure of Cu-benzenedicarboxylate framework



The method used to prepare this material is very different from that reported by Zimmermann *et al.* Their procedure consisted of combining copper nitrate hydrate and benzenedicarboxylic acid in methanol and an aqueous ammonia solution and allowing the solvent to evaporate. If the structure prepared by the ionothermal route is exactly the same as that prepared by Zimmermann *et al* it implies that the urea has broken down during synthesis to provide the ammonia ligands. The eutectic mixture is therefore incorporated into the structure, which was a main aim of this work. It is anticipated that changing the reaction conditions may result in a porous framework templated by ammonia or ammonium. However, initial attempts at changing the reactant ratios and the reaction temperature proved to be unsuccessful.

To check if the sample was phase pure a powder x-ray pattern was collected from 5 to 80 °C on a STOE stadip diffractometer using Cu K_{α1} radiation. Le Bail fitting of the pattern in triclinic P-1 did not satisfactorily model all the observed peaks, implying that even though the majority of the product was the Cu-BDC chain framework there was another crystalline material in the sample (wRp = 15.77 %, $\chi^2 = 16.36$). This was expected as the sample could be seen to not be a homogenous blue colour. However purification of the sample by sonification was not possible as this resulted in transformation of the product to an unknown green phase.

Figure 3.3.9 Plot of the Reitveld refinement of the PXRD Pattern of the Cu-BDC framework. The red crosses are of the observed powder pattern and the green line is the calculated powder pattern. The purple line shows the difference between the observed and calculated patterns.



3.4 Conclusion

It has been demonstrated that eutectic mixtures can be utilised in the preparation of coordination polymers, either as the reaction solvent or part of the coordination polymer framework. It is not possible to form frameworks just by mixing succinic acid/choline chloride with a metal salt. This is probably due to the pH of the reaction mixture. Adding a base to the mixture does result in the formation of a framework, although the use of aqueous sodium hydroxide means the reaction does not take place under ionothermal conditions. Further studies need to be undertaken to see if a framework can be formed whilst retaining the ionothermal nature of the synthesis.

The synthesis of metal-diphosphonate frameworks is possible under ionothermal conditions. No novel frameworks were formed, which indicates that the eutectic mixture is acting similarly to a normal solvent and not affecting the reaction that much. However, a copper-benzenedicarboxylate framework was formed under ionothermal conditions where the eutectic mixture directly contributed to the formation of the coordination polymer. The framework contained ammonia ligands that were a result of the urea decomposing during the reaction

Even though no porous coordination polymers were formed using a eutectic mixture in this study other studies have shown it to be possible to do so. Therefore, by altering more reaction variables novel porous materials may potentially be formed using the organic building units studied in this chapter. Otherwise, there are many

other organic building blocks that can be used that might give novel framework topologies when reacted under ionothermal conditions.

3.5 References

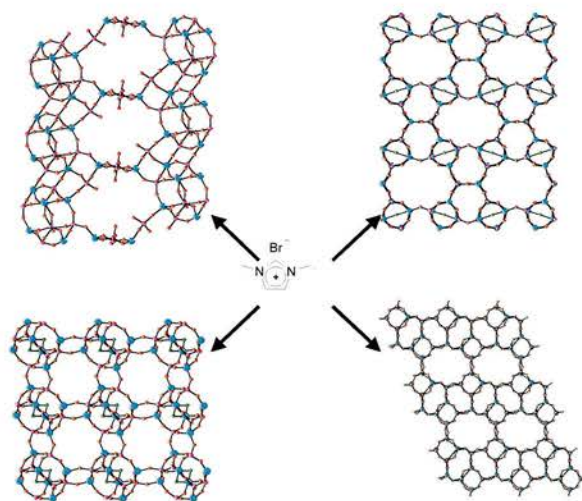
1. J.-H. Liao, P.-C. Wu and Y.-H. Bai, *Inorg. Chem. Commun.*, **2005**, 8, 390-392
2. A. P. Abbott, D. Boothby, G. Capper, D. L. Davies and R. K. Rasheed, *J. Am. Chem. Soc.*, **2004**, 126, 9142-9147
3. A. P. Abbott, G. Capper, D. L. Davies & R. Rasheed, *Inorg. Chem.*, **2004**, 43, 3447-3452
4. M. Friel, *Metal Organic Frameworks for the Generation, Storage and Delivery of Nitric Oxide*, University of St Andrews, **2004**
5. CCLRC Daresbury Synchrotron Radiation Source website: www.srs.ac.uk/src
6. S. G. Ang, B. W. Sun and S. Gao, *Inorg. Chem. Commun.*, **2004**, 7, 795-798
7. (a) N. L. Rosl, J. Eckert, M. Eddaoudi, D. T. Vodak, J. Kim, M. O'Keeffe & O. M. Yaghi, *Science*, **2003**, 300, 1127 (b) H. K. Chae, D. Y. Siberio-Pérez, J. Kim, Y. Go, M. Eddaoudi, A. J. Matzger, M O'Keeffe & O. M. Yaghi, *Nature*, **2004**, 427, 523 (c) S. Subramanian & M. J. Zaworotko, *Angew. Chem. Int. Ed. Eng.*, **1995**, 34, 2127
8. N. Stock & T. Bein, *J. Solid St. Chem.*, **2002**, 167, 330-336
9. (a) E. Irran, T. Bein & N. Stock, *J. Solid St. Chem.*, **2003**, 173, 293-298 (b) D. Riou, F. Belier, C. Serre, M. Nogues, D. Vichard & G. Férey, *Int. J. Inorg. Mater.* 2, **2000**, 29-33
10. B. Paul, B. Zimmermann, K. M. Fromm and C. Janiak, *Zeitschrift Fur Anorganische Und Allgemeine Chemie*, **2004**, 630, 1650-1654

4. Eutectic Mixtures in the Synthesis of Aluminium Cobalt Phosphate Frameworks

4.1 Introduction

It was reported in 2004 by Morris *et al* that novel porous aluminophosphate frameworks could be prepared by using ionic liquids as both the reaction solvent and template (figure 4.1.1) [1]. This new methodology was termed ionothermal synthesis and has numerous advantages over the conventional hydrothermal route to zeolitic frameworks. Firstly, because the ionic liquid can act as both solvent and template there is no competition between the solvent and template to direct the structure, possibly allowing for closer templating. Therefore there is an increased possibility of novel framework topologies being formed and more rational design of zeolitic materials.

Figure 4.1.1 AlPO frameworks from ionic liquids as solvent and template [1]. Blue, pink and red spheres correspond to aluminium, phosphorus and oxygen respectively.



Furthermore, as ionic liquids have a vanishingly low vapour pressure it can be possible to perform the synthesis of porous frameworks in an open flask. This eliminates the safety concerns over autoclave synthesis where high pressures can be built up during the reaction. Other advantages are that ionic liquids can have unusual solvation properties and that it is potentially possible to synthesise 10^{18} ionic liquids compared to around six hundred conventional solvents, therefore also increasing the probability of novel frameworks being formed.

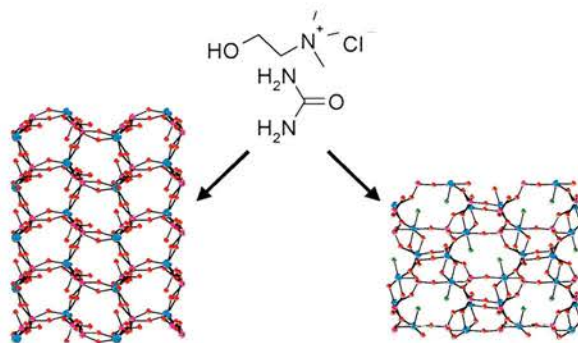
Morris *et al* furthered this work by reporting the synthesis of a layered aluminophosphate material (termed SIZ-6) and three aluminium cobalt phosphate frameworks (SIZ-7, SIZ-8 and SIZ-9) [2]. Each of the frameworks was prepared using 1-ethyl-3-methylimidazolium bromide as solvent and template. The only other zeolitic materials to be made in this way were reported by Xu *et al* in 2005 [3]. The ionic liquids 1-ethyl-3-methylimidazolium bromide and 1-hexyl-3-methylimidazolium bromide were used in the synthesis of silicoaluminophosphate frameworks with the AEL topology, which was carried out at atmospheric pressure in a round-bottomed flask.

Also reported by Morris *et al* was the use of a eutectic mixture as solvent and template in the formation of a porous aluminophosphate (figure 4.1.2) [1]. This methodology was also included in the definition of ionothermal synthesis due to the ionic character of eutectic mixtures. A novel framework with an interrupted structure was synthesised using a urea/choline chloride mixture as the solvent. It was expected that the quaternary amine choline chloride would act as the template however the

template was found to be ammonium, formed *in situ* from the partial decomposition of the urea.

In the same paper the synthesis of the non-zeolitic framework AIPO-CJ2 was reported, prepared with the addition of fluoride, again with ammonium as the template (figure 4.1.2). These results suggest that in these systems ammonium formed *in situ* is the preferred template over choline. Therefore, to prepare a framework templated by choline an alternative to urea has to be used.

Figure 4.1.2 AIPO frameworks from eutectic mixtures as solvent and template [1]. Blue, pink, red and green spheres correspond to aluminium, phosphorus, oxygen and fluoride respectively.



In this chapter the use of carboxylic acid/choline chloride eutectic mixtures as solvent and template in the synthesis of aluminium phosphate materials is studied. It was anticipated that the competition between which molecules would act as template would be removed and new porous frameworks would be formed templated by choline. This is desirable as choline is very cheap and very safe (it is used in baby food), making it an ideal choice of template.

4.2 Experimental

4.2.1 Preparation of Eutectic Mixtures

Eutectic mixtures were prepared by mixing choline chloride with a multi-carboxylic acid containing molecule (x) in the correct ratio.

Eutectic mixture	x	ratio x: choline chloride
EM1	succinic acid	1:1
EM2	glutaric acid	1:1
EM3	citric acid	1:2

4.2.2 Attempted Preparation of Aluminium Phosphate Frameworks

General method for unsuccessful attempts at preparing a porous AIPO. Into a Teflon lined autoclave was placed the succinic acid/choline chloride eutectic mixture (4 g), an aluminium source and phosphoric acid (85 wt% in H₂O). In some reactions cyclam or cobalt acetate tetrahydrate was also added to the reaction mixture. The autoclave was heated in the oven for 3 days. The white solid product was recovered by dissolving the eutectic mixture in distilled water followed by filtration. It was then washed with distilled water and acetone and air dried.

E.M. (g)	Al source (g, mmol)	H ₃ PO ₄ (g, mmol)	Other (g, mmol)	T (°C)	time (days)
EM1 (4.98)	Al(O ⁱ Pr) ₃ (0.11, 0.61)	0.19, 1.65	none	150	3
EM1 (5.08)	Al(O ⁱ Pr) ₃ (0.10, 0.55)	0.17, 1.48	none	180	3
EM1 (4.07)	Al(O ⁱ Pr) ₃ (0.16, 0.88)	0.23, 2.00	Cyclam (0.11, 0.55)	150	3
EM1 (4.22)	Al(O ⁱ Pr) ₃ (0.23, 1.26)	0.32, 2.78	Cyclam (0.25, 1.24)	150	3
EM1 (4.07)	Al(O ⁱ Pr) ₃ (0.10, 0.55)	0.18, 1.56	Cyclam (0.12, 0.60)	180	3
EM1 (4.22)	Al(O ⁱ Pr) ₃ (0.22, 1.21)	0.32, 2.78	Cyclam (0.24, 1.20)	180	3
EM1 (4.12)	Al(O ⁱ Pr) ₃ (0.21, 1.15)	0.31, 2.69	Co(OAc) ₂ .4H ₂ O (0.21, 0.84)	150	3
EM1 (3.95)	Al(O ⁱ Pr) ₃ (0.22, 1.21)	0.29, 2.52	Co(OAc) ₂ .4H ₂ O (0.20, 0.80)	180	3
EM1 (4.03)	Al(OH) ₃ (0.19, 2.44)	0.38, 3.30	none	150	3
EM1 (3.94)	Al(OH) ₃ (0.20, 2.56)	0.37, 3.21	Cyclam (0.12, 0.60)	150	3
EM1 (4.06)	Al(OH) ₃ (0.19, 2.44)	0.36, 3.12	Cyclam (0.12, 0.60)	180	3

4.2.3 Preparation of Aluminium Cobalt Phosphate Frameworks

CoAlPO-1. Into a Teflon lined autoclave was placed the succinic acid/choline chloride eutectic mixture (4 g), aluminium isopropoxide (0.23 g, 1.26×10^{-3} mol), phosphoric acid (0.31 g 85 wt% in water, 2.69×10^{-3} mol), cobalt acetate tetrahydrate (0.20 g, 8.03×10^{-4} mol) and cyclam (0.13 g, 6.49×10^{-4} mol). The reaction mixture was heated at 150 °C for 6 days. The blue solid product was recovered by dissolving the eutectic mixture in distilled water followed by filtration. It was then washed with distilled water and acetone and air dried.

Solution ^1H NMR of the template was obtained by dissolving a sample in hydrochloric acid (0.8 ml, 6 M) and D_2O (4 drops). ^1H NMR (D_2O , 300 MHz): δ_{H} 1.35 (9H, s, CH_3), 2.19 (2H, m, NCH_2) and 2.75 (2H, m, CH_2OH).

CoAlPO-1 could also be prepared under the same conditions except using the glutaric acid/choline chloride (EM2) and citric acid/choline chloride (EM3) eutectic mixtures as solvent.

Attempted CoAlPO-1 synthesis in a round-bottomed flask. Into a round-bottomed flask fitted with a drying tube was placed the succinic acid/choline chloride eutectic mixture (4 g), aluminium isopropoxide (0.23 g, 1.26×10^{-3} mol), phosphoric acid (0.31 g 85 wt% in water, 2.69×10^{-3} mol), cobalt acetate tetrahydrate (0.20 g, 8.03×10^{-4} mol) and cyclam (0.13 g, 6.49×10^{-4} mol). The reaction mixture was stirred and heated at $150\text{ }^\circ\text{C}$ for 7 days. The white solid product was recovered as for before.

CoAlPO-3. Into a Teflon lined autoclave was placed the succinic acid/choline chloride eutectic mixture (4 g) aluminium isopropoxide (0.22 g, 1.08×10^{-3} mol), phosphoric acid (0.32 g 85 wt% in water, 2.78×10^{-3} mol), cobalt acetate tetrahydrate (0.21 g, 8.43×10^{-4} mol) and cyclam (0.15 g, 7.49×10^{-4} mol). The reaction mixture was heated at $180\text{ }^\circ\text{C}$ for 3 days. The blue solid product was recovered by dissolving the eutectic mixture in distilled water followed by filtration. It was then washed with distilled water and acetone then air dried.

Solution NMR of the template was obtained as for the layered CoAlPO structure. ^1H NMR (D_2O , 300 MHz): δ_{H} 1.83 (9H, s, CH_3), 2.13 (2H, m, NCH_2) and 2.69 (2H, m, CH_2OH). ^{13}C NMR (D_2O , 75 MHz): δ_{C} 53.07 (3C, CH_3), 54.83 (1C, NCH_2) and 66.35 (1C, CH_2OH).

CoAlPO-3 could also be prepared under the same conditions except using pyridine instead of cyclam.

4.3 Results and Discussion

4.3.1 Attempted Preparation of Aluminium Phosphate Frameworks

Attempts to synthesis a porous aluminium phosphate framework by simply heating an aluminium and phosphate source in an autoclave with succinic acid/choline chloride were found to be unsuccessful. By using aluminium isopropoxide as the aluminium source an aluminophosphate dense phase was formed, previously reported by Mooney [4]. Switching to aluminium hydroxide as the aluminium source resulted in the formation of the dense phase berlinite [5].

It was therefore thought that choline would not act as a template so to make an open framework another possible template would have to be added. For this the macrocycle cyclam (1,4,8,11-tetraazacyclotetradecane) was chosen. Nitrogen containing macrocycles have been shown to be excellent templates in the synthesis of zeolitic materials due to their size, shape and high charge density [6].

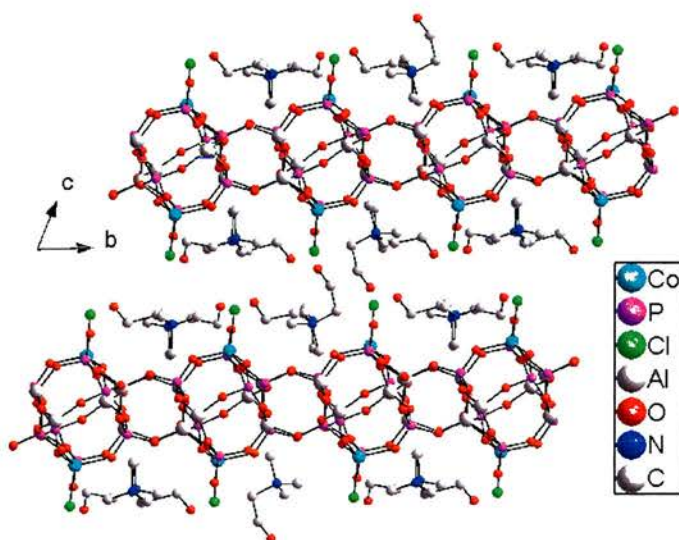
Furthermore, macrocycles with different heteroatoms and ring sizes have varying affinities to metal ions, which may play a role in the crystallisation of transition metal containing zeotypes [7]. With regards to this work, macrocycles have the added advantage over other possible templates in that they are solid rather than liquid. This means that there is no possibility of products forming due to solvothermal reaction conditions, or intermediate conditions, instead of the desired ionothermal conditions.

Cyclam has been used before in the synthesis of zeolitic materials, where it is either located as a template unbound to the framework [8] or is coordinated to a metal in the framework and is part of an inorganic-organic hybrid structure [9]. However, the addition of cyclam to this reaction mixture did not result in the formation of a porous material.

4.3.2 CoAlPO-1

On addition of cobalt acetate tetrahydrate to the reaction mixture as well as the cyclam a blue crystalline solid was formed after heating in an autoclave at 150 °C (figure 4.3.1). This solid, termed CoAlPO-1, was initially thought to be a layered aluminium cobalt phosphate templated by cyclam, however on solution of the structure by single crystal x-ray diffraction the template was found to be choline.

Figure 4.3.1 Crystal Structure of CoAlPO-1 showing layers of CoAlPO separated by a layer of choline molecules.



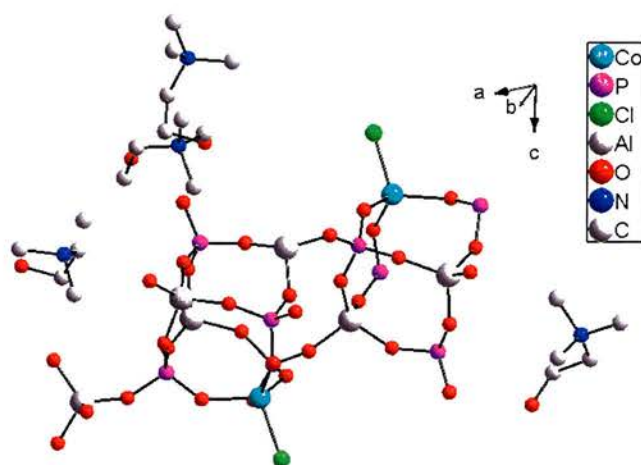
The asymmetric unit of CoAlPO-1 consists of two cobalt, six aluminium, eight phosphorus, thirty-two oxygen and two chlorines, with four choline molecules in ordered positions (figure 4.3.2). The chemical formula is $[\text{Al}_3\text{CoP}_4\text{O}_{16}\text{Cl}]^{2-} \cdot [\text{C}_5\text{H}_{13}\text{NOH}]_2^+$.

Table 4.3.1 Crystal data and structure refinement for CoAlPO-1

Identification code	CoAlPO-1
Empirical formula	$\text{C}_{20}\text{Al}_6\text{Cl}_2\text{Co}_2\text{N}_4\text{O}_{36}\text{P}_8$
Temperature	293(2) K
Wavelength	1.54180 Å
Crystal system, Space Group	Triclinic, P-1
Unit cell dimensions	$A = 14.167(7)$ Å $\alpha = 67.69(6)^\circ$, $B = 15.045(5)$ Å $\beta = 75.26(6)^\circ$, $C = 15.104(3)$ Å $\gamma = 89.65(6)^\circ$.
Volume	$2865.6(18)$ Å ³
Crystal size	0.1 x 0.05 x 0.01 mm ³
Theta range for data collection	3.19 to 68.06°.
Index ranges	-16 ≤ h ≤ 17, -17 ≤ k ≤ 17,

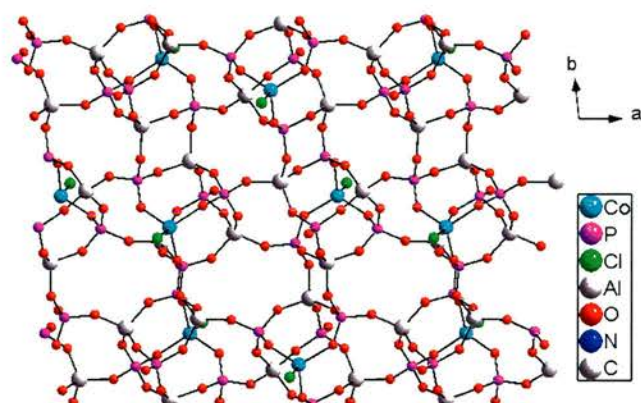
	-17<= <=18
Reflections collected	35630
Completeness to theta = 68.06°	91.3 %
Refinement method	Full-matrix least-squares on F ²
Data / restraints / parameters	9538 / 0 / 703
Goodness-of-fit on F ²	1.710
Final R indices [I>2sigma(I)]	R1 = 0.1869, wR2 = 0.4371
R indices (all data)	R1 = 0.2468, wR2 = 0.5038
Largest diff. peak and hole	1.930 and -1.942 e.Å ⁻³

Figure 4.3.2 Asymmetric unit of CoAlPO-1



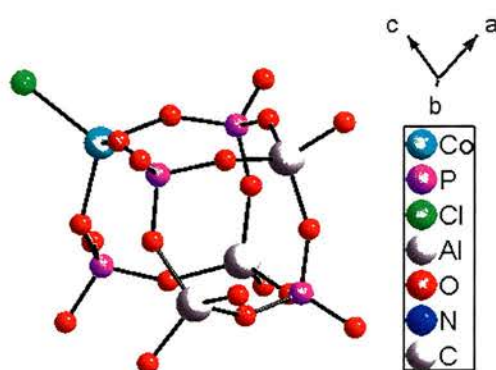
The framework topology is very similar to the layered gallium phosphate material, DMAP-GaPO, reported by Wragg and Morris [10]. It consists of alternating inorganic and organic layers. The secondary building unit (SBU) is a double four-membered ring (D4R) opened out on one edge, linking it to another of the repeating units to form a chain. The chains are linked through phosphorus and aluminium centred tetrahedra to form sheets (figure 4.3.3).

Figure 4.3.3 Crystal structure of CoAlPO-1 showing a CoAlPO sheet



The cobalt atoms are coordinated tetrahedrally to three oxygens and one chlorine. The cobalt-chlorine bond is the first to be found in zeolitic frameworks. This may be due to the conditions in this system being less harsh than conventional zeotype synthesis, where it would have been hydrolysed to a cobalt-oxygen bond. This opens up the opportunity for these bond types to be utilised in some way and also the possibility of more novel bond types in zeolitic materials being formed.

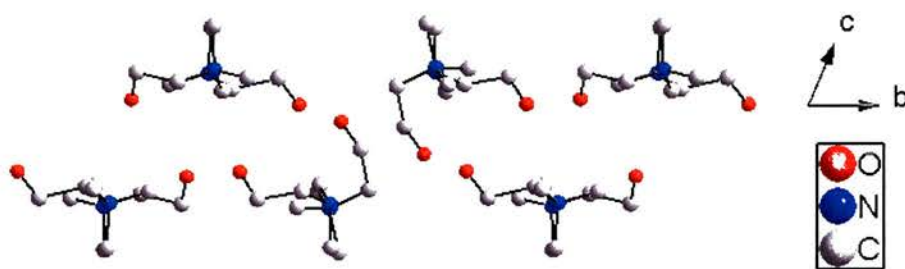
Figure 4.3.4 Crystal structure of the CoAlPO-1 SBU



Often cobalt sites in zeolitic frameworks are disordered, sharing occupancy of aluminium sites. However, in this structure the cobalt is ordered. The cobalt positions are on the corner of every D4R-like unit, with the cobalt-chlorine bond alternating between pointing to the layer above and pointing to the layer below.

Unexpectedly, choline was found to be the template rather than cyclam (figure 4.3.5). It is therefore presumed that the addition of cyclam alters the pH of the reaction mixture to a value more suited to CoAIPO synthesis. There may be competition between the choline and cyclam as to which acts as template, such as the competition between ammonium and choline in the previous AIPO synthesis using this methodology, but in this system choline is the favoured template. This may be due to the formation of hydrogen bonds between the chlorine atoms in the framework and the hydroxide groups of the choline.

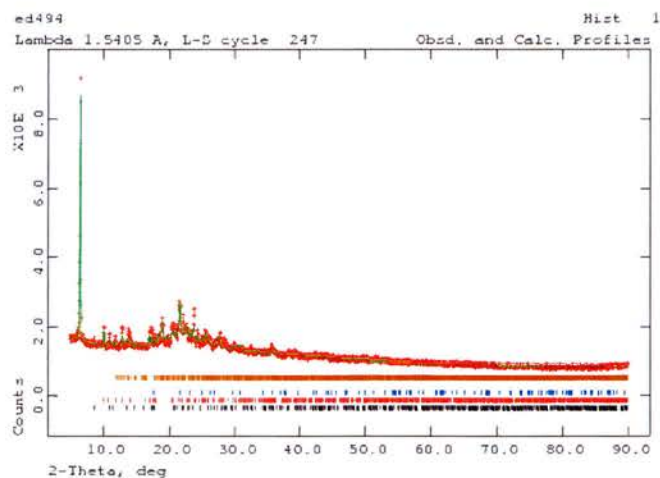
Figure 4.3.5 Crystal structure of the choline layer in CoAIPO-1



The crystal data for CoAIPO-1 collected on the in house diffractometer (Bruker SMART diffractometer with graphite-monochromated Cu K_{α} radiation) is not good due to the small size and weak x-ray scattering of the crystals. Unfortunately better data was not obtained at the SRS so a Reitveld refinement on the powder data was

attempted, although this was complicated as the sample was not phase pure or highly crystalline. The powder x-ray pattern was collected from 5 to 90 °C on a STOE stadip diffractometer using Cu K_{α1} radiation. Le Bail fitting of the pattern in triclinic P-1 did not satisfactorily model all the observed peaks. This was expected as it was known that there were additional phases in the sample. Addition of the aluminophosphate dense phase and two other aluminium cobalt phosphate phases (discussed later) gave a much more reasonable fit (wRp = 4.99 %, $\chi^2 = 2.958$). The liveplot (figure 4.3.6) of the calculated pattern does not match entirely with the observed pattern as some of the modelled peak shapes and heights aren't exact fits to the observed data. However, it confirms that the crystalline material in the sample is mostly CoAlPO-1 and the dense phase.

Figure 4.3.6 Plot of the Reitveld refinement of the PXRD Pattern of CoAlPO-1. The red crosses are of the observed powder pattern and the green line is the calculated powder pattern. The purple line shows the difference between the observed and calculated patterns. There are four phases: CoAlPO-1 (brown ticks), CoAlPO-2 (purple ticks), CoAlPO-3 (black ticks) and the AlPO dense phase (blue ticks).



Although this result further elucidates the potential of eutectic mixtures in the synthesis of crystalline porous materials it was not possible to obtain a phase pure sample or better crystals of CoAlPO-1 by changing the reaction conditions and stoichiometry. Changing the solvent to either the glutaric acid or citric acid/choline chloride eutectic mixture also resulted in CoAlPO-1 as the major product at 150 °C. In all three cases also present was the dense phase formed in the absence of cobalt acetate and cyclam, the amount of which seemed to decrease with extended reaction times.

An attempt was made to synthesise CoAlPO-1 in a round bottomed flask under atmospheric pressure, as achieved by Morris *et al* in the preparation of AlPO frameworks using ionic liquids [1]. However, all that formed was the same aluminium phosphate dense phase present in successful syntheses of CoAlPO-1. This suggests that the slight increase in pressure that happens in an autoclave is required to make CoAlPO frameworks using this eutectic mixture.

4.3.3 CoAlPO-2

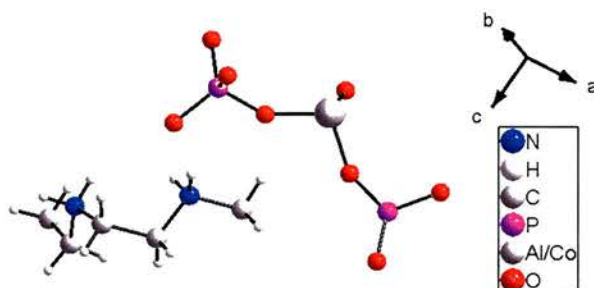
Present in each sample of CoAlPO-1 obtained was also a very minor blue crystalline product found to be a CoAlPO chain structure templated by cyclam. This material, termed CoAlPO-2, has an asymmetric unit containing one aluminium/cobalt site, two phosphorus, eight oxygen, five carbon, two nitrogen and fourteen hydrogen (figure 4.3.7). The chemical formula is $[Al_{0.982}Co_{0.018}P_4O_{16}] \cdot [C_{10}H_{28}N_4]^+$. The crystal

structure was solved using single crystal X-ray diffraction data collected on station 9.8 of the synchrotron radiation source (SRS) at Daresbury [11].

Table 4.3.2 Crystal data and structure refinement for CoAlPO-2

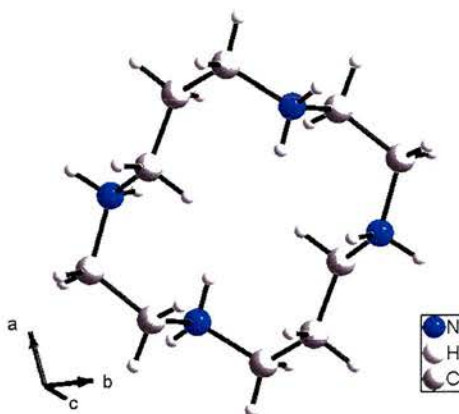
Identification code	CoAlPO-2
Empirical formula	C ₁₀ H ₂₈ Al _{1.96} Co _{0.04} N ₄ O ₁₆ P ₄
Temperature	150(2) K
Wavelength	0.69100 Å
Crystal system, Space group	Triclinic, P-1
Unit cell dimensions	a = 7.8215(13) Å α = 102.253(2)°. b = 8.7905(15) Å β = 97.237(3)°. c = 8.9928(15) Å γ = 102.486(3)°.
Volume	580.27(17) Å ³
Crystal size	0.075 x 0.05 x 0.005 mm ³
Theta range for data collection	2.38 to 30.05°.
Index ranges	-11 ≤ h ≤ 11, -12 ≤ k ≤ 12, -12 ≤ l ≤ 12
Reflections collected	6612
Completeness to theta = 30.05°	94.0 %
Refinement method	Full-matrix least-squares on F ²
Data / restraints / parameters	3473 / 0 / 164
Goodness-of-fit on F ²	1.097
Final R indices [I > 2σ(I)]	R1 = 0.0703, wR2 = 0.2282
R indices (all data)	R1 = 0.0778, wR2 = 0.2330
Largest diff. peak and hole	2.364 and -0.860 e.Å ⁻³

Figure 4.3.7 Asymmetric unit of CoAlPO-2



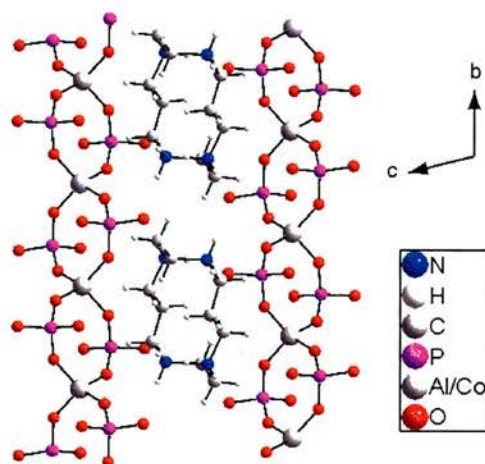
The framework is made up of linear chains where each aluminium/cobalt position is connected by two oxygen-phosphorus-oxygen bridges (figure 4.3.9). Each phosphorus has two hanging phosphorus to oxygen bonds that hydrogen bond to the hydrogens on the nitrogen atoms of the template cyclam. The cyclam is in the trans-IV conformation, which is one of five possible conformations (figure 4.3.8) [12]. Conformations of cyclam differ in the direction the hydrogens on the nitrogens are facing. The trans-IV conformation has the nitrogen hydrogens on one NH-CH₂-CH₂-NH section pointing in one direction and the nitrogen hydrogens on the other NH-CH₂-CH₂-NH section pointing in the opposite direction.

Figure 4.3.8 Crystal structure showing the conformation of cyclam between the CoAlPO-2 chains.



There appears to be no relationship between CoAlPO-2 and CoAlPO-1. Therefore, it would appear that CoAlPO-2 is not a parent chain that is condensed into the layered structure but is the result of a very minor side reaction.

Figure 4.3.9 Crystal Structure of CoAlPO-2



4.3.4 CoAlPO-3

When the reaction temperature was increased from 150 °C to 180 °C the major reaction product was another aluminium cobalt phosphate framework. This material, termed CoAlPO-3, was found to be a three-dimensional zeolitic framework with the levyne topology (LEV). This topology was first reported as an aluminium silicate by Barrer and Kerr in 1959 [13]. The crystal structure was solved using single crystal X-ray diffraction data collected on station 9.8 of the synchrotron radiation source (SRS) at Daresbury [11].

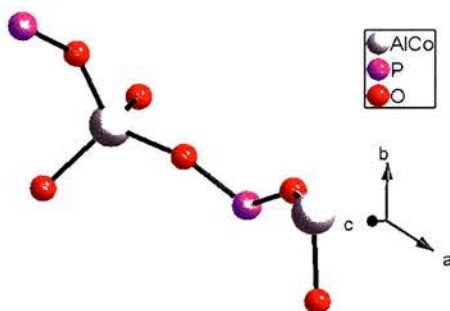
Table 4.3.3 Crystal Data and Structure Refinement for CoAlPO-3

Identification code	CoAlPO-3
Empirical formula	Al _{44.66} Co _{9.34} O ₂₁₆ P ₅₄
Temperature	293(2) K
Wavelength	0.7103 Å
Crystal system, Space group	Rhombohedral, R-3c
Unit cell dimensions	a = 13.0970(9) Å a = 90°.
	b = 13.0970(9) Å b = 90°.

	$c = 45.627(6) \text{ \AA}$ $\beta = 120^\circ$.
Volume	$6778.0(11) \text{ \AA}^3$
Crystal size	$0.05 \times 0.05 \times 0.05 \text{ mm}^3$
Theta range for data collection	2.01 to 30.99° .
Index ranges	$-16 \leq h \leq 18$,
	$-18 \leq k \leq 18$,
	$-65 \leq l \leq 64$
Reflections collected	18199
Independent reflections	2317 [R(int) = 0.0822]
Completeness to theta = 30.99°	96.3 %
Refinement method	Full-matrix least-squares on F^2
Data / restraints / parameters	2317 / 0 / 84
Goodness-of-fit on F^2	1.076
Final R indices [I > 2sigma(I)]	R1 = 0.0787, wR2 = 0.2681
R indices (all data)	R1 = 0.1328, wR2 = 0.3207
Largest diff. peak and hole	2.301 and $-0.626 \text{ e.\AA}^{-3}$

The asymmetric unit of the inorganic framework consists of two aluminium/cobalt positions, two phosphorus and six oxygen (figure 4.3.10). It was not possible to find the organic template crystallographically due the high symmetry of the structure. The chemical formula of the material is $[\text{Al}_{0.817}\text{Co}_{0.183}\text{PO}_4]^{-1.183} \cdot [\text{C}_5\text{H}_{13}\text{NOH}]_{1.183}^+$

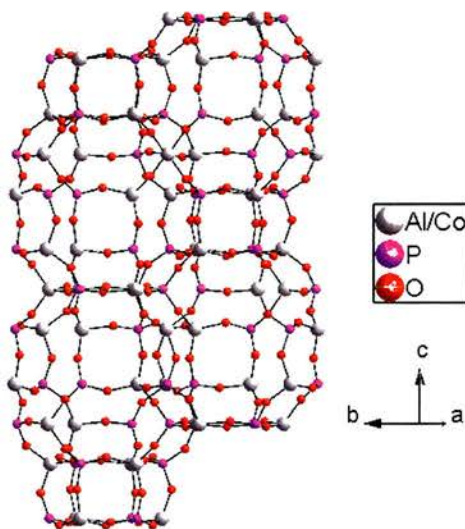
Figure 4.3.10 Asymmetric Unit of CoAlPO-3



The levyne topology is very similar to the chabazite topology. It consists of large cages with dimensions of approximately $3.6 \times 4.8 \text{ \AA}$, which are linked through eight ring windows or by double four rings and are capped by double six rings (figure

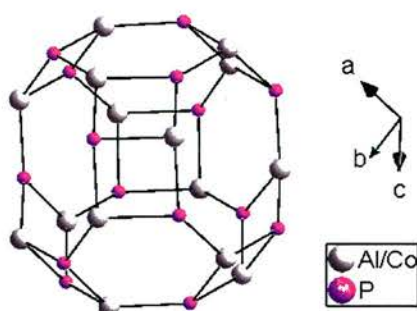
4.3.11). If the template was removed the structure would have a two-dimensional channel system allowing for passage of very small molecules through the material.

Figure 4.3.11 Crystal Structure of CoAlPO-3



An aluminium cobalt phosphate material with the levyne topology has already been reported by Barrett and Jones in 2000 [14]. This material, termed CoDAF-4, was made hydrothermally using 2-methylcyclohexylamine as template. The ratio of aluminium to cobalt was 4.45:1, which is very similar to the ratio of 4.46:1 obtained for CoAlPO-3. Using resonant (anomalous) powder x-ray diffraction Barrett and Jones found that the cobalt ions preferred to occupy aluminium sites that minimised the potential number of Co-O-P-O-Co linkages.

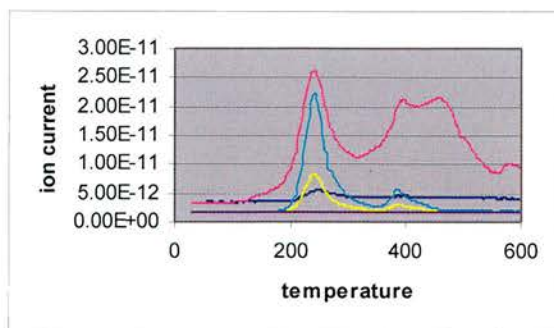
Figure 4.3.12 Crystal structure of the large cages of CoAlPO-3 (only T atoms shown)



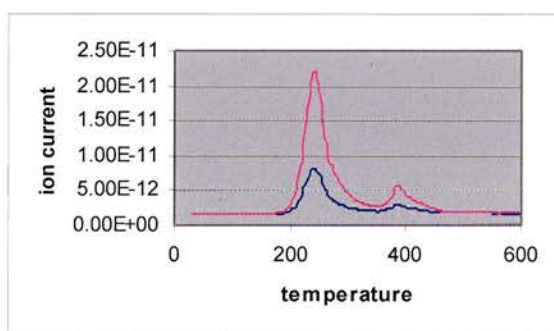
Not only was it not possible to locate the template crystallographically, it was also not possible to assign it by solid state NMR due to the paramagnetism of cobalt. Therefore, an attempt was made to identify the template by comparison of thermogravimetric mass spectroscopy (TG-MS) data for CoAlPO-3 with that of CoAlPO-1. Since it was known that the template of CoAlPO-1 is choline it was expected that if CoAlPO-3 had the same template there would be significant similarities in the two spectra.

Although the TG-MS data of CoAlPO-1 was not of high quality it did show a few expected masses from fragments of choline (35.19, 44.22, 50.22, 52.21 and 70.19). The CoAlPO-3 data also showed these same masses but in far less quantity as for CoAlPO-1, especially masses 50.22 and 52.11, which could with most certainty be assigned to choline. This is possibly due to there being less template and it having difficulties escaping from the framework cages. Neither set of data showed any expected masses of fragments of cyclam.

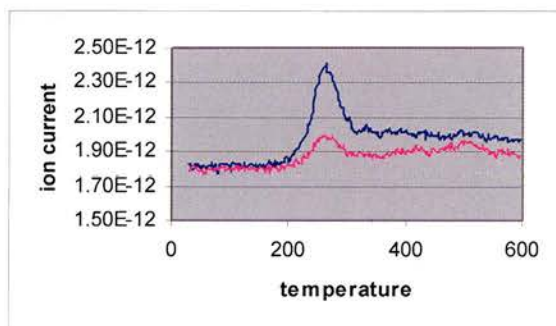
Figure 4.3.13 TG-MS Data for CoAlPO-1 and CoAlPO-2



a. Data for CoAlPO-1 showing masses 35.19 (purple), 44.22 (blue), 50.22 (yellow), 52.22 (cyan) and 70.19 (dark purple).



b. Data for CoAlPO-1 showing only masses 50.22 (purple) and 52.21 (blue).



c. Data for CoAlPO-3 showing masses 50.22 (blue) and 52.21 (purple).

The TG-MS data was far from conclusive so therefore after sonicating the sample in distilled water to ensure complete removal of any extra-framework species, the

framework was dissolved in hydrochloric acid and deuterium oxide for analysis by solution state NMR. The ^1H NMR spectrum obtained showed only a slightly shifted downfield choline resonance pattern (δ_{H} 1.83, 2.13 and 2.69; choline chloride in D_2O gives signals at 2.23, 2.56 and 3.08 respectively) and no signals for cyclam. The ^{13}C NMR also showed only signals from choline (δ_{C} 53.07, 54.83 and 66.35; choline chloride in D_2O has signals at 54.17, 55.81 and 67.56). It was therefore deduced that the template of CoAlPO-3, like CoAlPO-1, was choline.

Despite slight alterations to the reactant stoichiometry a phase pure sample of CoAlPO-3 was not obtained, therefore further analysis was not performed. Also, these alterations to the reactant stoichiometry did not result in the formation of another framework as the major product, as is often the case with zeolite synthesis. Substituting the cyclam for pyridine also resulted in the major product being CoAlPO-3. It would therefore appear that the levyne topology is the default structure for this system at 180 °C.

4.4 Conclusion

These results provide further evidence that eutectic mixtures can be used as solvent and template in the formation of new crystalline framework topologies. Both CoAlPO-1 and CoAlPO-3 are templated by choline proving that choline from the eutectic mixture can act as a template in the formation of CoAlPO frameworks. This is an excellent result as choline is inexpensive and very safe, making it an ideal template. It also means that derivatives of choline chloride could be used to form a

eutectic mixture and used as both solvent and template in zeotype synthesis, resulting in the formation of different framework topologies and compositions. Using chiral derivatives of choline may lead to the formation of chiral frameworks if close templating can be achieved.

CoAlPO-1 is the first aluminium cobalt phosphate framework to contain cobalt-chlorine bonds. Since this study was completed copper-chlorine bonds have also been formed in coordination polymers using choline chloride containing eutectic mixtures, proving that using eutectic mixtures in porous material synthesis gives reaction conditions that may have the potential to form more novel bond types [15].

The CoAlPO-2 framework was formed as a minor side-product in the synthesis of CoAlPO-1. Unlike CoAlPO-1 and CoAlPO-3 it is templated by cyclam rather than choline. This shows that the template in ionothermal synthesis needn't come from the solvent but that a templating agent can also be added to the reaction mixture, allowing the eutectic mixture or ionic liquid to act solely as a solvent. This technique would still have many benefits over the use of conventional solvents. For example, the vanishingly low vapour pressure of ionic liquids and eutectic mixtures means that reactions can be performed at lower pressure than in traditional methods, which eliminates some of the safety concerns of zeotype synthesis.

No phase pure samples of the CoAlPO frameworks were obtained. It can be seen from other studies that control over phases formed in all ionothermal synthesis is difficult. However, if the correct reaction conditions and stoichiometry are found

phase pure samples and more control over the product formed may be achieved, so the inability to achieve this in this study should not deter further work in this area.

4.5 References

1. E. R. Cooper, C. D. Andrews, P. S. Wheatley, P. B. Webb, P. Wormald and R. E. Morris, *Nature*, **2004**, *430*, 1012-1016
2. (a) E. R. Parnham, P. S. Wheatley & R. E. Morris, *Chem. Commun.*, **2006**, 380-382 (b) E. R. Parnham & R. E. Morris, *J. Am. Chem. Soc.*, **2006**, in press
3. Xu Yunpeng, Tian Zhijian, Xu Zhusheng, Wang Bingchun, Li Peng, Wang Shaojun, Hu Yue, Ma Yingchong, Li Kunlan, Liu Yanjun, Yu Jiayou and Lin Liwu, *Chinese Journal of Catalysis*, **2005**, *26*, 446-448
4. R. C. L. Mooney, *Acta Cryst.*, **1956**, *9*, 728
5. H. N. Ng & C. Calvo, *Canadian. J. Phys.*, **1976**, *54*, 638-647 and references therein
6. (a) R. Garcia, E. F. Philp, A. M. Z. Slawin, P. A. Wright & P. A. Cox, *J. Mater. Chem.*, **2001**, *11*, 1421-1427 (b) R. Garcia, T. D. Coombs, I. J. Shannon, P. A. Wright & P. A. Cox, *Topics in Catalysis*, **2003**, *24*, 115
7. (a) P. A. Wright, M. J. Maple, A. M. Z. Slawin, V. Patinec, R. A. Aitken, S. Welsh & P. A. Cox, *J. Chem. Soc. Dalton Trans.*, **2000**, 1243-1248 (b) C. Baerlocher, L. B. McCusker & R. Chiappetta, *Micropor. Mater.*, **1994**, *2*, 269-280 (c) F. Delprato, L. Delmotte, J. L. Guth & L. Huve, *Zeolites*, **1990**, *10*, 546-552
8. V. Patinec, P. A. Wright, P. Lightfoot, R. A. Aitken & P. A. Cox, *J. Chem. Soc. Dalton Trans.*, **1999**, 3909-3911

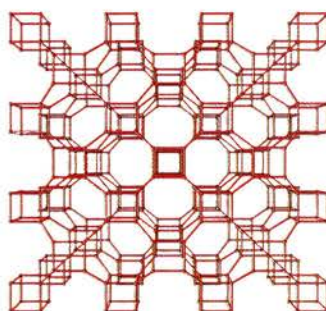
9. M. J. Maple, E. F. Philp, A. M. Z. Slawin, P. Lightfoot, P. A. Cox & P. A. Wright, *J. Mater. Chem.*, **2001**, *11*, 98-104
10. D. S. Wragg & R. E. Morris, *J. Phys. Chem. Solids*, **2001**, *62*, 1493-1497
11. CCLRC Daresbury Synchrotron Radiation Source website: www.srs.ac.uk/src
12. V. J. Thöm. C. C. Fox, J. C. A. Boeyens and R. D. Hancock, *J. Am. Chem. Soc.*, **1984**, *106*, 5947-5955
13. R. M. Barrer & I. S. Kerr, *Trans. Farad. Soc.*, **1959**, *55*, 1915
14. P. A. Barrett and R. H. Jones, *Phys. Chem. Chem. Phys.*, **2000**, *2*, 407-412
15. Z. Lin & R. E. Morris, manuscript in preparation

5. Attempted Synthesis of Carboxylic Acid Functionalised POSS

5.1 Introduction

A carboxylic acid or carboxylate functionalised POSS is desirable as it could be used to form a porous framework. The carboxylic acid POSS can either form an extended network through intermolecular hydrogen bonding or carboxylate groups can be coordinated to a metal cation to form a coordination polymer. If the POSS molecules are linked together through all eight corners in either of these ways the resultant porous framework can only have a few possible topologies [1], one of which is the aluminium cobalt phosphate 1 (ACO) topology (figure 5.1.1) [2].

Figure 5.1.1 ACO Topology

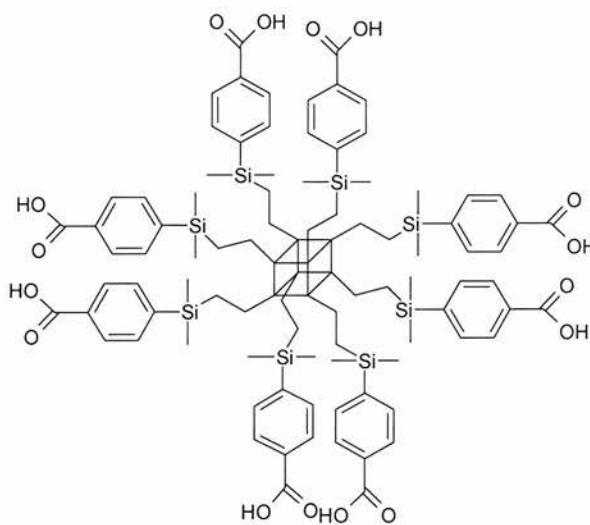


There is one example of POSS molecules that have crystallised into a porous framework [3]. This POSS was a tertiary alcohol functionalised species prepared from the hydrosilation reaction between octahydridesilsesquioxane and an alcohol-alkene molecule at high pressure. The framework has cavities between 8-9 Å,

however it is only held together by hydrogen bonding between the alcohols and water molecules so is not as stable a framework as that which would be formed through hydrogen bonding between carboxylate groups or by coordination of carboxylates to metals.

Only one carboxylic acid functionalised POSS species has been reported, formed through a multistep procedure resulting in a benzaldehyde functionalised POSS (figure 5.1.2) [4]. Controlling oxidation of the aldehyde groups by synthetic methods proved difficult but it was found that the aldehyde groups oxidised in air over a period of several months. It was intended for this molecule to be used in the synthesis of POSS frameworks and attempts were made at using it for this purpose, but all were unsuccessful.

Figure 5.1.2 Carboxylic acid POSS (Si_8O_{12} core drawn as a cube for clarity)

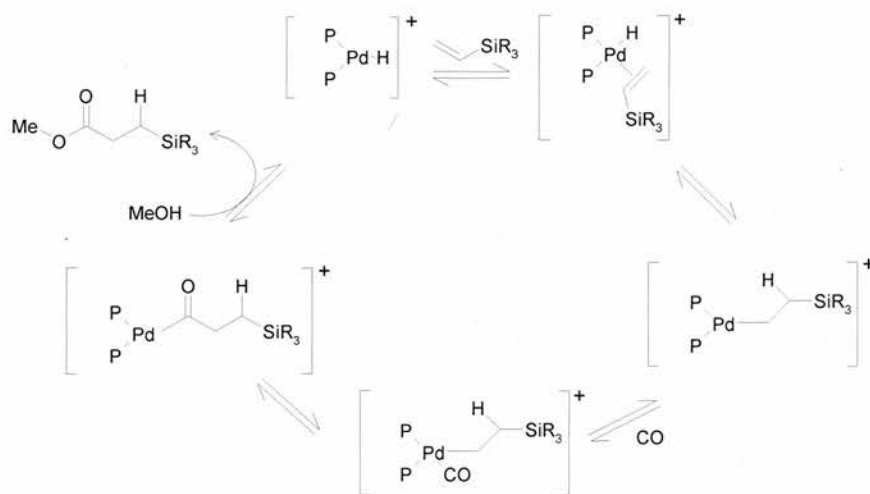


Other POSS molecules have been made with groups that can possibly be converted to carboxylic acid groups such as alcohols, aldehydes and esters [4,5]. Due to the

potential difficulty in controlling oxidation reactions required to convert alcohols and aldehydes to carboxylic acids, it was decided to pursue the route of forming an ester functionalised POSS and then hydrolysing this species to give an octacarboxylic acid species.

One possible route was by the methoxycarbonylation of octavinylsilsesquioxane to form an octamethylpropanoate functionalised POSS followed by hydrolysis of the ester groups under mild basic conditions. Alkoxy carbonylation of alkenes has been recently reported as a highly selective route to industrially important esters [6]. Methoxycarbonylation involves the addition of carbon monoxide and a methoxy group (from methanol) to a vinyl group to form a methyl ester. It has been used previously with great success in the conversion of ethene to methyl propanoate, where a palladium catalyst with the highly sterically hindered bidentate phosphine ligand 1,2-bis(di-*tert*-butylphosphinomethyl)-benzene (DTBPMB) gives exceptional selectivity (99.9 %) for the linear product [7]. The reaction has been shown by deuterium labelling to progress through the ‘hydride’ mechanism (figure 5.1.3) [8].

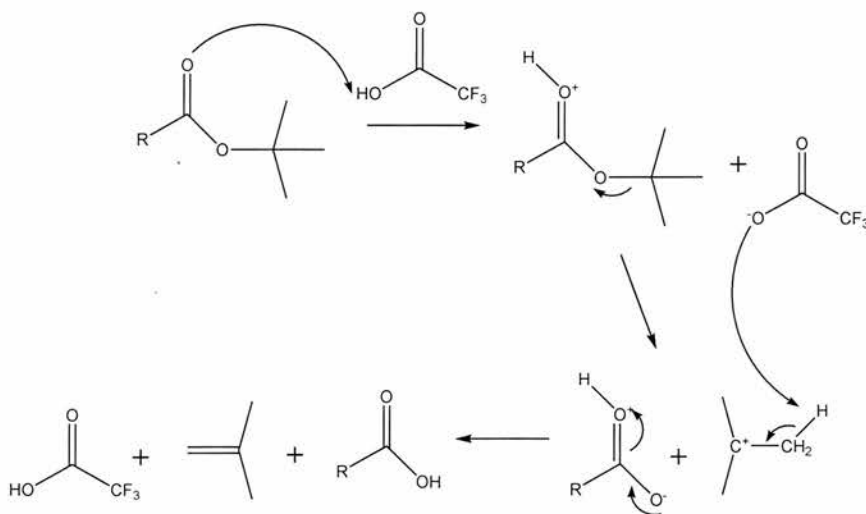
Figure 5.1.3 Methoxycarbonylation hydride mechanism



It was thought that hydrolysis of the ester-substituted POSS to form a carboxylate functionalised material should be possible. However, since the POSS core is sensitive to strongly acidic and basic conditions hydrolysis would have to be carried out under as mild conditions as possible in order to keep it intact. Hydrolysis of the ester was attempted under basic conditions, as hydrolysis has already proved unsuccessful under acidic conditions [9]. Also, the carboxylate ion is very unreactive towards nucleophilic substitution so the reaction is irreversible.

A second technique for converting ester functional groups on POSS to carboxylic acid groups was also investigated. This technique involved the synthesis of a tertiary butyl ester functionalised POSS and conversion of the esters to carboxylic acids (figure 5.1.4). This conversion is not a hydrolysis reaction as above but still involves the use of an acid, so there was still the possibility of breaking the POSS core.

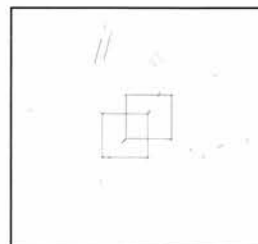
Figure 5.1.4 Mechanism of the reaction between a tertiary butyl ester and trifluoroacetic acid



5.2 Experimental

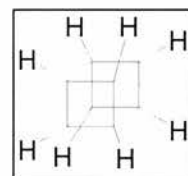
5.2.1 Preparation of Vinyl and Hydride Precursors

Octavinylsilsesquioxane [10]. To a mixture of ethanol (1.6 L) and water (100 ml) at 0 °C was added trichlorovinylsilane (80 ml, 0.62 mol) dropwise. The reaction mixture was stirred at room temperature for 7 weeks. The precipitate was



filtered, washed with cold acetone and dried under vacuum to yield a white solid (10.88 g, 22%). ^1H NMR (CDCl_3 , 300 MHz): δ_{H} 5.7-6.1 (24H, m, vinyl-H). ^{13}C NMR (CDCl_3 , 300 MHz): δ_{C} 129.05 ($\text{CH}=\text{CH}_2$) and 137.40 ($\text{CH}=\text{CH}_2$).

Octahydridesilsesquioxane [11]. To iron (III) chloride (50 g, 0.31 mol) was added concentrated hydrochloric acid (20 ml), methanol (40 ml), hexane (350 ml) and toluene (50 ml). To this mixture was



added trichlorosilane (20 ml, 0.20 mol) in hexane (150 ml) dropwise over a period of 12 hours and the reaction mixture was stirred overnight. The top layer was then removed and dried over K_2CO_3 (14 g) and CaCl_2 (10 g). The mixture was filtered and the solution was reduced *in vacuo* to ~20 ml. On cooling a white crystalline product precipitated, which was recovered by filtration and washed with hexane (1.04 g, 10 %). The mother liquor and washings were then reduced *in vacuo* to ~10 ml and a second crop of crystals was collected (0.31 g, 3 %). ^1H NMR (CDCl_3 , 300 MHz): δ_{H} 4.25 (8H, s, SiH). MS (ESI) m/z (relative intensity): 422.80 (100), 423.80 (33), 424.80 (29) and 425.80 (9).

The iron (III) chloride layer was recycled and the procedure was repeated as above to yield a white crystalline solid (2.21 g, 21 %). ^1H NMR (CDCl_3 , 300 MHz): δ_{H} 4.25 (8H, s, SiH).

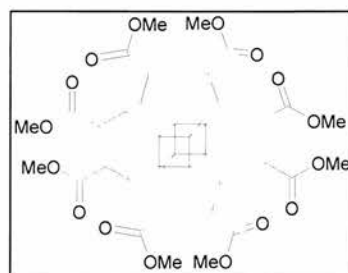
5.2.2 Attempted Preparation of a Carboxylic Acid POSS via Methoxycarbonylation of Octavinylsilsesquioxane

1,3,5,7,9,11,13,15-Octakis[methylpropanoate]-

octasiloxane. $\text{Pd}_2(\text{dba})_3$ (45.7 mg, 7.283×10^{-5} mol)

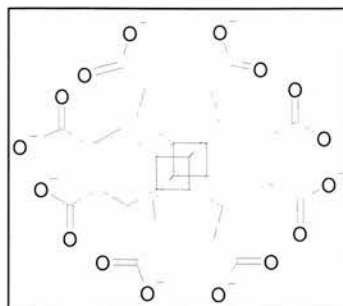
[dba = dibenzylidene-acetone], 1,2-bis(di-*tert*-butylphosphinomethyl)-benzene (0.198 g, 5.018×10^{-4}

mol) and octavinylsilsesquioxane (0.50 g, 7.90×10^{-4} mol) were dissolved in dry toluene (30 ml) under argon. Dry methanol (5 ml) and methanesulfonic acid (65 μl , 1×10^{-3} mol) were added and the reaction mixture was transferred into a Hastelloy autoclave that had been evacuated and fitted with a paddle stirrer. The autoclave was pressurised to 30 bar CO and heated to 80 $^\circ\text{C}$ for 41 hours. The autoclave was then cooled, vented, the contents were removed and the product was purified on a florisil column (ethyl acetate/petroleum ether) and recrystallised from ethyl acetate/petroleum ether to yield small, white needle like crystals (0.38 g, 43 %). ^1H NMR (CDCl_3 , 300 MHz): δ_{H} 0.9 (16H, m, SiCH_2CH_2), 2.3 (16H, m, SiCH_2CH_2) and 3.6 (24H, s, OMe). ^{13}C NMR (CDCl_3 , 75 MHz) δ_{C} 7.17 (8C, SiCH_2CH_2), 27.64 (8C, SiCH_2CH_2), 52.10 (8C, OMe) and 174.65 (8C, COO). ^{29}Si NMR (CDCl_3 , 59.6 MHz): δ_{Si} -67 (8Si, CH_2SiO_3). IR (nujol mull): ν/cm^{-1} 1738 (CO-O str.), 1236 (CO str.) and 1095 (CO str.). CHN (calc): 34.90 (34.52) C, 4.71 (5.07) H.



Attempted preparation of 1,3,5,7,9,11,13,15-Octakis[lithium propanoate]octasiloxane.

Octakis[methyl-propanoate]octasiloxane (150 mg, 1.347×10^{-4} mol) was dissolved in a mixture of THF and water (ratio 5:2). Lithium hydroxide (11 ml, 0.15

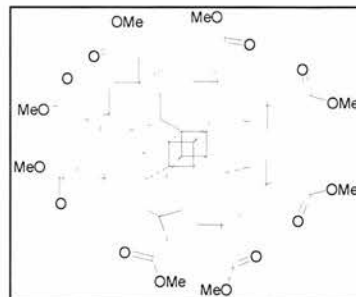


M, 1.65×10^{-3} mol) was added and the reaction mixture was stirred at RT for 3 days. The solvent was removed *in vacuo* and the product was precipitated from a water/acetone mixture to yield a white solid. ^1H NMR (D_2O , 300 MHz): δ_{H} 0.76 (16H, m, SiCH_2CH_2) and 2.25 (16H, m, SiCH_2CH_2). ^{13}C NMR (D_2O , 75.5 MHz): δ_{C} 13.63 (8C, SiCH_2CH_2), 34.50 (8C, SiCH_2CH_2) and 188.31 (8C, COO). ^{29}Si NMR (D_2O , 59.6 MHz): δ_{Si} -42.32, -50.00, -50.43 and -58.00 to -58.50.

Attempted preparation of 1,3,5,7,9,11,13,15-Octakis[lithium propanoate]-octasiloxane 2. Octakis[methyl-propanoate]octasiloxane (0.05 g, 4.49×10^{-5} mol) was dissolved in methanol (9 ml) and distilled water (1 ml). Lithium hydroxide (0.0175 g, 4.17×10^{-4} mol) was added and the reaction mixture was refluxed for 7 hours. The solvent was removed *in vacuo* to yield the product as a white solid. ^1H NMR (D_2O , 300 MHz): δ_{H} 0.79 (4H, m, SiCH_2), 0.93 (12H, bs, SiCH_2), 2.21 (16H, m, SiCH_2CH_2) and 3.30 (8H, s, OMe). ^{13}C NMR (D_2O , 75.5 MHz): δ_{C} : 9.31 & 9.45 (8C, SiCH_2CH_2), 30.70 & 30.76 (8C, SiCH_2CH_2), 48.79 (OMe) and 184.36 (8C, C=O). δ_{Si} ^{29}Si NMR (D_2O , 59.6 MHz) -39.38, -48.49 and -56.58. MS (ESI) m/z (relative intensity): 157.13 (5) and 433.24 (100).

5.2.3 Attempted Preparation of a Carboxylic Acid POSS *via* a Tertiary Butyl Ester POSS

1,3,5,7,9,11,13,15-octakis[methyl-3,3-dimethyl-pentanoate]octasiloxane. Octahydridesilsesquioxane (0.3 g, 7.06×10^{-4} mol) and methyl-3,3-dimethyl-4-pentenoate (1.2 ml, 7.59×10^{-3} mol) were dissolved



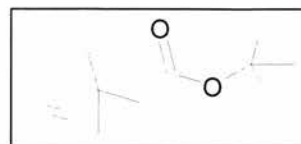
in hexane (60 ml) and the solution was cooled to 0 °C. Platinum(0)-1,3-divinyl-1,1,3,3-tetramethyldisiloxane complex (Karstedt's catalyst) solution in xylenes (200 μ l) was added and the reaction mixture was allowed to warm to RT and stirred for three days until there was no Si-H resonance visible in the ^1H NMR. The platinum was removed on a short silica plug eluted with diethyl ether, the solvent was removed and the product was recrystallised from methanol to yield a white crystalline solid (0.752 g, 68 %). ^1H NMR (CDCl_3 , 300 MHz): δ_{H} 0.57 (16H, m, 0.58, SiCH_2), 0.97 (48H, s, 2 x Me), 1.41 (16H, m, SiCH_2CH_2), 2.19 (16H, s, $\text{CCH}_2\text{CO}_2\text{Me}$) and 3.64 (24H, s, OMe). ^{13}C NMR (CDCl_3 , 75 MHz): δ_{C} 6.46 (SiCH_2), 26.89 (2 x Me), 34.22 (SiCH_2CH_2), 35.72 ($\text{CCH}_2\text{CO}_2\text{Me}$), 45.36 ($\text{CH}_2\text{C}(\text{CH}_3)_2\text{CH}_2$), 51.48 (OMe) and 173.16 (C=O). IR (nujol mull): ν/cm^{-1} 1737 (CO-O str). CHN (calc): 48.56 (49.20) C, 8.18 (7.74) H.

Reaction of 1,3,5,7,9,11,13,15-octakis[methyl-3,3-dimethylpentanoate]octasiloxane with trifluoroacetic acid. 1,3,5,7,9,11,13,15-octakis[methyl-3,3-dimethylpentanoate]octasiloxane (0.07 g, 4.48×10^{-5} mol) in trifluoroacetic acid (5 ml) was stirred at RT for 1 hour. The trifluoroacetic acid was removed *in vacuo* and

the residue was dissolved in dichloromethane (40 ml), washed with distilled water (3 x 10 ml) and dried over MgSO₄. The product was recovered as a white solid and shown to be POSS starting material. ¹H NMR (CDCl₃, 300 MHz): δ_H 0.57 (16H, m, 0.58, SiCH₂), 0.96 (16H, s, 2 x Me), 1.40 (16H, m, SiCH₂CH₂), 2.19 (48H, s, CCH₂CO₂Me) and 3.63 (24H, s, OMe). ²⁹Si NMR (CDCl₃, 59.6 MHz): δ_{Si} -65.09, -65.79 and -65.90 (O₃SiC).

Attempted transesterification of Methyl-3,3-dimethyl

4-pentenoate. Methyl-3,3-dimethyl 4-pentenoate (5 ml, 0.032 mol) and concentrated sulphuric acid (8 drops)



were heated in *tert*-butanol (75 ml) in a distillation setup for 8 hours. The solvent was removed *in vacuo* to yield a colourless oil that was shown to be the methyl ester starting material. ¹H NMR (CDCl₃, 300 MHz): δ_H 1.13 (6H, s, CH₃), 2.31 (2H, s, CH₂), 3.64 (3H, s, OMe), 4.92-5.00 (2H, m, CH₂=CH) and 5.84-5.94 (1H, m, CH₂=CH).

Hydrolysis of Methyl-3,3-dimethyl-4-pentenoate. Methyl-3,3-dimethyl-4-pentenoate (5 ml) in aqueous NaOH solution (3 M, 120 ml) was refluxed for 45 minutes. Two layers were still



present so ethanol (2 x 10 ml) was added and the reaction was refluxed for a further 3 hours. The reaction was cooled and acidified with dilute HCl. The organic layer was extracted with dichloromethane (3 x 100 ml), dried over MgSO₄, filtered and the solvent was removed to yield a clear, colourless oil (3.40 g, 84 %). ¹H NMR (CD₃OD, 300 MHz): δ_H 1.04 (6H, s, CH₃), 2.17 (2H, s, CH₂), 4.80-4.92 (2H, m,

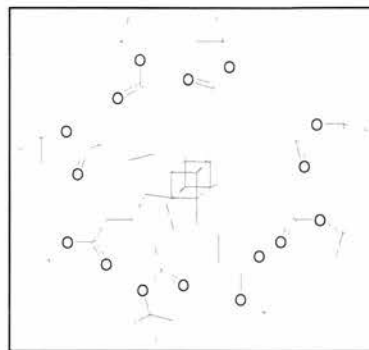
CH=CH₂) and 5.79-5.88 (1H, m, CH=CH₂). ¹³C NMR (CD₃OD, 75 MHz): δ_C 27.40 (CH₃), 36.80 (Me₂CCH₂), 47.57 (CH₂), 111.30 (CH=CH₂), 148.30 (CH=CH₂) and 175.60 (COOH). MS (ESI) *m/z* (relative intensity): 127.02 (100). IR: ν/cm⁻¹ 1708 (saturated CO₂H str.). CHN (calc): 65.21 (65.60) C, 10.06 (9.44) H.

Attempted esterification of 3,3-dimethyl-4-pentenoic acid. 3,3-dimethyl-4-pentenoic acid (0.410 g, 3.20 x 10⁻³ mol) and concentrated sulphuric acid (10 drops) were refluxed in *tert*-butanol (50 ml) for 12 hours. The solvent was removed *in vacuo* to yield a yellow oil that was shown to be the carboxylic acid starting material. ¹H NMR (CDCl₃, 300 MHz): δ_H 1.16 (6H, s, 2 x Me), 2.34 (2H, s, CCH₂CO₂Me), 4.94-5.03 (2H, m, CH=CH₂) and 5.86-5.96 (1H, m, CH=CH₂).

Attempted conversion of 3,3-dimethyl-4-pentenoic acid to a *tert*-butyl ester via an acid chloride. Into dry dichloromethane (10 ml) under argon was added 3,3-dimethyl-4-pentenoic acid (0.54 g, 4.21 x 10⁻³ mol), dimethylformamide (3 drops) and oxalyl chloride (4 ml, 4.59 x 10⁻² mol). A bubbler was fitted and the reaction mixture stirred overnight at room temperature. The solvent and excess oxalyl chloride were then removed *in vacuo* and the residue was redissolved in dry dichloromethane (10 ml). *tert*-Butanol (0.5 ml, 5.23 x 10⁻³ mol) was added and the reaction mixture was cooled to -78 °C. Pyridine (0.4 ml, 4.95 x 10⁻³ mol) was added and the reaction was stirred at RT overnight. The solvent was removed *in vacuo* to yield a brown solid. No satisfactory spectral data was obtained.

Attempted synthesis of 1,3,5,7,9,11,13,15-octakis[t-butylbutanoate]octasiloxane.

Octahydridesilsesquioxane (0.05 g, 7.90×10^{-5} mol) was dissolved in dry toluene (5 ml) under an argon atmosphere. *Tert*-butylbutanoate (0.1 ml, 6.17×10^{-4} mol) was added and the solution was cooled to 0



$^{\circ}\text{C}$ before addition of Kartstedt's catalyst in xylenes (100 μl). The reaction mixture was then allowed to warm to room temperature and stirred for two days under argon. The solvent was removed *in vacuo* to yield a brown oil, which was redissolved in diethyl ether and filtered through a florisil plug eluted with diethyl ether to remove the platinum. The solvent was then removed *in vacuo* to yield an oily solid. ^1H NMR (CDCl_3 , 300 MHz): δ_{H} 0.44-0.54 (1H, broad hump, unknown), 0.56-0.68 (9H, broad hump, $\text{SiCH}_2\text{CH}_2\text{CH}_2$), 0.93-1.02 (11H, multiplet, unknown), 1.37 (72H, s, $\text{C}(\text{CH}_3)_3$), 1.56-1.72 (10H, multiplet, $\text{CH}_2\text{CH}_2\text{CH}_2$), 1.90-2.08 (6H, multiplet, unknown), 2.12-2.24 (9H, multiplet, $\text{CH}_2\text{CH}_2\text{CH}_2$) and 2.32-2.46 (6H, multiplet, unknown). ^{13}C NMR (CDCl_3 , 75 MHz): δ_{C} 12.53 (SiCH_2), 12.61 (unknown), 17.54 (SiCH_2CH_2), 27.10 ($\text{C}(\text{CH}_3)_3$), 36.00 ($\text{SiCH}_2\text{CH}_2\text{CH}_2$), 37.50 (unknown), 79.70 ($\text{C}(\text{CH}_3)_3$) and 171.50 ($\text{C}=\text{O}$). MS (ESI) (m/z) (relative intensity): 1331.28 (100), 1332.27 (65) and 1333.29 (20). IR (nujol mull): ν/cm^{-1} 1731 (CO-O str).

The reaction was repeated under reflux with dry toluene as the solvent and at RT using dry hexane as solvent. Each yielded a yellow oil with the same ^1H NMR as above.

5.3 Results and Discussion

5.3.1 Attempted Preparation of Carboxylic Acid POSS via Methoxycarbonylation of Octavinylsilsesquioxane

Methoxycarbonylation of octavinylsilsesquioxane formed a silsesquioxane species functionalised with eight methyl propanoate groups. It was accomplished using the zero valent $L_2Pd(dba)_3$ complex [where $L_2 = 1,2$ -bis(di-*tert*-butylphosphinomethyl)benzene and $dba = trans,trans$ -dibenzylideneacetone] as the catalyst. The reaction was performed under 30 bar of CO at 80 °C in a Hastelloy autoclave but it could also be performed at room temperature on a smaller scale by bubbling CO through the solution. However, scaling up this procedure was difficult due to problems in controlling the flow rate of carbon monoxide over a long period of time.

Nuclear magnetic resonance spectroscopy (1H and ^{13}C) indicated that all the vinyl resonances (δ_H 5.7-6.1) of octavinylsilsesquioxane had disappeared after 41 hours. The 1H NMR showed the emergence of two multiplet resonances (δ_H 0.9 and 2.3), which were assigned to the CH_2 groups and a singlet peak (δ_H 3.6) assigned to the methoxy group. In line with the steric requirements of the system, there was no evidence of formation of the branched ester product. Therefore, as far as could be deduced from NMR 100 % conversion to the linear ester product had been achieved.

Chemical analysis and ^{29}Si NMR further proved that addition to all corners of the cube had been achieved. The IR spectrum showed the expected ester carbonyl stretch at 1738 cm^{-1} . Purification of the product by chromatography followed by recrystallisation resulted in the formation of crystals suitable for obtaining single crystal x-ray data.

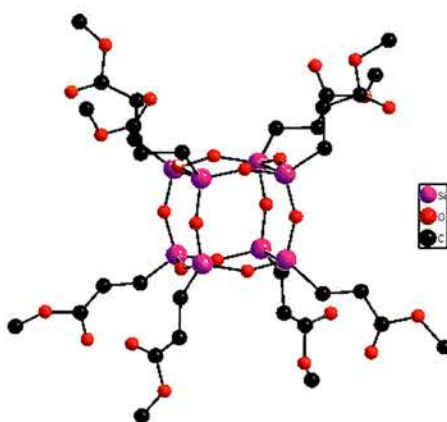
The crystal structure was obtained on a Bruker SMART diffractometer with graphite-monochromated Mo K_{α} radiation ($\lambda = 0.71074$) at 293 K. The silsesquioxane core of the structure is crystallographically well behaved, however the atoms on the organic arms do not refine as well. The further away from the silsesquioxane core the atom is the larger the anisotropic displacement parameters become, which must be due to some unresolved disorder and/or molecular motion of the terminal units. Disorder of the terminal carbon and oxygen atoms is resolvable for about half of the ester groups, but there remains some significant disorder that cannot be modelled satisfactorily.

Table 5.3.1 Crystal Data and Structure Refinement Details

Identification code	Ester POSS
Empirical formula	$(\text{Si}_8\text{O}_{12})(\text{CH}_2\text{CH}_2\text{CO}_2\text{CH}_3)_8$
Formula weight	1273.45
Temperature (K)	293(2)
Wavelength (\AA)	0.71074
Crystal system	Tetragonal
Space group	P4/ncc
Unit Cell Dimensions	
a (\AA)	17.813(2)
b (\AA)	17.813(2)
c (\AA)	15.704(3)
α ($^\circ$)	90
β ($^\circ$)	90
γ ($^\circ$)	90
V (\AA^3)	4982.9(12)
Z_s	4

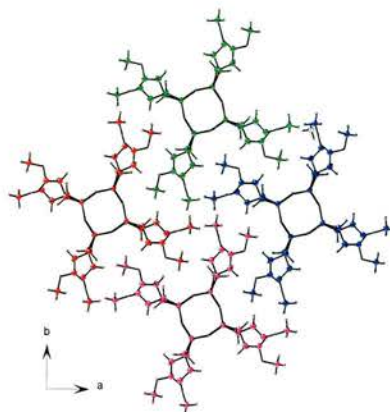
Calculated density (Mg/m ³)	1.654
$F(0\ 0\ 0)$	2592
Crystal size (mm)	0.07 × 0.07 × 0.07
Reflections collected/unique [R_{int}]	20 040/1797 [0.131]
Refinement method	full-matrix least-squares on F^2
Data/restraints/parameters	1797/70/170
Goodness-of-fit on F^2	2.544
Final R indices [$I > 2\sigma(I)$]	$R_1 = 0.1989$, $wR_2 = 0.5647$
R indices (all data)	$R_1 = 0.2221$, $wR_2 = 0.5745$
Largest difference in peak and hole (e \AA^{-3})	1.156 and -1.027

Figure 5.3.1 Crystal structure of Octakis[methylpropanoate]octasiloxane molecule



Collecting data at 150 K at the synchrotron source at Daresbury did not improve the quality of the diffraction data to any great degree. This type of problem is common with silsesquioxane materials of this kind. In fact, as already seen, there are examples where the disorder of the organic part is such that only the cubic silsesquioxane core can be found using single crystal x-ray diffraction [4]. In this case all the non-hydrogen atoms were found from the difference Fourier syntheses, although the subtle details of the structure could not be elucidated unambiguously.

Figure 5.3.2 Crystal Structure of the Packing of Octakis[methylpropanoate]-octasiloxane. For clarity, individual molecules are represented in different colours.



It was unnecessary to purify the ester POSS for the hydrolysis step as the methoxycarbonylation catalyst did not interfere with the reaction, so only the palladium was removed on a small florisil plug eluted with ethyl acetate. The methoxycarbonylation catalyst's ligand was removed after hydrolysis was complete due to its insolubility in water.

Hydrolysis of the octamethylpropanoate silsesquioxane was attempted with an excess of aqueous lithium hydroxide to form the octa-lithium propanoate salt. This method of ester hydrolysis has been employed successfully before using low temperatures and dilute solutions of lithium hydroxide giving very high yields of the carboxylate [12].

The ^1H NMR of the resulting hydrolysis product showed the loss of the methoxy hydrogen signals and the transformation of the signals of CH_2 's from second order triplets to multiplets with an $[\text{AX}]_2$ splitting pattern (δ_{H} 0.76 and 2.25) (figure 5.3.3). This is usually due to a predominance of the *trans* configuration along the silicon-

carbon-carbon-carbon chain, resulting in inequivalent hydrogen environments on each carbon.

Figure 5.3.3 *[AX₂] Splitting Pattern*



Hydrolysis of the ester groups was confirmed by the loss of the methoxy carbon signal in the ¹³C NMR spectrum and the absence of the ester carbonyl stretch in the IR. However, ²⁹Si NMR did not show the expected single POSS peak at about -65 ppm but showed a peak at -42 ppm and several peaks around -50 to -58 ppm. Furthermore, satisfactory mass spectrometry or MALDI-TOF data for the sample was not obtained so it was concluded that the POSS cube had broken up or undergone rearrangement.

It was thought that if a 1:1 ratio of ester groups to lithium hydroxide was used the ester groups would hydrolyse before the silicon-oxygen bonds, minimising the amount of POSS cube break-up. Performing the reaction at room temperature did not result in significant ester hydrolysis, but by refluxing the reaction mixture almost complete conversion of the esters to carboxylate groups occurred. However, examination of the product using ²⁹Si NMR again showed more than one signal (δ_{Si} -

39.38, -48.49 and -56.58), of which none were in the expected region. Again POSS break-up had resulted.

5.3.2 Attempted Preparation of a Carboxylic Acid POSS *via* a Tertiary Butyl Ester POSS

No milder methods of base promoted hydrolysis could be identified so it was concluded that a different approach to preparing a carboxylic acid functionalised POSS would have to be found. Trifluoroacetic acid is very efficient at converting tertiary butyl esters to carboxylic acid groups [13]. The reaction only works with tertiary alkyl groups as the intermediate carbocation is stabilised. Since the reaction is not a hydrolysis reaction it was anticipated that it could be used to make carboxylic acid functionalised POSS.

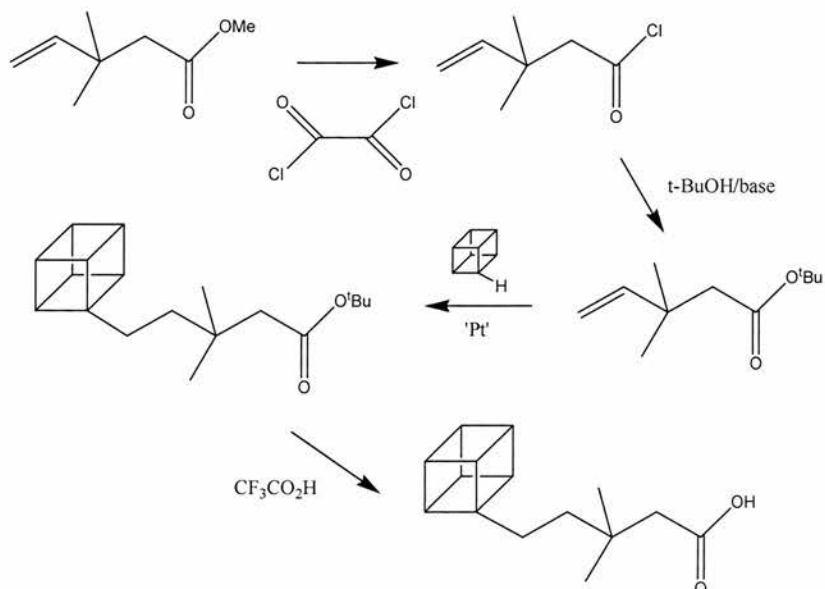
Before starting on preparing this POSS it was decided to check what would happen to the molecule's core under the conditions expected to result in the formation of carboxylic acid groups. For this 1,3,5,7,9,11,13,15-octakis[methyl-3,3-dimethylpentanoate]octasiloxane, reported by Feher *et al* was used [5(a)]. It was prepared by Feher's method except that hydrosilation was performed using Karstedt's catalyst instead of Speirs catalyst. This allowed the reaction to be carried out at room temperature. Even though longer reaction times are required, this promotes formation of the silicon-carbon bond at the α -carbon rather than β carbon of the vinyl group [9]. Cooling the reaction mixture to 0 °C before addition of the catalyst also aids formation of the linear product.

After stirring the ester POSS in trifluoroacetic acid for one hour at room temperature, it was recovered without any break-up or rearrangement of the POSS core, shown by the ^{29}Si NMR (δ_{Si} -65.90) being exactly the same as for the starting material. Therefore the preparation of a tertiary butyl ester POSS was pursued.

It was originally believed that methyl-3,3-dimethyl-4-pentenoate, used in the synthesis of Feher's ester POSS, could be converted to the tertiary butyl ester and then hydrosilated to the octahydridesilsesquioxane core. However, acid catalysed transesterification and esterification of the 3,3-dimethyl-4-pentenoic acid proved unsuccessful.

This implies that the methyl ester and carboxylic acid molecules are too unreactive to convert to the tertiary butyl ester. Converting carboxylic acid groups to acyl chlorides, the most reactive of the acid derivatives, and then to a less reactive derivative is a common method in the preparation of esters, amides and anhydrides. Oxalyl chloride is often used for the conversion of carboxylic acids to acyl chlorides and it was anticipated that an intermediate could be formed that could be used to make a tertiary butyl ester, which could then be attached to the POSS by hydrosilation (figure 5.3.4).

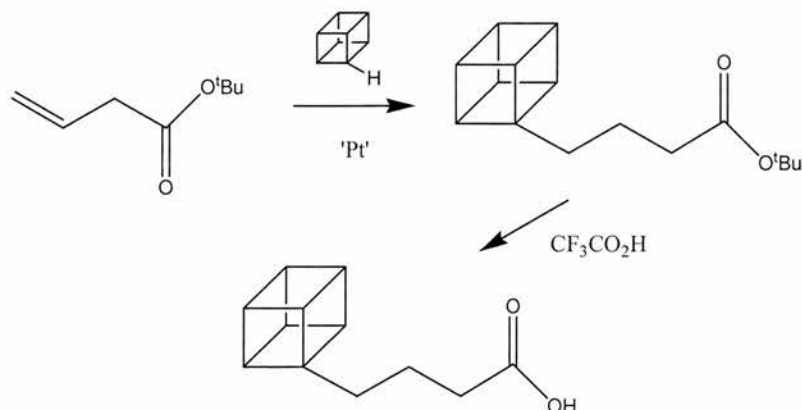
Figure 5.3.4 Preparation of a carboxylic acid POSS via a *t*-butylester POSS reaction mechanism (Si_8O_{12} core depicted as a cube and only one organic 'arm' shown for clarity)



Addition of oxalyl chloride and DMF to the 3,3-dimethylpentenoic acid in dry dichloromethane resulted in effervescence of the reaction mixture. This was expected as carbon monoxide and hydrochloric acid are formed along with the acid chloride. Tertiary butanol and pyridine were added to convert the intermediate to the tertiary butyl ester and after stirring overnight the product was analysed. No satisfactory NMR data were obtained implying that the reaction was unsuccessful.

Due to the lack of time remaining for the project to be completed it was decided to postpone this work and attempt to hydrosilate tertiary-butylbutenoate to the octahydride POSS and convert the product to a carboxylic acid functionalised POSS (figure 5.3.5).

Figure 5.3.5 Reaction mechanism for the preparation of an octabutanoic acid POSS (Si_8O_{12} core depicted as a cube and only one organic 'arm' shown for clarity)

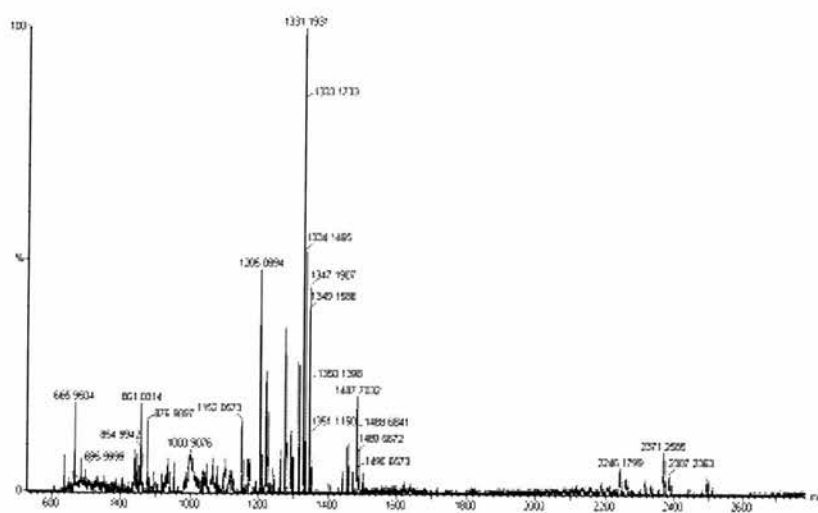


It was anticipated that hydrosilation of tertiary-butylbutenoate to octahydridesilsesquioxane would be as straightforward as hydrosilation of methyl-3,3-dimethylpentenoate to octahydridesilsesquioxane. However, the initial attempt in toluene using Karstedt's catalyst at room temperature resulted in a more complicated ^1H NMR spectrum than expected. No vinyl resonances of the alkene were present suggesting full hydrosilation had taken place but whereas three CH_2 signals and a t-butyl signal were predicted, there were in fact six resonances other than the t-butyl signal.

Although the resolution of the splitting patterns of the proton resonances is poor and the integration does not add up to exactly the correct number of protons, it is postulated that the reaction results in the formation of two types of organic arms attached to the POSS core: the expected linear t-butylbutanoate and the branched t-butylbutanoate resulting from β -addition across the double bond. If this is the case the ratio between the two types of functionality is approximately 1:1.

Further characterisation of the reaction product by mass spectrometry and MALDI-TOF appears to show that the product has a mass of 1331 g mol^{-1} , or breaks down to a product with this mass in the spectrometer. It could be that this mass correlates to a POSS molecule with four t-butyl ester functionalised arms and four carboxylic acid functionalised arms. However, this seems unlikely as it expected that there would be some evidence of POSS molecules with other numbers of t-butyl ester functional groups.

Figure 5.3.6 MALDI-TOF spectrum of the product in the attempted synthesis of a tertiary butyl ester POSS



It is not clear why a mixture of functionalisation occurs in this case as room temperature hydrosilation reactions are usually very ‘clean’ reactions and are better at giving linear products than reactions carried out under reflux. It could also have been expected that the steric bulk of the t-butyl group would aid linear product formation as this would be the least hindered product to form.

Similar results were obtained when the solvent was changed to hexane. It was therefore decided to attempt the reaction under reflux conditions. Performing the reaction at higher temperature may have resulted in a change in the ratio of products forming due to the change in kinetics and which product was favoured. However, no change in ratios was observed.

5.4 Conclusion

The synthesis of carboxylic acid functionalised POSS was attempted *via* the conversion of ester functionalised POSS. A carboxylic acid POSS was not synthesised, however a novel ester functionalised POSS was synthesised *via* the methoxycarbonylation of octavinylsilsesquioxane. Alkoxy carbonylation is a one-step catalytic reaction where a carbonyl group followed by an alkoxy group is inserted onto the terminal end of a vinyl group. It is an extremely efficient reaction with a high conversion rate and selectivity, making it ideal for use on POSS molecules. Although it is possible to perform the reaction at room temperature and under 1 bar CO it was found to work better at 30 bar CO and at 80 °C, reaching 100 % conversion to the desired product after 41 hours. A full catalytic study was not undertaken as it was not the aim of this project, but it may be that different quantities of catalyst and different reaction conditions result in a quicker reaction time.

It was anticipated that the methoxycarbonylation product could be converted to a carboxylic acid functionalised POSS by hydrolysis under mild basic conditions. However, although the conditions used gave full hydrolysis of the ester groups they

were not mild enough to prevent break-up of the POSS core, which is susceptible to acids, bases and oxidising agents. Despite this ester POSS being unsuitable for conversion to a carboxylic acid POSS it may have other applications, for example in the synthesis of dendrimers or polymers.

The preparation of a carboxylic acid POSS may be possible by conversion of a tertiary butyl ester functionalised POSS as it would appear that the core is not susceptible to attack by trifluoroacetic acid. However, this study was unsuccessful in the preparation of a pure, linear chain, t-butyl ester POSS. Therefore significant progress would have to be made on the preparation of this type of functionalised POSS.

Even if a carboxylic acid POSS is synthesised preparation of a coordination polymer will probably not be a trivial matter due to the difficulties in ordered assembly of molecules with such high functionality. It may actually be that this approach to a crystalline porous framework is unfeasible due to the inherent disorder of the organic 'arms' of the POSS molecules and because of the eight fold functionality, which is much higher than that of any other molecule used in coordination polymer synthesis.

5.5 References

1. C. Mellot-Draznieka, S. Girard & G. Férey, *J. Am. Chem. Soc.*, **2002**, *124*, 15326-15335
2. P. Feng, X. Bu & G. D. Stucky, *Nature*, **1997**, *21*, 735
3. M. S. Said, H. W. Roesky, C. Rennekamp, M. Andruh, H.-G. Schmidt & M. Noltemeyer, *Angew. Chem. Int. Ed. Eng.*, **1999**, *38*, 661
4. B. W. Manson, J. J. Morrison, P. I. Couper, P.-A. Jaffrès & R. E. Morris, *J. Chem. Soc. Dalton Trans.*, **2001**, 1123-1127
5. (a) C. Zhang & R. M. Laine, *J. Am. Chem. Soc.*, **2000**, *122*, 6779-6988 (b) F. J. Feher & K. D. Wyndham, *Chem. Commun.*, **1998**, 323-324 (c) F. J. Feher, K. D. Wyndham, D. Soulivong & F. Nguyen, *J. Chem. Soc. Dalton. Trans.*, **1999**, 1491-1497
6. C. Jimenez Rodriguez, D. F. Foster, G. R. Eastham & D. J. Cole-Hamilton, *Chem. Commun.*, **2004**, 1720-1721
7. W. Clegg, G. R. Eastham, M. R. J. Elsegood, R. P. Tooze, X.L. Wang & K. Whiston, *Chem. Commun.*, **1999**, 1877-1878
8. G. R. Eastham, R. P. Tooze, M. Kilner, D. F. Foster & D. J. Cole-Hamilton, *J. Chem. Soc. Dalton Trans.*, **2002**, 1613-1617
9. B. Manson, *Chemical Manipulation of Polyhedral Oligomeric Silsesquioxanes for the Synthesis of Modular Materials and Catalysts*, University of St Andrews, **2002**
10. M. G. Voronkov, T. N. Martynova, R. G. Mirskov & V. L. Belyi, *Zh. Obsch. Khim.*, **1979**, *49*, 1522-1525
11. P. A. Agaskar, *Inorg. Chem.*, **1991**, *30*, 2707

12. B. W. Jennings & M. T. H. Liu, *J. Am. Chem. Soc.*, **1976**, *98*, 6417
13. (a) J. G. Stack, D. P. Curran, S. V. Geib, J. Rebek & P. Ballester, *J. Am. Chem. Soc.*, **1992**, *114*, 7007-7018 (b) B. M. Bachmann & D. Seebach, *Helvetica Chim. Acta*, **1998**, *81*, 2430

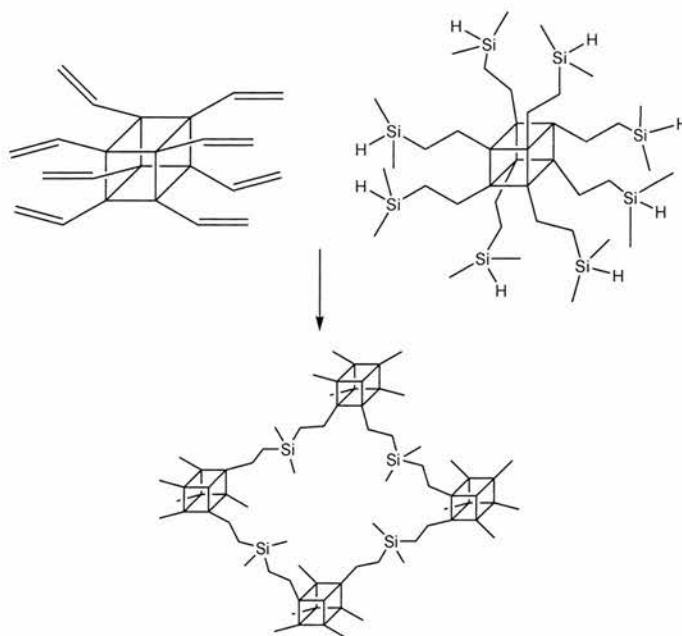
6. Synthesis and Use of Furyl Functionalised POSS in Diels-Alder Reactions

6.1 Introduction

As described earlier, it is possible to prepare porous network polymers from the copolymerisation of cubic POSS. Functionalised materials of this type have the potential to be used in heterogeneous catalysis, challenging silica supported catalysis, organic polymers and zeolites. The porosity of these materials can be altered by varying the length and rigidity of the organic linkers and is also dependent on the efficiency of the polymerisation reaction.

Harrison *et al* and Laine *et al* have shown that porous polymers can be formed by the hydrosilation reaction between octavinyl-POSS and octahydride-POSS (figure 6.1.1) [1]. The polymers have high surface areas with pore sizes in the mesoporous range and are thermally stable to temperatures beyond 300 °C. It was found that the most reactive species for polymerisation were molecules with spacer units between the vinyl and hydride groups and the POSS cage. This is due to improved segmental mobility and increased reactive group flexibility and accessibility.

Figure 6.1.1 Polymer formation through hydrosilation reactions between octavinyl-POSS and octahydride-POSS (Si_8O_{12} core depicted as a cube for clarity)



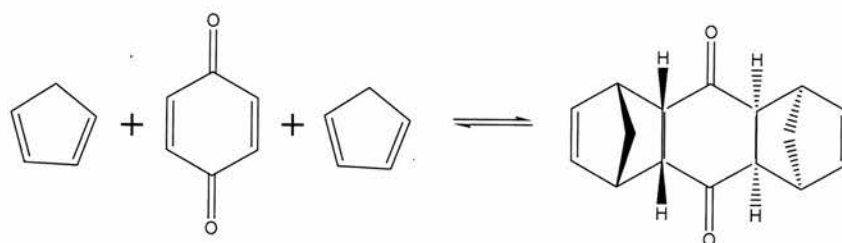
Morris *et al* furthered this work by showing that functionalisation is possible post creation of the polymer by ‘ring-opening’ the sides of some of the POSS units and incorporating metals to give the polymer catalytic properties [2]. It has already been shown that titanium-POSS species are excellent homogeneous catalysts and that titanium-containing silicates are excellent oxidation catalysts [3]. Therefore, further studies of POSS based polymers functionalised with metals such as titanium could see them become rivals of traditional and more established porous heterogeneous catalysts.

This chapter is concerned with the preparation of furyl functionalised POSS species and their reaction with maleimide. It was anticipated that a Diels-Alder reaction (1,4-cycloaddition of alkenes) would occur. Co-polymerisation with a maleimide

functionalised silsesquioxane would then result in the linking of the POSS cubes together to form a porous polymer.

The Diels-Alder reaction is one of the most important reactions in synthetic chemistry [4], utilised in the formation of widely used organic molecules such as morphine [5]. Prof. Otto Diels and his student Kurt Alder first reported it in 1928 when they correctly identified the product of the reaction between cyclopentadiene and quinone (figure 6.1.2) [6]. They won the Nobel Prize for their discovery in 1950.

Figure 6.1.2 Diels-Alder Reaction between cyclopentadiene and quinone

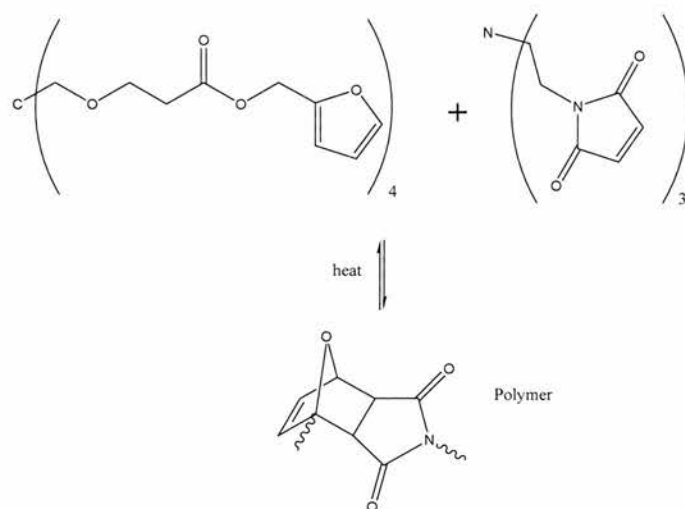


Generally the reaction is between a conjugated diene (a four π electron system) and a dienophile (a two π electron system) [7]. The product (or adduct) contains two new σ bonds that are formed at the expense of two π bonds. σ bonds are stronger than π bonds so the formation of the adduct is energetically favourable although the reaction is generally reversible. The reaction can be made more favourable if the dienophile contains electron-withdrawing groups and the diene has electron-donating groups or *vice versa*.

Additionally, the Diels-Alder reaction is a concerted process, i.e. bond breaking and bond forming happens at the same time. The reaction is highly stereospecific *syn* addition and the configuration of the dienophile is retained in the product. Also, it is necessary for the diene to react in *cis* conformation rather than the *trans* conformation. This is because reaction in the *trans* conformation would result in a six-membered ring with a severely strained *trans* double bond.

Wudl *et al* reported a polymeric material with individual units linked through Diels-Alder reactions in 2002 when a multi-diene (multi-furan) and a multi-dienophile (multi-maleimide) were polymerised to form a highly cross-linked network (figure 6.1.3) [8]. The polymerisation reaction was very efficient, reaching completion ($95\pm 5\%$) after just three hours heating at $75\text{ }^{\circ}\text{C}$. The polymer is a tough solid at room temperatures with excellent mechanical properties. Its most interesting property is that it has the ability to repeatedly mend itself under mild conditions without having to undergo special surface treatment. This property is a direct result of the thermal reversibility of the Diels-Alder reactions that link the individual monomers together and allows fractured parts of the polymer to be fixed many times.

Figure 6.1.3 Polymer formed through Diels-Alder reactions between the monomers reported by Wudl *et al* [8]



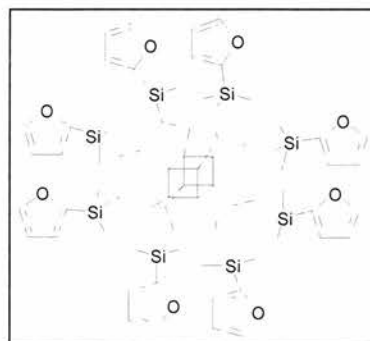
Polymers where only the cross-links between the polymer backbones were formed using Diels-Alder reactions have also been prepared. Chujo *et al* again utilised the reaction between furan and maleimide groups to form an organic-inorganic polymer hybrid [9]. In this case the reaction was performed at ambient temperature with acid catalysis.

The reversibility of Diels-Alder reactions in which bonds can form and break many times is similar to the crystallisation process in zeotype synthesis. It is this reversibility in zeotype synthesis that allows for highly ordered materials as mistakes in the framework formation can be fixed and growth of the crystalline framework continued. It was therefore postulated that if the desired POSS monomers could be prepared they could be polymerised into a highly ordered polymer. As with POSS coordination polymers, by linking cubes through only their corners it is geometrically difficult to fill all available space so a porous material was expected to result.

6.2 Experimental

6.2.1 Preparation of Furyl POSS 1 (FP1) and attempted Diels-Alder Reaction between FP1 and Maleimide

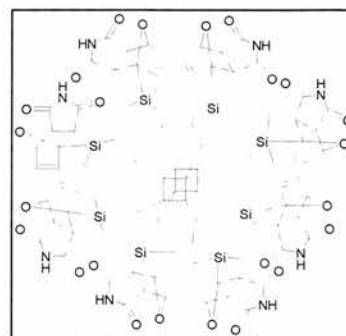
1,3,5,7,9,11,13,15-octakis[dimethylfurylethane]-octasiloxane (FP1). Octavinylsilsesquioxane (0.30 g, 4.739×10^{-4} mol) was dissolved in dry toluene (25 ml) under an argon atmosphere. The solution was cooled to 0 °C and chlorodimethylsilane (0.5 ml, 4.54×10^{-3} mol) and Karstedt's catalyst in xylenes (250 μ l, 1.12×10^{-3} mol) added. The reaction mixture was allowed to warm to RT and stirred for 3 days, resulting in the formation of a green solution. A small amount of the reaction mixture was removed and the solvent was removed *in vacuo* to check for completion of the reaction. ^1H NMR (CDCl_3 , 300 MHz): δ_{H} 0.35 (48H, m, CH_3), 0.60 (16H, m, SiCH_2CH_2) and 0.80 (16H, m, SiCH_2CH_2).



On completion of the hydrosilation *n*-butyl lithium in hexane (2 ml, 2.5 M, 5.00×10^{-3} mol) and furan (0.8 ml, 5.52×10^{-3} mol) were added to dry THF at -78 °C under argon. The reaction mixture was allowed to warm to RT and stirred for 2 hrs 30 mins then transferred by cannular over to the POSS solution and stirred at 0 °C for 3 hrs 30 mins. Any unreacted organolithium was quenched with isopropanol and the solvent was removed *in vacuo* to yield a yellow oil. The oil was dissolved in hexane, filtered to remove the precipitate and purified on a florisil column eluted with diethyl ether.

The solvent was removed *in vacuo* and the residue recrystallised in methanol to yield white needle crystals (0.17 g, 22 %). ^1H NMR (CDCl_3 , 300 Mhz): δ_{H} 0.23 (48H, s, Si- CH_3), 0.55 (16H, m, Si CH_2CH_2), 0.75 (16H, m, Si CH_2CH_2), 6.35 (8H, m, furyl H), 6.61 (8H, m, furyl H) and 7.61 (8H, m, furyl H). ^{13}C NMR (CDCl_3 , 75 MHz): δ_{C} -3.98 (Si- CH_3), 4.31 (Si CH_2), 6.64 (Si CH_2), 109.25 (furyl-C), 119.97 (furyl-C), 146.62 (furyl-C) and 159.21 (furyl-C).

General method for unsuccessful Diels-Alder reactions between FP1 and maleimide. FP1 and maleimide in approximately a ratio of 8:1 moles (1:1 ratio between furyls and maleimide) were dissolved in the desired solvent and stirred or heated for a period of time. In each case no reaction was observed.

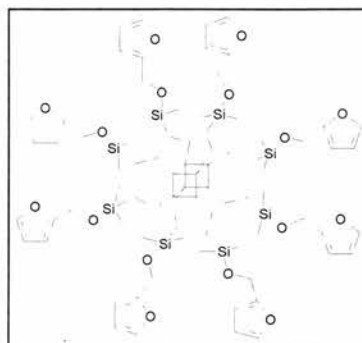


FP1 (g, mol)	Maleimide (g, mol)	Solvent (ml)	T	Time
0.10, 6.09×10^{-5}	0.067, 6.90×10^{-4}	Diethyl ether (10 ml)	RT	4 days (in the dark)
0.10, 6.09×10^{-5}	0.067, 6.90×10^{-4}	Diethyl ether (10 ml)	reflux	2 days
0.08, 4.87×10^{-5}	0.08, 4.87×10^{-5}	toluene (25 ml)	reflux	24 hrs
0.10, 6.09×10^{-5}	0.067, 6.90×10^{-4}	THF (15 ml)	reflux	2 days
0.06, 3.65×10^{-5}	0.06, 6.18×10^{-4}	DCM (3 ml)	reflux	5 hours
0.04, 2.44×10^{-5}	0.03, 3.09×10^{-4}	methanol (12 ml) DCM (0.12 ml)	RT	5 days

6.2.2 Attempted Preparation of Furyl POSS 2 (FP2)

Attempted preparation of Furyl POSS 2 (FP2).

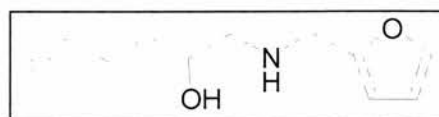
Furfuryl alcohol (0.6 ml, 6.82×10^{-3} mol) and triethylamine (0.9 ml, 6.49×10^{-3} mol) were stirred in dry diethyl ether (30 ml) under an argon atmosphere at 0 °C. To this chlorodimethylsilane (2 ml, 0.018 mol) in dry diethyl ether (15 ml) under



argon was added dropwise with vigorous stirring over a period of 1 hour, during which time a white precipitate formed. The reaction mixture was stirred at 0 °C for 1.5 hours then allowed to warm and stirred at RT for 1 hour. The mixture was filtered by cannular and the solvent removed to yield a clear, colourless oil that was found to be only furfuryl alcohol. ^1H NMR (CDCl_3 , 300 MHz): δ_{H} 4.40 (2H, s, CH_2OH), 6.10 (1H, m, furyl-H), 6.18 (1H, m, furyl-H) and 7.21 (1H, m, furyl-H).

6.2.3 Preparation of Furyl POSS 3 (FP3) and attempted Diels-Alder Reaction Between FP3 and Maleimide

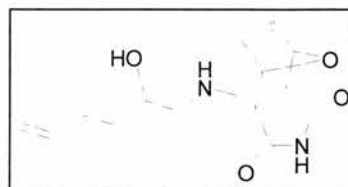
Preparation of a furyl alkene (FA). 1,2-epoxyhexene (1 ml, 8.86×10^{-3} mol) and



furfurylamine (3 ml, 0.034 mol) were refluxed in isopropanol (15 ml) for 4.5 hours. The solvent and excess furfurylamine were removed *in vacuo* to yield a red/brown oil (1.23 g, 71 %). ^1H NMR (CDCl_3 , 300 Mhz): δ_{H} 1.50 (2H, m, $\text{CH}_2\text{CH}_2\text{CH}$), 2.15 (2H, m, $\text{CH}_2\text{CH}_2\text{CH}$), 2.45 (1H, m, CHCH_2NH), 2.70 (1H, CHCH_2NH), 3.63 (1H, m,

CHOH), 3.79 (2H, s, NHCH₂C), 4.94-5.04 (2H, m, CH=CH₂), 5.75-5.89 (1H, m, CH=CH₂), 6.17 (1H, d, J_H 3.07, furyl-H), 6.31 (1H, dd, J_H 1.79 and 1.54, furyl-H) and 7.36 (1H, dd, J_H 1.28 and 0.77, furyl-H). ¹³C NMR (CDCl₃, 75 MHz): δ_C 30.28 (CH₂=CHCH₂), 34.40 (CH₂CH₂CH), 46.19 (NHCH₂C), 54.80 (CHCH₂NH), 69.43 (CHOH), 107.50 (furyl-CH), 110.55 (furyl-CH), 115.12 (CH₂=CH), 138.11 (CH₂=CH), 142.29 (furyl-CH) and 153.90 (furyl-C).

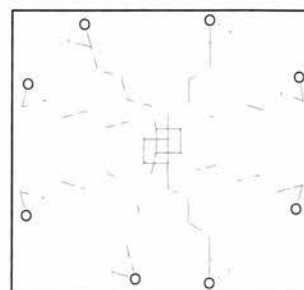
Reaction of FA with maleimide. FA (0.132 g, 6.47×10^{-4} mol) and maleimide (0.098 g, 1.00×10^{-3} mol) were stirred in dichloromethane (10 ml) for 3 days.



The solvent was removed *in vacuo* to yield an orange oil. ¹H NMR (CDCl₃, 300 Mhz): δ_H 1.50 (4H, m, CH₂CH₂CH), 2.15 (4H, m, CH₂CH₂CH), 2.30-3.45 (4H, m, CHCH₂NH and 3H, m, D-A adduct H), 3.63 (2H, m, CHOH), 3.79 (4H, s, NHCH₂C), 4.94-5.04 (4H, m, CH=CH₂), 5.23 (1H, m, D-A adduct H), 5.75-5.89 (2H, m, CH=CH₂), 6.17 (1H, m, furyl-H), 6.25 (1H, m, D-A adduct H), 6.35-6.50 (1H, m, furyl-H), 6.63 (1H, s, maleimide H) and 7.36 (1H, m, furyl-H). MS (ESI) *m/z* (relative intensity): 196.11 (87), 293.12 (4), 294.17 (58), 315.09 (100) and 316.16 (4).

1,3,5,7,9,11,13,15-octakis[epoxyhexane]octasiloxane.

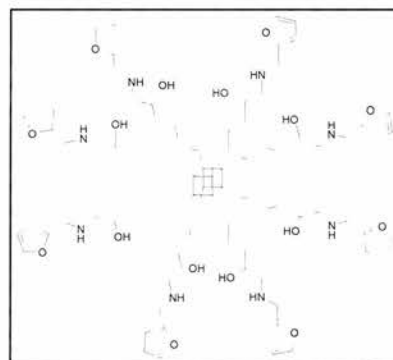
Octahydridesilsesquioxane (0.25 g, 5.86×10^{-4} mol) was dissolved in dry toluene (10 ml) under argon. 1,2-Epoxyhexene (1.2 ml, 0.011 mol) was added and the reaction mixture was cooled to 0 °C. Karstedt's catalyst



in xylenes (70 μ l) was added and the reaction mixture was allowed to warm to RT and stirred for 3 days. The solvent was reduced *in vacuo* and filtered through a florisil plug eluted with diethyl ether (300 ml) to remove the catalyst. The solvent was removed *in vacuo* to yield a clear, colourless oil (0.56 g, 78 %). ^1H NMR (CDCl_3 , 300 Mhz): δ_{H} 0.56 (16H, m, SiCH_2), 1.42 (32H, m, SiCH_2CH_2), 2.39 (8H, m, CH), 2.67 (8H, m, CH), 2.82 (8H, m, CH). ^{13}C NMR (CDCl_3 , 300 MHz): δ_{C} 12.32 ($\text{SiCH}_2\text{CH}_2\text{CH}_2\text{CH}_2$), 23.06 ($\text{SiCH}_2\text{CH}_2\text{CH}_2\text{CH}_2$), 29.40 ($\text{SiCH}_2\text{CH}_2\text{CH}_2\text{CH}_2$), 32.52 ($\text{SiCH}_2\text{CH}_2\text{CH}_2\text{CH}_2$), 52.65 (CH_2CHCH_2), 66.27 (CH_2CHCH_2). ^{29}Si NMR (CDCl_3 , 59.6 MHz): δ_{Si} -66.91, -67.70 and -68.69. MS (ESI) m/z (relative intensity): 1231.06 (100), 1232.07 (64) and 1233.09 (17) (+Na). CHN (calc): 46.30 (47.65) C, 7.87 (7.33) H.

Preparation of furyl POSS 3 (FP3).

1,3,5,7,9,11,13,15-octakis[epoxyhexane]octasiloxane (0.25 g, 2.07×10^{-4} mol) and furfurylamine (0.7 ml, 7.92×10^{-3} mol) were refluxed in isopropanol (20 ml) overnight. The majority of the solvent and excess furfurylamine



were removed *in vacuo* to yield an orange oil (0.35 g, 91 %). ^1H NMR (CDCl_3 , 300 Mhz): δ_{H} 0.60 (16H, bs, SiCH_2), 1.39 (48H, m, $\text{CH}_2\text{CH}_2\text{CH}_2$), 2.40-2.75 (16H, m, CHCH_2NH), 3.57-3.75 (8H, m, CHOH), 3.83 (16H, m, NHCH_2C), 6.11-6.20 (8H, m, furyl-CH), 6.27-6.31 (8H, m, furyl-CH) and 7.32-7.37 (8H, m, furyl-CH). ^{13}C NMR (CDCl_3 , 75 MHz): δ_{C} 21.88 (SiCH_2), 27.45 (SiCH_2CH_2), 32.25 ($\text{SiCH}_2\text{CH}_2\text{CH}_2$), 33.90 (CH_2CHCH_2), 44.80 (NHCH_2C), 53.64 (CHCH_2NH), 68.29 (CHOH), 107.48

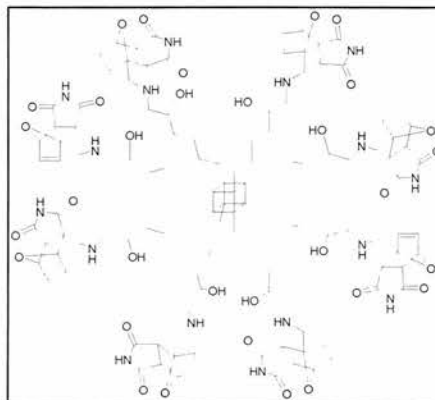
(furyl-CH), 109.28 (furyl-CH), 140.96 (furyl-CH) and 151.80 (furyl-C). ^{29}Si NMR (CDCl_3 , 59.6 MHz): δ_{Si} -66.92, -67.64 and -68.56. CHN (calc): 51.63 (53.20) C, 7.39 (7.31) H, 4.16 (5.64) N.

Reaction between FP3 and maleimide. FP3

(0.14 g, 6.95×10^{-5} mol) and maleimide (0.54 g, 5.56×10^{-4} mol) were stirred in dichloromethane (5 ml) overnight. ^1H NMR

(DMSO, 300 MHz): δ_{H} 0.46-0.66 (80H, bs, SiCH_2), 1.07-1.45 (240H, m, $\text{CH}_2\text{CH}_2\text{CH}_2$),

2.26-2.48 (64H, m, CHCH_2NH and 24H, m, D-A adduct H), 3.24-3.40 (40H, m, CHOH), 3.41-3.85 (80H, m, NHCH_2C), 5.04-5.20 (8H, m, D-A adduct H), 6.20-6.32 (64H, m, furyl-CHs and 8H, m, D-A adduct H), 6.90 (H, s, maleimide H) and 7.50-7.62 (32H, m, furyl-CH).



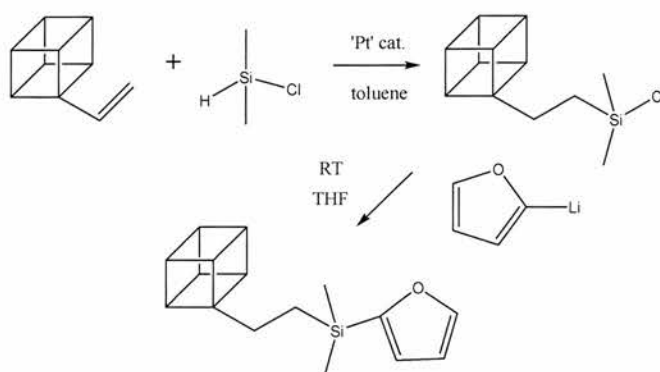
6.3 Results and Discussion

6.3.1 Furyl POSS 1 (FP1) and attempted Diels-Alder Reaction between FP1 and Maleimide

It was believed that a furfurylsilane functionalised POSS would be an ideal target for a monomer with which to perform Diels-Alder reactions. The first target molecule was a POSS molecule with a furfuryl group attached to the end of a dimethylethylsilyl arm

(FP1) as it was anticipated that this molecule would not have any difficulties in undergoing a Diels-Alder reaction with maleimide.

Figure 6.3.1 Mechanism for the preparation of FP1. The POSS core is shown as a cube with only one organic 'arm' for clarity.



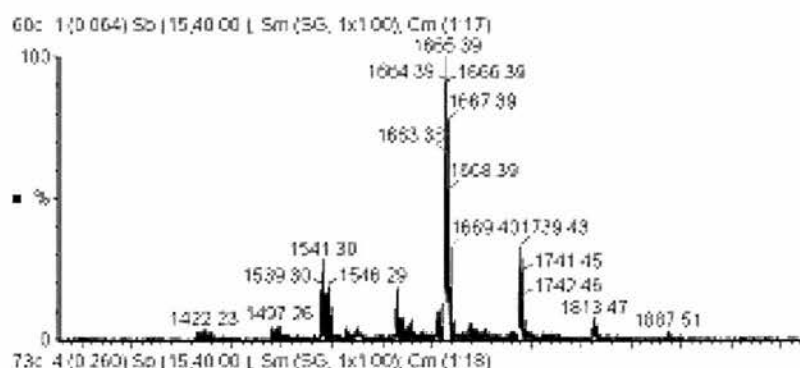
The furyl POSS was prepared by first functionalising octavinylsilsesquioxane with a chlorosilane group by hydrosilation of chlorodimethylsilane to the POSS core. After three days of stirring at room temperature in the presence of Karstedt's catalyst the ¹H NMR of the product showed the expected signals of the desired product (δ_{H} 0.35, 0.60 and 0.80) and no signals of the octavinylsilsesquioxane. Therefore, as far as could be deduced from ¹H NMR, 100 % conversion to the octakis[chloro-dimethylsilyl]ethane]octasiloxane had been achieved.

Due to the sensitivity of the silicon-chlorine bond to moisture, the product was not isolated and the reaction with the furyl lithium was carried out *in situ*. NMR (¹H and ¹³C) confirmed that the desired product had been formed. Purification of the product by chromatography followed by recrystallisation gave the furyl functionalised POSS product as very small, colourless needle crystals. The yield of 22 % was very low

suggesting that the best chromatography conditions were not found. However, despite trying numerous other conditions a better yield could not be obtained.

Despite the presence of single crystals a crystal structure was not obtained due to the poor diffraction of the crystals. As mentioned in chapter five, this is a common problem with POSS materials due to the inherent disorder of the organic arms. However, further confirmation that FPI had been made was obtained from MALDI-TOF spectroscopy. The spectrum showed a large peak at $m/z = 1665$ (figure 6.3.2), which matches the mass of the furyl POSS plus a sodium ion.

Figure 6.3.2 MALDI-TOF spectrum of FPI



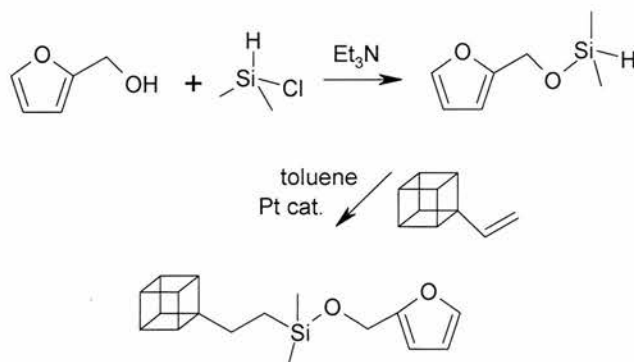
Diels-Alder reactions of this POSS were then attempted with maleimide. The reaction was first tried by stirring the two reactants in the dark as performed by Kwart and Burchuk [10]. No reaction was observed after four days so the reaction mixture was refluxed for a further two days, but still no reaction was observed. Further experiments were carried out under different conditions and using previously reported techniques for similar systems, such as refluxing in toluene, refluxing in

dichloromethane and using copper nitrate as a catalyst, however in each case no reaction was observed [4, 11].

6.3.2 Attempted Preparation of Furyl POSS 2 (FP2)

It was believed that the lack of a reaction happening might be due to the steric hindrance around the furyl group as a result of the close proximity of the two methyl groups and silicon atom. It was therefore decided to attempt to make a POSS molecule where there was less steric hindrance around the furyl group. This was initially attempted by reacting furfuryl alcohol with chlorodimethylsilane to form a furysilane molecule with a spacer group between the furyl and the dimethylsilyl group. It was anticipated that this molecule could then be hydrosilated to the octavinylsilsesquioxane to form a furyl POSS (FP2) on which Diels-Alder reactions could be performed (figure 6.3.3). However, the furysilane molecule could not be prepared successfully so it was decided to follow an entirely different approach.

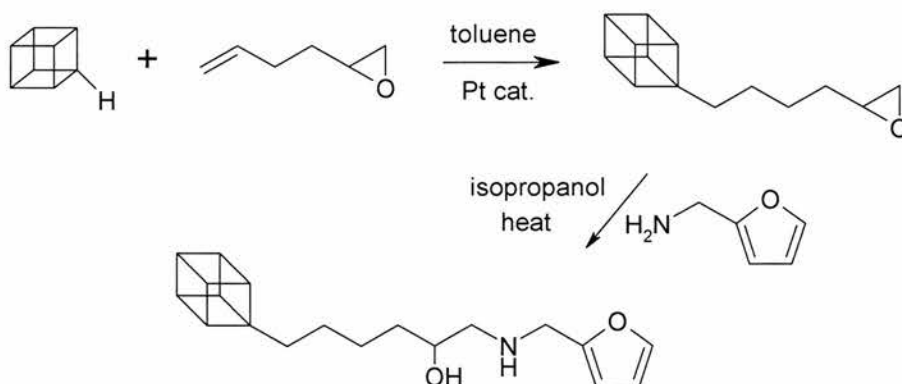
Figure 6.3.3 Mechanism for the proposed synthesis of FP2. The POSS core is shown as a cube with only one organic 'arm' for clarity.



6.3.3 Furyl POSS 3 (FP3) and attempted Diels-Alder Reaction between FP3 and Maleimide

An efficient reaction is between epoxide and amine functionalised molecules [12] and it was anticipated that this reaction could be used to convert an epoxy functionalised POSS to a furyl functionalised POSS by the reaction with furfurylamine (FP3). This would result in a furyl POSS with little steric hindrance around the furyl group and therefore a more likely possibility of a Diels-Alder reaction taking place. It would also have accessible secondary alcohol and amine groups on which further reactions could be performed, so enhancing a polymer formed in this ways utility.

Figure 6.3.4 Mechanism for the preparation of FP3. The POSS core is shown as a cube with only one organic 'arm' for clarity.



However, before attempting to synthesise this molecule it was decided to first check whether the molecule formed between the reaction of 1,2-epoxyhexene and furfurylamine would undergo a Diels-Alder reaction with maleimide. The furyl molecule was prepared by refluxing the two reactants in isopropanol. An

approximately three-fold excess of furfurylamine was used to ensure that only one epoxide reacted with each furfuryl molecule.

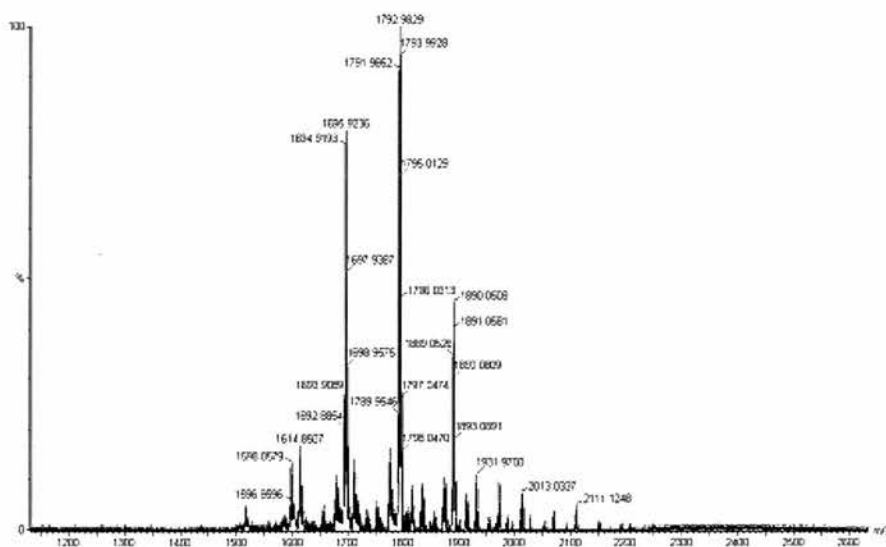
An attempted Diels-Alder reaction of this molecule with maleimide was carried out in refluxing dichloromethane. Although the ^1H NMR was very complicated it suggested that a Diels-Alder reaction had partially taken place. Mass spectrometry confirmed that a product with the same mass as the Diels-Alder adduct had formed ($m/z = 294.17$ [M^+H] and 315.09 [M^+Na]). The mass spectrum also showed the presence of the furfuryl alkene (FA) in the reaction mixture ($m/z = 196.11$). An attempt at purifying the furfuryl alkene Diels-Alder adduct was not made due to a lack of time and because it was only a test reaction, which when applied to the POSS system would not be necessary. Therefore, as it appeared that a Diels-Alder reaction had occurred, the synthesis of a furyl functionalised POSS by this route was proceeded with.

1,2-Epoxyhexene has been used to prepare an epoxy functionalised POSS before by He *et al* in 2004 [12]. Even though the organic arms of this molecule would probably be too long and ‘floppy’ to create an ordered polymer it was decided to synthesise it and convert it to the furyl functionalised molecule, as if polymerisation was successful it may have resulted in a large pored polymer. Preparing shorter chained (or chains with less rotational freedom) epoxy POSS could then be attempted at a later date for the preparation of other polymeric materials.

The epoxyhexane functionalised POSS was prepared by the hydrosilation of 1,2-epoxyhexene to octahydridesilsesquioxane using Karstedt's catalyst. As far as could be deduced from ^1H and ^{13}C NMR the desired product had formed, although the ^{29}Si NMR showed more than one peak (δ_{Si} -66.91, -67.70 and -68.69). As the peak at -66.91 was much larger than the other peaks it was clear that the vast majority of the product was the desired epoxy POSS. Therefore, it was then heated in isopropanol with an excess of furfurylamine to form the furyl functionalised POSS. ^1H NMR confirmed the desired product had formed and did not show any epoxy signals. The ^{29}Si NMR was similar to that of the epoxy POSS showing that the silicate core had remained intact during the reaction and subsequent purification.

The MALDI-TOF spectrum of this furyl POSS contained a large signal at $m/z = 1792$. This correlates to the desired product with a furfurylamine segment lost from one of the arms. The spectrum also showed species where two, three and four furfurylamine segments had been lost. There was no evidence to suggest that products where two epoxide groups had reacted with the same amine group had formed, either from the same POSS molecule or from different molecules to form dimers or larger species.

Figure 6.3.5 MALDI-TOF spectrum of FP3

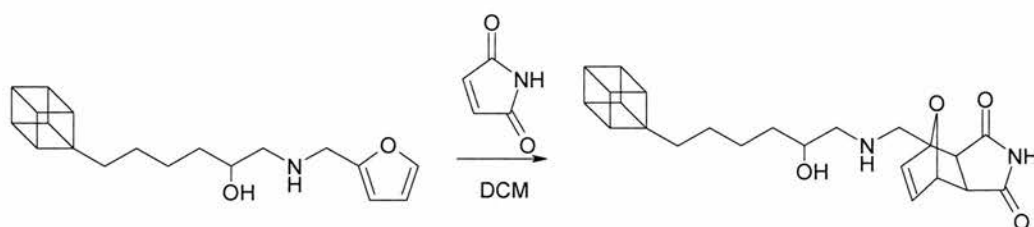


The majority of the solvent and excess furfurylamine could be removed by heating the product under vacuum for a few hours. Lengthening the time of this procedure did not increase the amount of isopropanol removed. This is probably due to it being entangled in the POSS molecule's organic arms, which is not an uncommon problem in POSS chemistry.

The furyl POSS was deemed pure enough to continue with as any impurities might have been able to be washed out on formation of a porous polymer. The reaction with maleimide was carried out at room temperature in dichloromethane (figure 6.3.6). After stirring overnight it could be seen from the ^1H NMR that a reaction had taken place and that about 20 % of the furyl groups had been converted to something else. Although the spectrum was complicated the additional peaks observed suggested that some of the furyl groups had undergone a reaction with the maleimide. Increasing the reaction time and temperature did not increase the level of

conversion. No further spectral analysis could be obtained so the formation of a Diels-Alder adduct on the furyl POSS has not yet been confirmed.

Figure 6.3.6 Mechanism for the formation of the Diels-Alder adduct of FP3. The POSS core is shown as a cube with only one organic 'arm' for clarity.



6.4 Conclusion

A novel dimethylfurylsilyl functionalised POSS (FP1) has been synthesised and obtained as a crystalline solid with a 22 % yield. This yield is very low but this is a common occurrence in POSS chemistry due to their instability in chromatography columns and because crystallisation is often not possible due to their inherent disorder.

The Diels-Alder reaction was attempted between this molecule and maleimide using a variety of conditions but no reaction was observed. This may have been due to too much steric hindrance around the furyl group, which is caused by the close proximity of the dimethylsilyl group. It was therefore attempted to synthesise furyl POSS species with less steric hindrance around the furyl group.

A second furyl POSS (FP3) that has more space around the furyl group was synthesised from an epoxyhexane POSS but it has not yet been fully purified. However, initial experiments suggest that it does undergo some Diels-Alder reaction with maleimide. It is therefore believed that should an appropriate furyl functionalised POSS be reacted with a maleimide functionalised POSS a polymeric material will result. The reversibility of the Diels-Alder reaction may lead to it being a highly ordered polymer.

6.5 References

1. (a) P. G. Harrison, *J. Organomet. Chem.*, **1997**, *542*, 141-183 and references therein (b) C. Zhang, F. Babonneau, C. Bonhomme, R. M. Laine, C. L. Soles, H. A. Hristov & A. F. Yee, *J. Am. Chem. Soc.*, **1998**, *11*, 8380-8391
2. J. J. Morrison, C. J. Love, B. W. Manson, I. J. Shannon & R. E. Morris, *J. Mater. Chem.*, **2002**, *12*, 3208-3212
3. (a) H. C. L. Abbenhuis, S. Krijnen & R. A. van Santen, *Chem. Commun.*, **1997**, 331-332 (b) T. Maschmeyer, F. Rey, G. Sankar & J. M. Thomas, *Nature*, **1995**, *378*, 159
4. K. C. Nicolaou, S. A. Snyder, T. Montagnon & G. Vassilikogiannakis, *Angew. Chem. Int. Ed. Eng.*, **2002**, *41*, 1668-1698 and references therein
5. M. Gates & G. Tschudi, *J. Am. Chem. Soc.*, **1952**, *74*, 1109-1110
6. O. Diels & K. Alder, *Justus Liebigs Ann. Chem.*, **1928**, *460*, 98-122
7. T. W. G. Solomons, *Organic Chemistry*, Wiley, New York, **1996**, 6th ed.

8. X. Che, M. A. Dam. K. Ono, A. Mal, H. Shen, S. R. Nutt, K. Sheran & F. Wudl, *Science*, **2002**, *295*, 1698
9. Y. Imai, H. Itoh, K. Naka & Y. Chujo, *Macromolecules*, **2000**, *33*, 4343-4346
10. H. Kwart & I. Burchuk, *J. Am. Chem. Soc.*, **1952**, *74*, 3094-3097
11. (a) A. Robertson, D. Philp & N. Spencer, *Tetrahedron*, **1999**, *55*, 11365-11384
(b) A. Grondin, D. C. Robson, W. E. Smith & D. Graham, *J. Chem. Soc. Perkin Trans. 2*, **2001**, 2136-2141
12. J. Huang, Y. Xiao, K. Y. Mya, X. Liu, C. He, J. Dai & Y. P. Siow, *J. Mater. Chem.*, **2004**, *14*, 2858-2868

7. General Conclusion

7.1 Eutectic Mixtures in the Synthesis of Porous Materials

The preparation of coordination polymers and aluminium cobalt phosphates using eutectic mixtures was moderately successful. Although no porous or novel coordination polymers were prepared and only one porous aluminium cobalt phosphate was formed, there was evidence that the eutectic mixture could play a significant part in the synthesis of these materials if the correct conditions were found.

Two layered cobalt/nickel-diphosphonate structures were formed; one with diphosphonate pillars containing two benzyl groups and one with diphosphonate pillars containing one benzyl group. The structures are very similar but differ in the orientation of the organic pillars and topology of the metal oxide layers. Although both frameworks have already been prepared before using solvothermal methods [1] they are of interest as they show that the metal that can be used in the formation of metal-diphosphonate frameworks is dependent on what eutectic mixture is used. Therefore, the eutectic mixture is playing an active role in the synthesis of the framework, which means that by altering or tuning the eutectic mixture further frameworks may be formed, some of which might be novel and only formed using eutectic mixtures as solvent.

Two copper-carboxylate frameworks with chain topologies were also formed using eutectic mixtures as solvent. Both frameworks have components that came directly from the eutectic mixture however neither framework is novel [2] and it appears likely that the copper-succinate framework was not formed ionothermally but on dissolving the eutectic mixture in water after the reaction was complete.

The copper-benzenedicarboxylate framework was formed ionothermally and contained amine ligands that came from the break-up of the eutectic mixture. Therefore, further reactions may result in a porous coordination polymer 'templated' by amine or ammonia. As there are other examples of eutectic mixture components forming part of the coordination polymer framework made from carboxylic acid containing building blocks [3] it appears that this route rather than the metal-diphosphonate route is the most promising for the synthesis of novel materials.

It was also shown that eutectic mixtures could be used successfully in the preparation of aluminium cobalt phosphates. Three frameworks were formed: a porous framework with the levyne topology and novel layered and chain materials. The layered material (CoAlPO-1) was found to consist of inorganic layers sandwiched between layers of well-ordered choline molecules. It is believed that it is the first zeolitic material formed ionothermally where the 'template' has not been prepared *in situ* but is an actual component of the solvent.

By raising the reaction temperature it was possible to prepare another aluminium cobalt phosphate framework. This material, termed CoAlPO-3, has the levyne

topology and has already been prepared solvothermally [4]. However, it does show that the succinic acid/choline chloride eutectic mixture can be used to prepare porous materials. This framework was also shown to be 'templated' by choline from the eutectic mixture proving that the use of stable eutectic mixtures is a viable way of template delivery in zeotype synthesis.

The incorporation of choline into the CoAlPO materials is a very significant step forward in ionothermal synthesis. Choline is very cheap and non-toxic, and showing that these solvent systems can provide such a template could make this a piece of work with significant impact. This is particularly true in industrial synthesis where there is a great need for cheap and safe synthetic methods.

Another interesting result of the cobalt aluminium phosphate syntheses is the presence of cobalt-chlorine bonds in the CoAlPO-1 framework, a bond type that has never been observed before in zeotype materials. It may be possible to use this functionality in the formation of interesting materials such as catalysts. It may also be possible to form other novel bond types by altering the eutectic mixture and utilising it in the preparation of functional materials.

Before such projects can be undertaken it will be necessary to synthesise phase pure cobalt aluminium phosphate frameworks. Both CoAlPO-1 and CoAlPO-3 samples also contained a dense aluminophosphate material and CoAlPO-1 was also found to contain an aluminium cobalt phosphate chain framework, termed CoAlPO-2. This minor product was 'templated' by the macrocycle cyclam, an additive that had to be

added to the reaction mixture in order to prepare CoAlPO-1. This result shows that eutectic mixtures can be used solely as the reaction solvent, which is still of interest as their vanishingly low vapour pressure means that reactions can be performed at lower pressure than in traditional methods, eliminating some of the safety concerns of zeotype synthesis.

7.2 POSS Molecules in the Synthesis of Porous Materials

The preparation of porous materials using POSS molecules as building blocks proved to be very difficult. Functionalising the POSS molecules with appropriate groups was complicated by the nature of the core, its instability to a number of reaction conditions, and the need to use extremely high-yielding reactions when attaching the organic arms.

Despite the problems associated with POSS synthesis a novel ester-functionalised POSS was prepared by use of a palladium complex catalysed methoxycarbonylation reaction. A crystal structure was obtained for this molecule, which is often not possible with POSS molecules due to the inherent disorder of the organic 'arms'. Attempts were made to convert this molecule to a carboxylic acid POSS for use in coordination polymer synthesis, but all were unsuccessful. However, even though this POSS could not be converted to a carboxylic acid functionalised material it may be possible to use it in the preparation of other potentially useful molecules such as dendrimers [5].

No other POSS molecules that could be used in the preparation of coordination polymers were synthesised but two novel furyl functionalised POSS were prepared that it was thought could be used in the formation a polymer. It was postulated that by linking appropriately functionalised POSS molecules through Diels-Alder reactions a highly ordered porous polymer would result with similar self-healing properties to that prepared by Wudl *et al* [6].

At first the idea seemed to be very promising but a POSS molecule functionalised with a furyl group attached to a dimethylsilyl group (FP1) did not undergo a Diels-Alder reaction with maleimide. This is possibly due to there being too much steric hindrance around the furyl group for the reaction to occur. An attempt at preparing a similar molecule but with more space between the furyl and the dimethylsilyl group was unsuccessful.

A second furyl POSS (FP3) prepared from an epoxyhexane POSS [7] precursor was obtained. This POSS has less steric hindrance around the furyl group but a pure sample was not obtained, possibly due to side reactions occurring on the POSS or due to impurities and the solvent being too entangled between the organic 'arms'. However, it did show at least some reaction with maleimide so it may be possible to use this molecule in the preparation of a porous polymer. If an appropriate maleimide POSS can be synthesised, multiple Diels-Alder reactions between the two species may result in a highly ordered porous polymer.

7.3 References

1. N. Stock & T. Bein, *J. Solid St. Chem.*, **2002**, *167*, 330-336
2. (a) S. G. Ang, B. W. Sun and S. Gao, *Inorg. Chem. Commun.*, **2004**, *7*, 795-798
(b) B. Paul, B. Zimmermann, K. M. Fromm and C. Janiak, *Zeitschrift Fur Anorganische Und Allgemeine Chemie*, **2004**, *630*, 1650-1654
3. (a) J.-H. Liao, P.-C. Wu and Y.-H. Bai, *Inorg. Chem. Commun.*, **2005**, *8*, 390-392
(b) Z. Lin & R. E. Morris, Manuscript in preparation.
4. P. A. Barrett and R. H. Jones, *Phys. Chem. Chem. Phys.*, **2000**, *2*, 407-412
5. (a) P. I. Coupar, P.-A. Jaffrès & R. E. Morris, *J. Chem. Soc. Dalton Trans.*, **1999**, 2183-2187 (b) B. Hong, T. P. S. Thoms, H. J. Murfee & M. J. Lebrun, *Inorg. Chem.*, **1997**, *36*, 6146-6147 (c) L. Ropartz, R. E. Morris, D. F. Foster & D. J. Cole-Hamilton, *Chem. Commun.*, **2001**, 361-362 (d) K. J. Haxton, D. J. Cole-Hamilton & R. E. Morris, *J. Chem. Soc. Dalton Trans.*, **2004**, 1665-169
6. X. Che, M. A. Dam. K. Ono, A. Mal, H. Shen, S. R. Nutt, K. Sheran & F. Wudl, *Science*, **2002**, *295*, 1698
7. J. Huang, Y. Xiao, K. Y. Mya, X. Liu, C. He, J. Dai & Y. P. Siow, *J. Mater. Chem.*, **2004**, *14*, 2858-2868

8. Further Work

8.1 Eutectic Mixtures in the Synthesis of Porous Materials

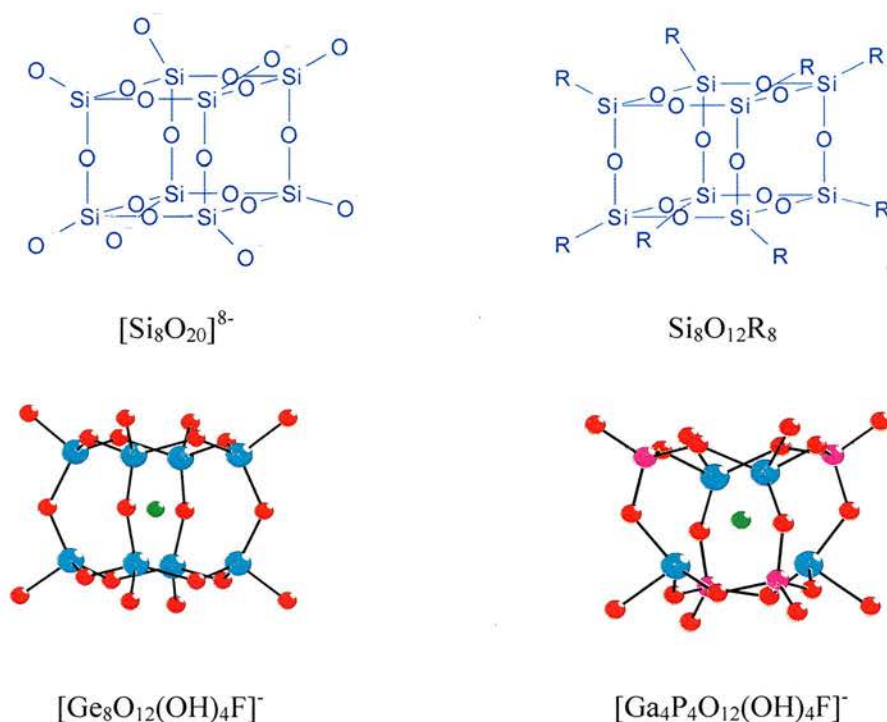
Although eutectic mixtures have shown great promise for use in the preparation of porous materials there is still a lot of progress to be made. All coordination polymers formed using eutectic mixtures in this project can be formed just as easily (and often more so) using conventional techniques. Therefore, a way has to be found in which the eutectic mixture plays a significant part in the preparation of novel crystalline porous materials.

In the synthesis of zeolitic materials using eutectic mixtures progress has to be made in preparing phase pure products. The potential of this method has been shown in the preparation of novel frameworks and bond types that can possibly be utilised in the preparation of novel materials. If this can be done there may then be a chance of materials formed in this way finding useful applications.

Not investigated in this project was the use of fluoride as a mineralising agent. It was not necessary for the synthesis of metal aluminophosphate frameworks but may be necessary for the formation of an aluminophosphate. Adding fluoride may facilitate P-O-Al formation and would significantly alter the pH of the system meaning that the addition of cyclam or other reagents could be avoided. Most importantly it would provide a negative charge for the framework, allowing 'templation' by the positively charged choline.

Perhaps the most promising use of eutectic mixtures (and ionic liquids) is in the preparation of designed zeolitic materials from molecular SBU analogues, such as the D4R silicates, germanates and gallium phosphates [1]. Previous attempts at using these molecular SBUs in zeolite synthesis by hydrothermal and solvothermal routes have resulted in them breaking up or rearranging during the reaction [2]. This is because it is difficult to control what bonds will form and which will break during the condensation process. Other difficulties include, for example, that the germanate D4R is very susceptible to break-up in water, the best results using it coming when an almost dry gel is used in the reaction.

Figure 8.1.1 Molecular double-four ring units (D4Rs)



Ionothermal synthesis is a much milder method than either hydrothermal or solvothermal techniques. Chains, layered and partially condensed structures form

frequently, showing that bond formation is not as facile as in hydrothermal synthesis [3]. It is presumed that bond breaking is just as difficult so this may therefore mean that the intermolecular bonds in the D4R analogues are less likely to break than new bonds between the molecules are to form.

The molecules which would show most potential for this type of designed zeotype synthesis are the gallium phosphate D4R analogue with occluded fluoride and the germanate D4R analogue. This gallium phosphate has perhaps a better chance of remaining intact than the analogue with occluded oxygen as fluoride is more commonly found inside D4R units in zeolites, so it may be that fluoride templates their formation better and would therefore be more likely to hold the D4R intact during the reaction.

The germanate D4R analogue is also attractive as it has been shown by O’Keeffe and Yaghi to be particularly stable because of the flexibility of the Ge-O-Ge linkages [4]. Additionally, Corma *et al* have shown that germanium can direct structures towards those containing D4Rs [5]. It is also noteworthy that the germanate D4R molecule synthesised contains an occluded fluoride, adding weight to the theory that fluoride helps to template D4R formation.

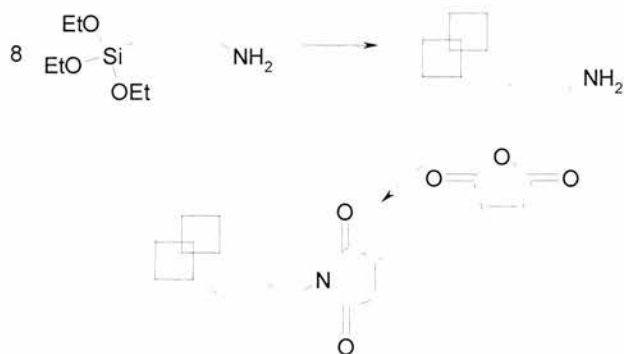
8.2 POSS Molecules in the Synthesis of Porous Materials

The future preparation of porous materials from octa-carboxylic acid functionalised POSS appears to be less promising than the ionothermal method. Perhaps if a tertiary butyl ester functionalised POSS can be synthesised and converted to a carboxylic acid functionalised material it could be used to prepare a porous material. It may be possible to achieve this by adapting the methoxycarbonylation reaction by using tertiary butanol instead of methanol (t-butoxycarbonylation). However, this may result in the reaction having a lower conversion rate due to the increased steric bulk of the solvent. It may also be possible to use water instead of methanol (hydroxycarbonylation) to form a carboxylic acid POSS in one step. Currently high enough conversion rates have not been achieved with this reaction for use on POSS systems but further advances may allow it to be tried on POSS molecules in the future. Even if a carboxylic acid POSS is synthesised, due to their complexity and inherent disorder the actual assembly of these molecules may prove to be just as difficult to achieve.

If an appropriate POSS is to be synthesised and used in this way it may have to be a nitrile, pyridine or phosphonic acid functionalised moiety. Although the product of the first two may not be as thermally stable as one prepared from carboxylic acid functionalised cubes, due to the octa-functionality it should still be stable. It is possible to prepare phosphonic acid functionalised POSS but as with the majority of reactions involving these molecules it is difficult to prepare a pure product in a high yield.

Using POSS molecules in polymer synthesis is perhaps more likely to achieve good results as a high degree of order does not have to be obtained. There are also a large variety of polymerisation reactions that can be utilised. Preparing a copolymer where the POSS monomers are linked through Diels-Alder reactions should be possible. For this to happen two monomers that readily undergo Diels-Alder reactions will have to be prepared. A maleimide functionalised POSS that may be suitable for Diels-Alder reaction could be prepared, for example, by the reaction between a primary amine functionalised POSS and maleic acid or maleic anhydride. It may be possible to carry out the polymerisation step using an ionic liquid or eutectic mixture as solvent and catalyst. The efficiency of Diels-Alder reactions has already been shown to be improved in a eutectic mixture prepared from zinc chloride and choline chloride [6].

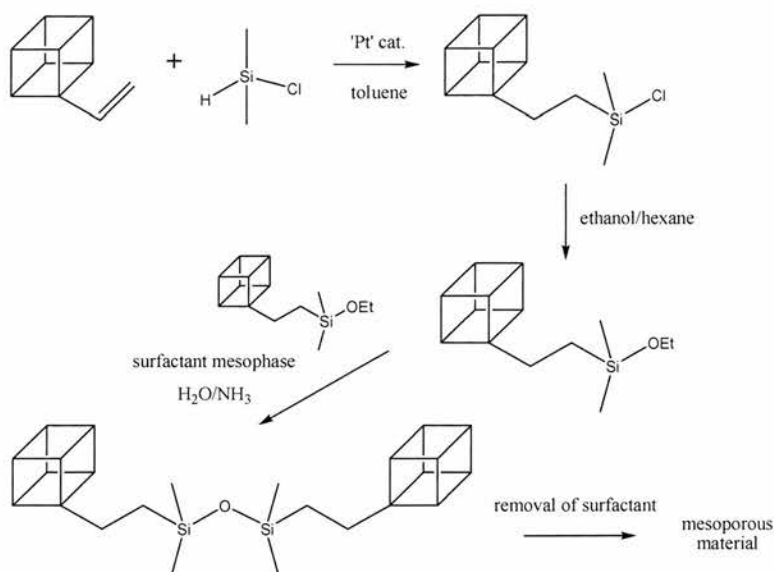
Figure 8.2.1 Possible mechanism for the preparation of a maleimide POSS (Si_8O_{12} core depicted as a cube and only one organic 'arm' shown for clarity)



It may be possible to form POSS networks with cavities in the mesopore range by using techniques adapted from mesoporous silicate chemistry. Cyclic silsesquioxanes with the chemical formula $[(EtO)_2Si(CH_2)]_3$ have been shown to be useful in the preparation of organosilicate materials with well-ordered mesopores [7]. The

materials are formed by the self-assembly of the silsesquioxane precursors around a surfactant mesophase *via* hydrolysis of the ethoxysilyl groups to form Si-O-Si linkages. This technique could be adapted to suit POSS molecules by conversion of octa-chlorodimethylsilyl functionalised POSS molecules to octa-dimethylethoxysilyl POSS molecules followed by the self-assembly reaction. Care would have to be taken though to ensure the reaction conditions were mild enough to keep the POSS core intact and that it was not destroyed on removal of the surfactant, although even if some POSS core breakage did occur the resultant material may still be of interest.

Figure 8.2.2 Possible mechanism for the preparation of a mesoporous organosilicate from POSS molecules (Si_8O_{12} core depicted as a cube and only one organic 'arm' shown for clarity).



8.3 References

1. (a) I. Hasegawa & S. Sakka, *ACS Symp. Ser.*, **1989**, 398, 140 (b) L. A. Villaescusa, P. Lightfoot & R. E. Morris, *Chem. Commun.*, **2002**, 2220-2221 (c) D. S. Wragg & R. E. Morris, *J. Am. Chem. Soc.*, **2000**, 122, 11246-11247 (d) S. Kallus, J. Patarin & B. Marler, *Microporous Mater.*, **1996**, 7, 89
2. (a) D. S. Wragg, A. M. Z. Slawin & R. E. Morris, *J. Mater. Chem.*, **2001**, 11, 1850-1857 (b) L. A. Villaescusa, P. S. Wheatley, R. E. Morris & P. Lightfoot, *J. Chem. Soc. Dalton Trans.*, **2004**, 820-824
3. (a) E. R. Cooper, C. D. Andrews, P. S. Wheatley, P. B. Webb, P. Wormald and R. E. Morris, *Nature*, **2004**, 430, 1012-1016 (b) E. R. Parnham, P. S. Wheatley & R. E. Morris, *Chem. Commun.*, **2006**, 380-382 (c) E. R. Parnham & R. E. Morris, *J. Am. Chem. Soc.*, **2006**, in press
4. M. O'Keeffe & O. M. Yaghi, *Chem. Eur. J.*, **1999**, 5, 2796
5. (a) A. Corma, M. T. Navaro & F. Rey, *Angew. Chem. Int. Ed. Eng.*, **2001**, 40, 2796 (b) A. Corma, F. Rey, J. Ruis, M. J. Sabater & S. Valencia, *Nature*, **2004**, 431, 287
6. A. P. Abbott, G. Capper, D. L. Davies, R. K. Rasheed & V. Tambyrajah, *Green Chemistry*, **2002**, 4, 24-26
7. K. Landskron, B. D. Hatton, D. D. Perovic & G. A. Ozin, *Science*, **2003**, 302, 266

9. Acknowledgements

Firstly, I would like to thank my supervisor, Professor Russell Morris, for his guidance and support. I would also like to thank the past and present members of the Morris group who have helped me and made it an enjoyable place to work, especially Lynsey Parke, Emily Parnham, Duncan Robertson, Chris Andrews, Paul Wheatley, Meredith Hearshaw and David Wragg.

Thanks also go to Cristina Jimenez-Rodriguez for her help with the methoxycarbonylation reaction and Professor David Cole-Hamilton and Lucite International for use of the methoxycarbonylation catalyst. I also thank Professor Alex Slawin for her assistance with obtaining and solving single crystal x-ray diffraction data and all the technical staff for their help.

I would also like to thank my family, Richard Riggs, Alison Dunwoody, Tim Coombs, Ross McCluskey, Jay Tzeng and all my other friends who have helped me with the chemistry or have provided much needed distractions from it.

Lastly, I thank the EPSRC/The Edinburgh and St Andrews Research School of Chemistry for funding the project.

10. Appendix

10.1 Crystal Data for CoAlPO-1

Table 1. Atomic coordinates ($\times 10^4$) and equivalent isotropic displacement parameters ($\text{\AA}^2 \times 10^3$) for CoAlPO-1. $U(\text{eq})$ is defined as one third of the trace of the orthogonalized U_{ij} tensor.

	x	y	z	$U(\text{eq})$
Co(1)	4829(2)	-3059(2)	7210(2)	39(1)
Co(2)	1014(2)	-1923(2)	2802(2)	37(1)
P(1)	5146(2)	-4479(3)	6036(3)	38(1)
Cl(2)	1386(3)	-1464(3)	1152(4)	67(1)
Cl(1)	4348(3)	-3462(3)	8859(3)	67(1)
P(4)	707(2)	-502(2)	3965(3)	38(1)
P(5)	3838(2)	-1343(2)	5871(3)	35(1)
P(6)	-694(2)	-3648(2)	4126(3)	32(1)
P(7)	6918(2)	-1863(3)	5739(3)	36(1)
P(8)	83(2)	-3068(3)	6999(3)	40(1)
P(9)	2327(2)	-3120(3)	4253(3)	37(1)
P(11)	6162(3)	-1934(3)	2991(3)	40(1)
Al(1)	1942(3)	-1744(3)	5370(3)	37(1)
Al(2)	4475(3)	-3598(3)	4131(3)	35(1)
Al(3)	5809(3)	-653(3)	4188(3)	37(1)
Al(4)	9006(3)	-1396(3)	5841(3)	36(1)
Al(6)	380(3)	-4339(3)	5799(3)	35(1)
Al(8)	7139(3)	-3262(3)	4663(3)	32(1)
O(1)	2027(7)	-2641(8)	3283(8)	53(3)
O(19)	6543(6)	-1735(7)	1929(7)	38(2)
O(20)	4016(6)	-597(6)	6310(8)	41(2)
O(21)	4946(6)	-5551(6)	6364(7)	38(2)
O(22)	4984(7)	-4256(6)	6917(8)	43(3)
O(23)	6603(7)	-1086(7)	4906(8)	49(3)
O(24)	270(7)	-5578(8)	6308(7)	50(3)
O(25)	6089(7)	-2285(7)	6685(7)	45(3)
O(26)	9674(7)	-991(6)	4571(8)	44(3)
O(27)	2820(6)	-1216(6)	5697(7)	38(2)
O(28)	-183(7)	-3303(7)	8073(7)	38(2)

O(29)	2500(7)	-2387(6)	4672(8)	45(3)
O(30)	9299(6)	-579(6)	6347(7)	40(2)
O(31)	3854(7)	-2341(7)	6566(9)	57(3)
O(32)	4486(7)	-3981(7)	5378(8)	48(3)
O(33)	1057(7)	-2437(7)	6498(8)	46(3)
O(34)	-281(7)	-2650(6)	3423(9)	50(3)
O(35)	162(7)	-4018(6)	6797(9)	49(3)
O(36)	6836(7)	-2555(7)	3583(8)	43(3)
O(37)	7329(7)	-2656(7)	5372(8)	50(3)
O(38)	1386(7)	-826(7)	4648(8)	48(3)
O(39)	3304(6)	-3553(7)	4022(7)	41(2)
O(40)	8211(6)	-3760(7)	4298(8)	47(3)
O(41)	5142(7)	-2481(6)	3406(9)	53(3)
O(42)	1025(7)	-738(7)	3053(8)	51(3)
O(43)	4599(7)	-1050(8)	4868(9)	58(3)
O(44)	6220(6)	-4196(6)	5360(9)	51(3)
O(45)	7755(6)	-1394(6)	5950(7)	39(2)
O(46)	9301(6)	-2555(6)	6519(9)	47(3)
O(47)	6083(7)	-984(6)	3192(8)	47(3)
O(48)	-472(8)	-3915(9)	5126(9)	62(3)
O(49)	1562(7)	-3927(7)	5006(8)	55(3)
O(201)	-2129(13)	-4025(11)	9022(11)	110(6)
O(202)	9083(9)	2831(10)	875(10)	79(4)
O(203)	8204(9)	-2202(9)	868(10)	76(4)
O(204)	5792(10)	-1086(12)	405(9)	90(5)
N(1)	-2780(10)	-5568(8)	8259(9)	43(3)
N(2)	8883(8)	548(12)	1651(9)	58(4)
N(3)	6133(10)	-485(11)	-1819(11)	67(5)
N(4)	7852(10)	-4522(11)	1661(9)	56(4)
C(2)	8683(17)	126(14)	2794(14)	75(6)
C(3)	9936(12)	976(18)	1192(19)	96(8)
C(4)	8189(11)	1268(14)	1366(17)	71(6)
C(5)	8266(13)	2201(13)	1560(14)	68(6)
C(7)	6374(16)	118(19)	-1305(19)	122(11)
C(9)	6280(16)	99(14)	-2875(15)	77(6)
C(11)	-2726(14)	-3874(13)	8308(17)	79(7)
C(13)	-2032(17)	-5969(17)	8799(17)	95(8)
C(14)	-3524(16)	-6398(16)	8445(13)	90(8)
C(15)	-2284(12)	-5138(14)	7142(12)	60(5)
C(16)	-3352(12)	-4865(12)	8558(14)	58(5)
C(17)	6999(15)	-4041(14)	1311(17)	81(6)
C(20)	6762(18)	-1300(18)	-1746(14)	93(8)
C(21)	7583(18)	-4970(30)	2724(19)	187(19)
C(22)	8684(15)	-2883(16)	1471(19)	87(7)
C(23)	8744(19)	-3830(20)	1250(20)	142(13)
C(24)	8150(30)	-5260(30)	1320(30)	220(20)
C(25)	8700(20)	-290(17)	1310(20)	113(10)
C(26)	5070(13)	-913(16)	-1399(12)	67(6)

Table 2. Bond lengths [Å] and angles [°] for CoAlPO-1.

Co(1)-O(25)	1.944(9)	Al(1)-O(33)	1.772(11)
Co(1)-O(31)	1.972(10)	Al(2)-O(39)	1.707(9)
Co(1)-O(22)	2.010(10)	Al(2)-O(41)	1.735(10)
Co(1)-Cl(1)	2.242(5)	Al(2)-O(32)	1.752(12)
Co(2)-O(1)	1.916(10)	Al(2)-O(21)#4	1.809(11)
Co(2)-O(34)	1.952(9)	Al(3)-O(47)	1.712(12)
Co(2)-O(42)	1.961(12)	Al(3)-O(23)	1.715(9)
Co(2)-Cl(2)	2.234(5)	Al(3)-O(20)#1	1.732(10)
P(1)-O(22)	1.454(11)	Al(3)-O(43)	1.732(11)
P(1)-O(21)	1.501(9)	Al(4)-O(45)	1.737(9)
P(1)-O(32)	1.524(10)	Al(4)-O(46)	1.766(10)
P(1)-O(44)	1.558(10)	Al(4)-O(26)	1.773(11)
P(4)-O(42)	1.509(12)	Al(4)-O(30)	1.774(11)
P(4)-O(30)#1	1.513(10)	Al(6)-O(35)	1.708(12)
P(4)-O(26)#2	1.529(9)	Al(6)-O(24)	1.716(11)
P(4)-O(38)	1.531(8)	Al(6)-O(48)	1.737(10)
P(5)-O(31)	1.474(10)	Al(6)-O(49)	1.747(10)
P(5)-O(43)	1.523(12)	Al(8)-O(37)	1.717(10)
P(5)-O(27)	1.528(8)	Al(8)-O(44)	1.726(9)
P(5)-O(20)	1.555(10)	Al(8)-O(36)	1.734(10)
P(6)-O(34)	1.485(9)	Al(8)-O(40)	1.745(10)
P(6)-O(40)#2	1.507(8)	O(20)-Al(3)#1	1.732(10)
P(6)-O(48)	1.523(11)	O(21)-Al(2)#4	1.809(11)
P(6)-O(24)#3	1.587(12)	O(24)-P(6)#3	1.587(12)
P(7)-O(25)	1.514(10)	O(26)-P(4)#5	1.529(9)
P(7)-O(23)	1.522(9)	O(30)-P(4)#1	1.513(10)
P(7)-O(45)	1.542(9)	O(40)-P(6)#5	1.507(8)
P(7)-O(37)	1.547(11)	O(46)-P(8)#5	1.524(9)
P(8)-O(28)	1.467(10)	O(201)-C(11)	1.49(2)
P(8)-O(46)#2	1.524(9)	O(202)-C(5)	1.40(2)
P(8)-O(33)	1.523(9)	O(203)-C(22)	1.39(2)
P(8)-O(35)	1.570(10)	O(204)-C(27)	1.49(2)
P(9)-O(49)	1.510(9)	N(1)-C(16)	1.46(2)
P(9)-O(29)	1.513(9)	N(1)-C(13)	1.49(2)
P(9)-O(1)	1.535(10)	N(1)-C(15)	1.527(19)
P(9)-O(39)	1.543(10)	N(1)-C(14)	1.53(2)
P(11)-O(19)	1.467(10)	N(2)-C(4)	1.47(2)
P(11)-O(41)	1.523(10)	N(2)-C(3)	1.51(2)
P(11)-O(36)	1.541(9)	N(2)-C(2)	1.54(2)
P(11)-O(47)	1.567(10)	N(2)-C(25)	1.57(3)
Al(1)-O(38)	1.731(9)	N(3)-C(9)	1.46(2)
Al(1)-O(29)	1.737(11)	N(3)-C(7)	1.49(3)
Al(1)-O(27)	1.745(9)	N(3)-C(20)	1.50(3)

N(3)-C(26)	1.52(2)	O(23)-P(7)-O(45)	107.6(5)
N(4)-C(24)	1.42(3)	O(25)-P(7)-O(37)	111.2(6)
N(4)-C(21)	1.43(3)	O(23)-P(7)-O(37)	108.6(6)
N(4)-C(23)	1.48(3)	O(45)-P(7)-O(37)	108.2(5)
N(4)-C(17)	1.51(2)	O(28)-P(8)-O(46)#2	112.2(6)
C(4)-C(5)	1.55(3)	O(28)-P(8)-O(33)	110.0(6)
C(7)-C(27)	1.53(3)	O(46)#2-P(8)-O(33)	109.4(5)
C(11)-C(16)	1.60(2)	O(28)-P(8)-O(35)	110.1(6)
C(22)-C(23)	1.58(4)	O(46)#2-P(8)-O(35)	105.2(5)
		O(33)-P(8)-O(35)	109.8(6)
O(25)-Co(1)-O(31)	110.7(4)	O(49)-P(9)-O(29)	110.9(7)
O(25)-Co(1)-O(22)	109.0(4)	O(49)-P(9)-O(1)	110.6(6)
O(31)-Co(1)-O(22)	107.9(4)	O(29)-P(9)-O(1)	111.2(6)
O(25)-Co(1)-Cl(1)	108.1(3)	O(49)-P(9)-O(39)	108.4(6)
O(31)-Co(1)-Cl(1)	111.2(4)	O(29)-P(9)-O(39)	107.2(5)
O(22)-Co(1)-Cl(1)	110.0(3)	O(1)-P(9)-O(39)	108.5(6)
O(1)-Co(2)-O(34)	112.8(4)	O(19)-P(11)-O(41)	110.7(6)
O(1)-Co(2)-O(42)	107.5(4)	O(19)-P(11)-O(36)	110.6(6)
O(34)-Co(2)-O(42)	110.5(5)	O(41)-P(11)-O(36)	108.0(5)
O(1)-Co(2)-Cl(2)	109.1(4)	O(19)-P(11)-O(47)	112.1(6)
O(34)-Co(2)-Cl(2)	110.2(4)	O(41)-P(11)-O(47)	107.6(6)
O(42)-Co(2)-Cl(2)	106.5(4)	O(36)-P(11)-O(47)	107.8(6)
O(22)-P(1)-O(21)	108.5(6)	O(38)-Al(1)-O(29)	108.6(6)
O(22)-P(1)-O(32)	113.0(6)	O(38)-Al(1)-O(27)	108.0(5)
O(21)-P(1)-O(32)	108.5(5)	O(29)-Al(1)-O(27)	110.1(5)
O(22)-P(1)-O(44)	113.5(6)	O(38)-Al(1)-O(33)	108.7(5)
O(21)-P(1)-O(44)	106.6(5)	O(29)-Al(1)-O(33)	115.1(5)
O(32)-P(1)-O(44)	106.6(6)	O(27)-Al(1)-O(33)	106.2(5)
O(42)-P(4)-O(30)#1	109.6(6)	O(39)-Al(2)-O(41)	109.7(5)
O(42)-P(4)-O(26)#2	109.7(6)	O(39)-Al(2)-O(32)	111.2(5)
O(30)#1-P(4)-O(26)#2	109.2(6)	O(41)-Al(2)-O(32)	111.8(5)
O(42)-P(4)-O(38)	113.5(6)	O(39)-Al(2)-O(21)#4	108.2(5)
O(30)#1-P(4)-O(38)	106.8(5)	O(41)-Al(2)-O(21)#4	106.9(5)
O(26)#2-P(4)-O(38)	108.0(6)	O(32)-Al(2)-O(21)#4	108.8(5)
O(31)-P(5)-O(43)	114.2(7)	O(47)-Al(3)-O(23)	110.6(6)
O(31)-P(5)-O(27)	109.2(5)	O(47)-Al(3)-O(20)#1	105.7(5)
O(43)-P(5)-O(27)	108.7(6)	O(23)-Al(3)-O(20)#1	108.4(5)
O(31)-P(5)-O(20)	111.6(6)	O(47)-Al(3)-O(43)	109.8(5)
O(43)-P(5)-O(20)	106.7(6)	O(23)-Al(3)-O(43)	111.8(6)
O(27)-P(5)-O(20)	106.0(5)	O(20)#1-Al(3)-O(43)	110.4(5)
O(34)-P(6)-O(40)#2	110.3(6)	O(45)-Al(4)-O(46)	111.2(5)
O(34)-P(6)-O(48)	112.4(6)	O(45)-Al(4)-O(26)	110.1(5)
O(40)#2-P(6)-O(48)	108.7(6)	O(46)-Al(4)-O(26)	110.4(5)
O(34)-P(6)-O(24)#3	111.4(6)	O(45)-Al(4)-O(30)	106.4(5)
O(40)#2-P(6)-O(24)#3	106.2(6)	O(46)-Al(4)-O(30)	109.1(5)
O(48)-P(6)-O(24)#3	107.5(6)	O(26)-Al(4)-O(30)	109.5(5)
O(25)-P(7)-O(23)	112.2(6)	O(35)-Al(6)-O(24)	104.5(5)
O(25)-P(7)-O(45)	108.8(6)	O(35)-Al(6)-O(48)	110.9(6)

O(24)-Al(6)-O(48)	110.9(5)	P(8)#5-O(46)-Al(4)	142.1(6)
O(35)-Al(6)-O(49)	112.6(6)	P(11)-O(47)-Al(3)	138.4(7)
O(24)-Al(6)-O(49)	108.6(5)	P(6)-O(48)-Al(6)	145.8(9)
O(48)-Al(6)-O(49)	109.3(6)	P(9)-O(49)-Al(6)	151.1(7)
O(37)-Al(8)-O(44)	109.7(6)	C(16)-N(1)-C(13)	115.6(14)
O(37)-Al(8)-O(36)	114.9(5)	C(16)-N(1)-C(15)	110.5(13)
O(44)-Al(8)-O(36)	108.3(5)	C(13)-N(1)-C(15)	109.1(14)
O(37)-Al(8)-O(40)	109.1(5)	C(16)-N(1)-C(14)	106.0(14)
O(44)-Al(8)-O(40)	107.9(5)	C(13)-N(1)-C(14)	108.7(15)
O(36)-Al(8)-O(40)	106.7(6)	C(15)-N(1)-C(14)	106.4(12)
P(9)-O(1)-Co(2)	140.2(7)	C(4)-N(2)-C(3)	112.4(15)
P(5)-O(20)-Al(3)#1	132.7(7)	C(4)-N(2)-C(2)	108.9(14)
P(1)-O(21)-Al(2)#4	132.4(6)	C(3)-N(2)-C(2)	108.6(15)
P(1)-O(22)-Co(1)	136.1(6)	C(4)-N(2)-C(25)	108.5(14)
P(7)-O(23)-Al(3)	152.3(6)	C(3)-N(2)-C(25)	109.6(16)
P(6)#3-O(24)-Al(6)	132.3(7)	C(2)-N(2)-C(25)	108.7(15)
P(7)-O(25)-Co(1)	140.7(6)	C(9)-N(3)-C(7)	110.3(15)
P(4)#5-O(26)-Al(4)	135.0(7)	C(9)-N(3)-C(20)	107.0(17)
P(5)-O(27)-Al(1)	141.4(7)	C(7)-N(3)-C(20)	112.7(16)
P(9)-O(29)-Al(1)	144.9(7)	C(9)-N(3)-C(26)	107.2(13)
P(4)#1-O(30)-Al(4)	133.3(6)	C(7)-N(3)-C(26)	111.5(16)
P(5)-O(31)-Co(1)	134.9(5)	C(20)-N(3)-C(26)	107.8(16)
P(1)-O(32)-Al(2)	138.9(7)	C(24)-N(4)-C(21)	106(3)
P(8)-O(33)-Al(1)	147.4(7)	C(24)-N(4)-C(23)	104(3)
P(6)-O(34)-Co(2)	137.0(6)	C(21)-N(4)-C(23)	113(2)
P(8)-O(35)-Al(6)	138.0(7)	C(24)-N(4)-C(17)	113(2)
P(11)-O(36)-Al(8)	154.3(7)	C(21)-N(4)-C(17)	109.9(17)
P(7)-O(37)-Al(8)	141.5(7)	C(23)-N(4)-C(17)	110.9(14)
P(4)-O(38)-Al(1)	149.2(7)	N(2)-C(4)-C(5)	118.4(13)
P(9)-O(39)-Al(2)	145.0(7)	O(202)-C(5)-C(4)	110.8(17)
P(6)#5-O(40)-Al(8)	142.6(7)	N(3)-C(7)-C(27)	119(2)
P(11)-O(41)-Al(2)	144.8(6)	O(201)-C(11)-C(16)	110.1(14)
P(4)-O(42)-Co(2)	134.9(6)	N(1)-C(16)-C(11)	114.4(15)
P(5)-O(43)-Al(3)	147.2(8)	O(203)-C(22)-C(23)	111.3(17)
P(1)-O(44)-Al(8)	145.3(7)	N(4)-C(23)-C(22)	118(3)
P(7)-O(45)-Al(4)	141.8(7)	O(204)-C(27)-C(7)	108.5(17)

Symmetry transformations used to generate equivalent atoms:

#1 -x+1,-y,-z+1 #2 x-1,y,z #3 -x,-y-1,-z+1

#4 -x+1,-y-1,-z+1 #5 x+1,y,z

Table 3. Anisotropic displacement parameters ($\text{\AA}^2 \times 10^3$) for CoAlPO-1. The anisotropic displacement factor exponent takes the form: $-2\pi^2[h^2a^*2U_{11} + \dots + 2hka^*b^*U_{12}]$.

	U ₁₁	U ₂₂	U ₃₃	U ₂₃	U ₁₃	U ₁₂
Co(1)	21(1)	34(1)	56(2)	-7(1)	-17(1)	1(1)
Co(2)	25(1)	32(1)	56(2)	-11(1)	-23(1)	3(1)
P(1)	18(2)	34(2)	52(2)	-4(2)	-16(2)	0(1)
Cl(2)	69(3)	64(3)	67(3)	-22(2)	-25(2)	9(2)
Cl(1)	63(3)	71(3)	60(3)	-18(2)	-17(2)	-4(2)
P(4)	18(2)	30(2)	56(2)	1(2)	-21(2)	1(1)
P(5)	17(2)	36(2)	49(2)	-11(2)	-16(1)	2(1)
P(6)	19(2)	28(2)	50(2)	-14(2)	-15(1)	3(1)
P(7)	18(2)	37(2)	48(2)	-6(2)	-16(1)	1(1)
P(8)	19(2)	34(2)	57(2)	-3(2)	-19(2)	7(1)
P(9)	17(2)	37(2)	48(2)	-3(2)	-15(1)	4(1)
P(11)	30(2)	33(2)	59(3)	-8(2)	-28(2)	3(2)
Al(1)	14(2)	44(2)	49(3)	-9(2)	-17(2)	3(2)
Al(2)	22(2)	27(2)	60(3)	-15(2)	-24(2)	4(2)
Al(3)	18(2)	34(2)	58(3)	-11(2)	-20(2)	6(2)
Al(4)	15(2)	36(2)	57(3)	-13(2)	-18(2)	7(2)
Al(6)	16(2)	31(2)	56(3)	-9(2)	-18(2)	0(2)
Al(8)	19(2)	38(2)	40(2)	-14(2)	-14(2)	8(2)
O(1)	32(5)	61(7)	75(8)	-25(6)	-32(5)	15(5)
O(19)	30(5)	59(6)	33(5)	-25(5)	-13(4)	17(4)
O(20)	26(5)	35(5)	72(7)	-24(5)	-28(5)	7(4)
O(21)	22(4)	21(4)	57(6)	2(4)	-13(4)	2(4)
O(22)	39(5)	20(5)	71(7)	-6(5)	-33(5)	15(4)
O(23)	35(5)	35(5)	78(8)	-8(5)	-40(5)	6(4)
O(24)	28(5)	60(7)	50(6)	-6(5)	-16(4)	3(5)
O(25)	41(6)	49(6)	49(6)	-21(5)	-17(4)	-11(5)
O(26)	34(5)	24(5)	62(7)	-4(5)	-11(5)	-12(4)
O(27)	23(4)	25(5)	55(6)	2(4)	-20(4)	1(4)
O(28)	35(5)	44(5)	43(6)	-22(5)	-14(4)	1(4)
O(29)	40(5)	37(5)	68(7)	-31(5)	-16(5)	2(4)
O(30)	33(5)	37(5)	43(6)	1(4)	-26(4)	4(4)
O(31)	36(6)	40(6)	90(8)	-6(6)	-40(6)	-11(4)
O(32)	29(5)	43(6)	73(8)	-15(5)	-25(5)	3(4)
O(33)	29(5)	45(6)	66(7)	-19(5)	-22(5)	-3(4)
O(34)	34(5)	22(5)	88(8)	-2(5)	-36(5)	-2(4)
O(35)	37(5)	22(5)	98(9)	-21(5)	-37(6)	18(4)
O(36)	30(5)	40(6)	56(6)	-8(5)	-23(4)	4(4)

O(37)	48(6)	54(6)	60(7)	-28(5)	-29(5)	-2(5)
O(38)	30(5)	38(5)	78(8)	-4(5)	-43(5)	9(4)
O(39)	29(5)	42(5)	49(6)	-7(5)	-19(4)	5(4)
O(40)	11(4)	42(6)	88(8)	-24(5)	-17(4)	0(4)
O(41)	36(6)	23(5)	99(9)	-13(5)	-34(6)	5(4)
O(42)	33(5)	53(6)	61(7)	-14(6)	-18(5)	5(5)
O(43)	27(5)	52(7)	83(9)	-16(6)	-12(5)	-4(5)
O(44)	20(5)	28(5)	99(9)	-12(5)	-24(5)	4(4)
O(45)	27(5)	36(5)	56(6)	-14(5)	-19(4)	2(4)
O(46)	19(4)	31(5)	98(9)	-23(5)	-29(5)	17(4)
O(47)	43(6)	17(4)	85(8)	-16(5)	-30(5)	-9(4)
O(48)	42(6)	75(8)	75(8)	-22(7)	-40(6)	1(6)
O(49)	22(5)	31(5)	76(8)	15(5)	-9(5)	-12(4)
O(201)	122(14)	111(12)	87(11)	-11(9)	-54(10)	-23(10)
O(202)	63(8)	102(10)	76(9)	-40(8)	-18(7)	-3(7)
O(203)	67(8)	61(8)	84(10)	-9(7)	-24(7)	-3(7)
O(204)	77(9)	143(13)	54(8)	-37(9)	-25(7)	16(9)
N(1)	61(8)	32(6)	34(7)	-8(5)	-16(6)	17(6)
N(2)	29(6)	104(12)	27(7)	-12(7)	-4(5)	22(7)
N(3)	40(8)	75(10)	56(9)	14(8)	-21(6)	-7(7)
N(4)	60(9)	70(9)	27(7)	-2(7)	-21(6)	11(7)
C(2)	122(18)	67(12)	58(12)	-31(10)	-51(12)	35(12)
C(3)	23(8)	125(19)	150(20)	-70(17)	-13(10)	33(10)
C(4)	25(8)	78(13)	131(18)	-46(12)	-48(10)	17(8)
C(5)	50(10)	61(11)	75(13)	0(10)	-27(9)	-3(9)
C(7)	72(15)	140(20)	115(19)	26(16)	-70(14)	-39(14)
C(9)	95(15)	76(13)	66(13)	-19(11)	-48(11)	-4(12)
C(11)	67(12)	54(11)	123(18)	-15(11)	-66(12)	1(9)
C(13)	99(17)	110(17)	91(16)	-35(14)	-62(14)	75(15)
C(14)	90(15)	107(16)	42(11)	-17(11)	16(10)	-60(13)
C(15)	43(9)	98(14)	40(9)	-35(9)	3(7)	-6(9)
C(16)	49(9)	61(11)	80(13)	-40(10)	-24(9)	5(8)
C(17)	59(12)	68(12)	102(17)	-10(12)	-35(11)	6(10)
C(20)	114(18)	118(18)	47(12)	-38(12)	-16(11)	70(16)
C(21)	64(15)	300(40)	77(18)	70(20)	-32(13)	20(20)
C(22)	73(14)	76(14)	150(20)	-65(15)	-56(14)	11(11)
C(23)	90(18)	120(20)	180(30)	10(20)	-100(20)	-14(16)
C(24)	250(50)	250(40)	310(50)	-240(40)	-140(40)	180(40)
C(25)	130(20)	88(17)	120(20)	-10(15)	-70(18)	-28(15)
C(26)	60(10)	116(16)	33(9)	-52(10)	10(7)	-8(11)
C(27)	77(15)	88(16)	112(19)	8(14)	-40(14)	-3(12)

10.2 Crystal Data for CoAlPO-2

Table 1. Atomic coordinates ($\times 10^4$) and equivalent isotropic displacement parameters ($\text{\AA}^2 \times 10^3$) for CoAlPO-2. $U(\text{eq})$ is defined as one third of the trace of the orthogonalized U_{ij} tensor.

	x	y	z	$U(\text{eq})$
N(1)	2290(4)	2237(4)	4019(4)	13(1)
N(2)	-563(5)	2858(4)	6026(4)	13(1)
C(1)	-953(6)	1465(5)	6754(5)	17(1)
C(2)	2602(5)	2773(5)	5742(5)	16(1)
C(3)	1352(6)	3766(5)	6343(5)	17(1)
C(4)	-2887(5)	504(5)	6146(5)	15(1)
C(5)	3334(5)	1082(5)	3392(5)	15(1)
P(1)	2824(1)	4819(1)	1359(1)	9(1)
P(2)	7694(1)	834(1)	1422(1)	9(1)
Al(1)	5060(2)	2493(1)	-50(1)	9(1)
Co(1)	5060(2)	2493(1)	-50(1)	9(1)
O(1)	6676(4)	2113(4)	1212(4)	17(1)
O(2)	3872(5)	3524(4)	1116(4)	22(1)
O(3)	3727(5)	740(4)	-1298(4)	22(1)
O(4)	4069(4)	6417(4)	1293(4)	20(1)
O(5)	8799(4)	1320(4)	3023(3)	16(1)
O(6)	2356(4)	4994(4)	2957(3)	16(1)
O(7)	1239(4)	4361(5)	39(4)	24(1)
O(8)	8745(5)	594(5)	118(4)	25(1)

Table 2. Bond lengths [\AA] and angles [$^\circ$] for CoAlPO-2.

N(1)-C(2)	1.493(5)	C(2)-C(3)	1.520(6)
N(1)-C(5)	1.500(5)	C(2)-HC2A	0.9700
N(1)-H(1A)	0.9008	C(2)-HC2B	0.9700
N(1)-H(1B)	0.9001	C(3)-HC3A	0.9700
N(2)-C(3)	1.497(5)	C(3)-HC3B	0.9700
N(2)-C(1)	1.500(5)	C(4)-C(5)#1	1.520(6)
N(2)-H(2A)	0.9004	C(4)-HC4A	0.9700
N(2)-H(2B)	0.8998	C(4)-HC4B	0.9700
C(1)-C(4)	1.531(6)	C(5)-C(4)#1	1.520(6)
C(1)-HC1A	0.9700	C(5)-HC5A	0.9700
C(1)-HC1B	0.9700	C(5)-HC5B	0.9700

P(1)-O(6)	1.512(3)	N(2)-C(3)-HC3A	108.7
P(1)-O(7)	1.523(3)	C(2)-C(3)-HC3A	108.7
P(1)-O(2)	1.535(3)	N(2)-C(3)-HC3B	108.7
P(1)-O(4)	1.544(3)	C(2)-C(3)-HC3B	108.7
P(2)-O(5)	1.506(3)	HC3A-C(3)-HC3B	107.6
P(2)-O(8)	1.519(3)	C(5)#1-C(4)-C(1)	113.5(3)
P(2)-O(1)	1.541(3)	C(5)#1-C(4)-HC4A	108.9
P(2)-O(3)#2	1.549(3)	C(1)-C(4)-HC4A	108.9
Al(1)-O(1)	1.726(3)	C(5)#1-C(4)-HC4B	108.9
Al(1)-O(2)	1.730(3)	C(1)-C(4)-HC4B	108.9
Al(1)-O(4)#3	1.730(3)	HC4A-C(4)-HC4B	107.7
Al(1)-O(3)	1.732(3)	N(1)-C(5)-C(4)#1	113.8(3)
O(3)-P(2)#2	1.549(3)	N(1)-C(5)-HC5A	108.8
O(4)-Co(1)#3	1.730(3)	C(4)#1-C(5)-HC5A	108.8
O(4)-Al(1)#3	1.730(3)	N(1)-C(5)-HC5B	108.8
		C(4)#1-C(5)-HC5B	108.8
C(2)-N(1)-C(5)	114.7(3)	HC5A-C(5)-HC5B	107.7
C(2)-N(1)-H(1A)	108.6	O(6)-P(1)-O(7)	115.00(19)
C(5)-N(1)-H(1A)	108.6	O(6)-P(1)-O(2)	107.83(18)
C(2)-N(1)-H(1B)	108.6	O(7)-P(1)-O(2)	108.7(2)
C(5)-N(1)-H(1B)	108.6	O(6)-P(1)-O(4)	108.82(18)
H(1A)-N(1)-H(1B)	107.5	O(7)-P(1)-O(4)	108.7(2)
C(3)-N(2)-C(1)	115.0(3)	O(2)-P(1)-O(4)	107.54(19)
C(3)-N(2)-H(2A)	108.5	O(5)-P(2)-O(8)	114.69(19)
C(1)-N(2)-H(2A)	108.5	O(5)-P(2)-O(1)	109.55(18)
C(3)-N(2)-H(2B)	108.6	O(8)-P(2)-O(1)	108.24(19)
C(1)-N(2)-H(2B)	108.5	O(5)-P(2)-O(3)#2	107.58(18)
H(2A)-N(2)-H(2B)	107.5	O(8)-P(2)-O(3)#2	109.9(2)
N(2)-C(1)-C(4)	109.4(3)	O(1)-P(2)-O(3)#2	106.64(19)
N(2)-C(1)-HC1A	109.8	O(1)-Al(1)-O(2)	105.14(17)
C(4)-C(1)-HC1A	109.8	O(1)-Al(1)-O(4)#3	113.05(17)
N(2)-C(1)-HC1B	109.8	O(2)-Al(1)-O(4)#3	111.52(17)
C(4)-C(1)-HC1B	109.8	O(1)-Al(1)-O(3)	111.83(17)
HC1A-C(1)-HC1B	108.2	O(2)-Al(1)-O(3)	112.47(19)
N(1)-C(2)-C(3)	113.3(3)	O(4)#3-Al(1)-O(3)	103.06(17)
N(1)-C(2)-HC2A	108.9	P(2)-O(1)-Al(1)	142.2(2)
C(3)-C(2)-HC2A	108.9	P(1)-O(2)-Al(1)	147.9(2)
N(1)-C(2)-HC2B	108.9	P(2)#2-O(3)-Al(1)	145.0(2)
C(3)-C(2)-HC2B	108.9	P(1)-O(4)-Co(1)#3	143.7(2)
HC2A-C(2)-HC2B	107.7	P(1)-O(4)-Al(1)#3	143.7(2)
N(2)-C(3)-C(2)	114.4(3)	Co(1)#3-O(4)-Al(1)#3	0.00(6)

Symmetry transformations used to generate equivalent atoms:

#1 -x,-y,-z+1 #2 -x+1,-y,-z #3 -x+1,-y+1,-z

Table 3. Anisotropic displacement parameters ($\text{\AA}^2 \times 10^3$) for CoAlPO-2. The anisotropic displacement factor exponent takes the form: $-2\pi^2[h^2a^2U^{11} + \dots + 2hka^*b^*U^{12}]$.

	U ¹¹	U ²²	U ³³	U ²³	U ¹³	U ¹²
N(1)	14(1)	12(1)	12(1)	4(1)	2(1)	3(1)
N(2)	16(2)	10(1)	14(1)	3(1)	6(1)	5(1)
C(1)	20(2)	12(2)	18(2)	6(1)	2(1)	4(1)
C(2)	14(2)	19(2)	12(2)	1(1)	0(1)	4(1)
C(3)	21(2)	14(2)	14(2)	0(1)	5(1)	2(1)
C(4)	14(2)	14(2)	18(2)	5(1)	5(1)	5(1)
C(5)	15(2)	15(2)	16(2)	5(1)	6(1)	4(1)
P(1)	10(1)	9(1)	11(1)	3(1)	4(1)	4(1)
P(2)	10(1)	10(1)	8(1)	2(1)	2(1)	3(1)
Al(1)	11(1)	7(1)	11(1)	3(1)	3(1)	4(1)
Co(1)	11(1)	7(1)	11(1)	3(1)	3(1)	4(1)
O(1)	19(1)	16(1)	19(1)	6(1)	2(1)	9(1)
O(2)	30(2)	22(2)	24(2)	10(1)	15(1)	20(1)
O(3)	25(2)	14(1)	22(2)	4(1)	0(1)	-2(1)
O(4)	25(2)	17(1)	17(1)	7(1)	5(1)	0(1)
O(5)	15(1)	20(1)	11(1)	1(1)	-2(1)	5(1)
O(6)	23(1)	16(1)	13(1)	6(1)	10(1)	10(1)
O(7)	17(1)	31(2)	19(2)	1(1)	-2(1)	5(1)
O(8)	27(2)	40(2)	20(2)	13(1)	14(1)	20(2)

10.3 Crystal Data for CoAlPO-3

Table 1. Atomic coordinates ($\times 10^4$) and equivalent isotropic displacement parameters ($\text{\AA}^2 \times 10^3$) for CoAlPO-3. $U(\text{eq})$ is defined as one third of the trace of the orthogonalized U_{ij} tensor.

	x	y	z	$U(\text{eq})$
Al(1)	9952(1)	2342(1)	340(1)	40(1)
Al(2)	14241(1)	3333	833	35(1)
Co(1)	9952(1)	2342(1)	340(1)	40(1)
Co(2)	14241(1)	3333	833	35(1)
P(1)	12371(1)	2437(1)	339(1)	45(1)
P(2)	9059(1)	3333	833	32(1)
O(1)	9635(4)	3227(4)	562(1)	79(1)
O(2)	13439(4)	3224(4)	524(1)	80(1)
O(3)	11367(4)	2626(5)	424(1)	79(2)
O(4)	8855(4)	843(3)	385(1)	71(1)
O(5)	9916(3)	2722(4)	-26(1)	66(1)
O(6)	14399(5)	2125(3)	870(1)	81(2)

Table 2. Bond lengths [\AA] and angles [$^\circ$] for CoAlPO-3.

Al(1)-O(3)	1.741(3)	O(6)-P(2)#3	1.484(3)
Al(1)-O(1)	1.741(4)		
Al(1)-O(5)	1.747(4)	O(3)-Al(1)-O(1)	108.1(2)
Al(1)-O(4)	1.772(4)	O(3)-Al(1)-O(5)	109.1(2)
Al(2)-O(6)	1.704(3)	O(1)-Al(1)-O(5)	108.5(2)
Al(2)-O(6)#1	1.704(3)	O(3)-Al(1)-O(4)	113.5(2)
Al(2)-O(2)#1	1.723(4)	O(1)-Al(1)-O(4)	109.8(2)
Al(2)-O(2)	1.723(4)	O(5)-Al(1)-O(4)	107.7(2)
P(1)-O(5)#2	1.505(4)	O(6)-Al(2)-O(6)#1	108.3(4)
P(1)-O(3)	1.506(3)	O(6)-Al(2)-O(2)#1	108.1(3)
P(1)-O(2)	1.512(4)	O(6)#1-Al(2)-O(2)#1	110.7(2)
P(1)-O(4)#3	1.520(4)	O(6)-Al(2)-O(2)	110.7(2)
P(2)-O(6)#4	1.484(3)	O(6)#1-Al(2)-O(2)	108.1(3)
P(2)-O(6)#5	1.484(3)	O(2)#1-Al(2)-O(2)	110.8(4)
P(2)-O(1)#1	1.491(4)	O(5)#2-P(1)-O(3)	110.1(2)
P(2)-O(1)	1.491(4)	O(5)#2-P(1)-O(2)	106.3(3)
O(4)-P(1)#5	1.520(4)	O(3)-P(1)-O(2)	109.3(3)
O(5)-P(1)#6	1.505(4)	O(5)#2-P(1)-O(4)#3	111.4(2)

O(3)-P(1)-O(4)#3	108.6(3)	O(1)#1-P(2)-O(1)	112.8(4)
O(2)-P(1)-O(4)#3	111.1(3)	P(2)-O(1)-Al(1)	147.9(3)
O(6)#4-P(2)-O(6)#5	109.6(4)	P(1)-O(2)-Al(2)	146.2(3)
O(6)#4-P(2)-O(1)#1	110.2(3)	P(1)-O(3)-Al(1)	146.3(3)
O(6)#5-P(2)-O(1)#1	107.0(3)	P(1)#5-O(4)-Al(1)	145.2(4)
O(6)#4-P(2)-O(1)	107.0(3)	P(1)#6-O(5)-Al(1)	144.3(4)
O(6)#5-P(2)-O(1)	110.2(3)	P(2)#3-O(6)-Al(2)	163.4(3)

Symmetry transformations used to generate equivalent atoms:

#1 $x-y+1/3, -y+2/3, -z+1/6$ #2 $y+1, -x+y+1, -z$ #3 $-x+y+2, -x+1, z$
 #4 $-x+7/3, -x+y+5/3, -z+1/6$ #5 $-y+1, x-y-1, z$ #6 $x-y, x-1, -z$

Table 3. Anisotropic displacement parameters ($\text{\AA}^2 \times 10^3$) for CoAlPO-3. The anisotropic displacement factor exponent takes the form: $-2\pi^2[h^2a^2U_{11} + \dots + 2hka^*b^*U_{12}]$.

	U11	U22	U33	U23	U13	U12
Al(1)	37(1)	49(1)	32(1)	-3(1)	7(1)	21(1)
Al(2)	33(1)	32(1)	39(1)	-6(1)	-3(1)	16(1)
Co(1)	37(1)	49(1)	32(1)	-3(1)	7(1)	21(1)
Co(2)	33(1)	32(1)	39(1)	-6(1)	-3(1)	16(1)
P(1)	54(1)	60(1)	38(1)	-11(1)	-17(1)	41(1)
P(2)	29(1)	27(1)	40(1)	-7(1)	-4(1)	14(1)
O(1)	90(3)	73(3)	66(3)	-6(2)	36(2)	35(2)
O(2)	85(3)	78(3)	75(3)	-18(2)	-44(2)	41(2)
O(3)	87(3)	132(4)	59(3)	-30(3)	-21(2)	86(3)
O(4)	62(2)	51(2)	81(3)	-4(2)	1(2)	14(2)
O(5)	70(3)	82(3)	47(2)	7(2)	7(2)	38(2)
O(6)	102(4)	48(2)	110(4)	-17(2)	-39(3)	51(3)

10.4 Crystal Data for octakis[methylpropanoate]octasiloxane

Table 1. Atomic coordinates ($\times 10^4$) and equivalent isotropic displacement parameters ($\text{\AA}^2 \times 10^3$) for octakis[methylpropanoate]octasiloxane. $U(\text{eq})$ is defined as one third of the trace of the orthogonalized U_{ij} tensor.

	x	y	z	$U(\text{eq})$
Si1	2022(3)	3644(2)	2317(3)	217(17)
Si2	2031(2)	3645(2)	0340(3)	220(17)
O1	1536(6)	2918(6)	0147(7)	280(4)
O2	1937(7)	3864(7)	1329(6)	320(4)
O3	2900(5)	3480(6)	2529(7)	210(3)
O4	1548(8)	5971(17)	-1010(2)	4000(3)
O5	342(9)	5683(10)	-9030(12)	860(8)
*O10	1926(16)	6427(10)	3257(15)	1170(17)
*O11	1335(17)	5634(13)	4120(2)	2400(3)
C1	1752(16)	4432(11)	-353(12)	710(11)
C2	1013(16)	4791(10)	-306(14)	1020(13)
C3	1076(10)	5551(9)	-792(12)	1700(2)
C6	164(9)	6340(16)	-1425(19)	1130(13)
C7	1635(10)	4400(8)	2997(10)	320(6)
C8	1972(12)	5168(9)	2865(11)	520(8)
C9	1738(12)	5824(9)	3445(14)	980(13)
*C12	1750(2)	7018(10)	3750(2)	2200(4)

Starred Atom sites have a S.O.F less than 1.0

Table 2. Bond lengths [\AA] and angles [$^\circ$] for octakis[methylpropanoate]octasiloxane.

Si(1)-O(2)	1.607(11)	O(10)-C(9)	1.16(3)
Si(1)-O(3)	1.626(10)	O(10)-C(12)	1.34(3)
Si(1)-C(7)	1.852(16)	O(11)-C(9)	1.32(4)
Si(1)-O(3_a)	1.633(10)	C(1)-C(2)	1.47(4)
Si(2)-O(1)	1.596(11)	C(2)-C(3)	1.56(3)
Si(2)-O(2)	1.610(11)	C(7)-C(8)	1.51(2)
Si(2)-C(1)	1.84(2)	C(8)-C(9)	1.54(3)
Si(2)-O(1_c)	1.641(11)	C(1)-H(1A)	0.9700
O(4)-C(3)	1.18(3)	C(1)-H(1B)	0.9700
O(5)-C(3)	1.34(2)	C(2)-H(2A)	0.9700
O(5)-C(6)	1.46(3)	C(2)-H(2B)	0.9700

C(7)-H(7A)	0.9700	O(5)-C(3)-C(2)	98.40(17)
C(7)-H(7B)	0.9700	Si(1)-C(7)-C(8)	115.6(12)
C(8)-H(8A)	0.9700	C(7)-C(8)-C(9)	120.0(16)
C(8)-H(8B)	0.9700	O(10)-C(9)-O(11)	127.0(2)
		O(10)-C(9)-C(8)	118.0(2)
O(2)-Si(1)-O(3)	109.4(7)	O(11)-C(9)-C(8)	115.3(17)
O(2)-Si(1)-C(7)	110.1(7)	Si(2)-C(1)-H(1A)	107.00
O(2)-Si(1)-O(3_a)	110.1(6)	Si(2)-C(1)-H(1B)	107.00
O(3)-Si(1)-C(7)	111.8(7)	C(2)-C(1)-H(1A)	107.00
O(3)-Si(1)-O(3_a)	109.8(6)	C(2)-C(1)-H(1B)	107.00
O(3_a)-Si(1)-C(7)	105.6(7)	H(1A)-C(1)-H(1B)	107.00
O(1)-Si(2)-O(2)	108.8(6)	C(1)-C(2)-H(2A)	110.00
O(1)-Si(2)-C(1)	110.9(9)	C(1)-C(2)-H(2B)	110.00
O(1)-Si(2)-O(1_c)	109.7(6)	C(3)-C(2)-H(2A)	110.00
O(2)-Si(2)-C(1)	110.9(8)	C(3)-C(2)-H(2B)	110.00
O(1_c)-Si(2)-O(2)	109.0(6)	H(2A)-C(2)-H(2B)	109.00
O(1_c)-Si(2)-C(1)	107.5(10)	Si(1)-C(7)-H(7A)	108.00
Si(2)-O(1)-Si(2_a)	148.8(8)	Si(1)-C(7)-H(7B)	108.00
Si(1)-O(2)-Si(2)	149.6(9)	C(8)-C(7)-H(7A)	108.00
Si(1)-O(3)-Si(1_c)	146.9(8)	C(8)-C(7)-H(7B)	108.00
C(3)-O(5)-C(6)	115.1(15)	H(7A)-C(7)-H(7B)	107.00
C(9)-O(10)-C(12)	121.0(3)	C(7)-C(8)-H(8A)	107.00
Si(2)-C(1)-C(2)	123.0(17)	C(7)-C(8)-H(8B)	107.00
C(1)-C(2)-C(3)	106.9(19)	C(9)-C(8)-H(8A)	107.00
O(4)-C(3)-O(5)	123.2(19)	C(9)-C(8)-H(8B)	107.00
O(4)-C(3)-C(2)	138.0(2)	H(8A)-C(8)-H(8B)	107.00

Symmetry transformations used to create equivalent atoms:

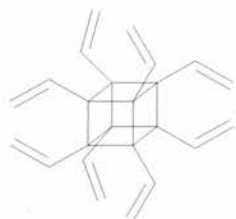
#1 $1/2-y, x, z$	#2 $1/2-x, 1/2-y, z$	#3 $y, 1/2-x, z$
#4 $1/2-y, 1/2-x, -1/2+z$	#5 $1/2-x, y, 1/2+z$	#6 $1/2-x, y, -1/2+z$
#7 $-1/2+y, 1/2+x, 1/2-z$	#8 $-x, 1-y, -z$	#9 $1/2-y, 1/2-x, 1/2+z$
#10 $1/2-x, 3/2-y, z$		

Table 3. Anisotropic displacement parameters ($\text{\AA}^2 \times 10^3$) for octakis[methylpropanoate]octasiloxane. The anisotropic displacement factor exponent takes the form: $-2\pi^2[h^2a^2U_{11} + \dots + 2hka^*b^*U_{12}]$.

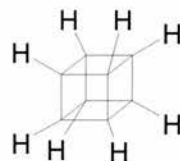
	U ₁₁	U ₂₂	U ₃₃	U ₂₃	U ₁₃	U ₁₂
Si1	38(3)	14(3)	13(3)	-1.1(16)	5.6(18)	10(2)
Si2	7(3)	14(3)	15(3)	0.4(17)	3.4(19)	12.1(19)
O1	31(6)	25(7)	28(7)	2(5)	-3(5)	-2(5)
O2	42(7)	35(7)	19(7)	2(5)	15(5)	7(6)
O3	25(6)	20(6)	17(6)	-2(5)	-3(4)	3(4)
O4	260(4)	550(8)	380(5)	430(6)	180(4)	310(5)
O5	63(12)	75(13)	119(15)	39(11)	12(11)	-6(10)
O10	230(4)	0(12)	120(3)	-19(12)	-30(2)	12(15)
O11	60(2)	120(3)	530(9)	-220(4)	90(4)	-50(2)
C1	170(3)	17(10)	27(12)	8(8)	-29(13)	25(13)
C2	170(3)	90(2)	46(15)	11(13)	26(16)	90(2)
C3	260(5)	140(3)	100(2)	80(2)	130(3)	220(3)
C6	58(17)	100(2)	180(3)	120(2)	54(18)	25(15)
C7	52(12)	18(9)	27(10)	0(7)	-11(8)	22(8)
C8	91(17)	26(10)	38(11)	-8(9)	-22(11)	22(10)
C9	63(19)	50(19)	180(3)	-20(2)	-30(2)	54(15)
C12	210(6)	150(5)	300(8)	-220(6)	-190(6)	130(4)

10.5 Molecular Structures

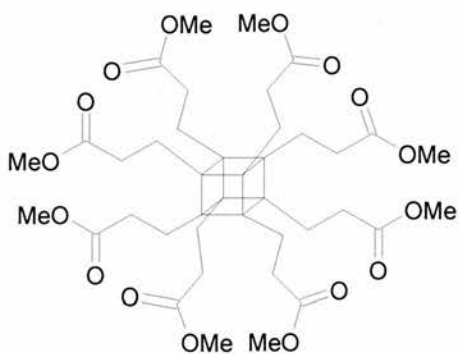
All POSS cores (Si_8O_{12}) drawn as cubes for clarity.



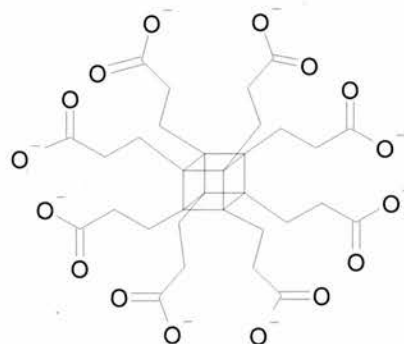
Octavinylsilsesquioxane



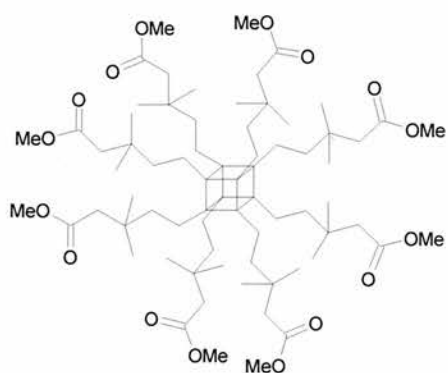
Octahydridesilsesquioxane



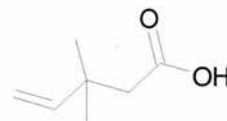
octakis[methylpropanoate]octasiloxane



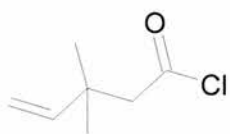
octakis[propanoate]octasiloxane



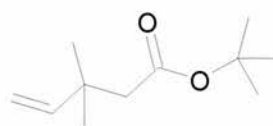
octakis[methyl-3,3-dimethylpentanoate]
octasiloxane



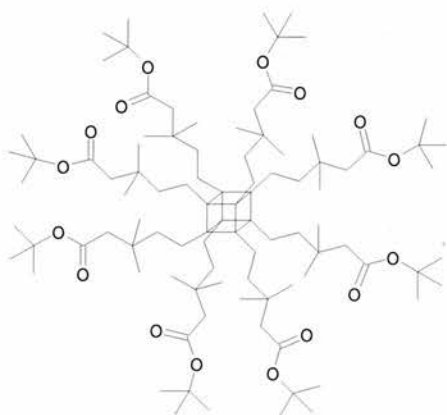
3,3-dimethyl-4-pentenoic acid



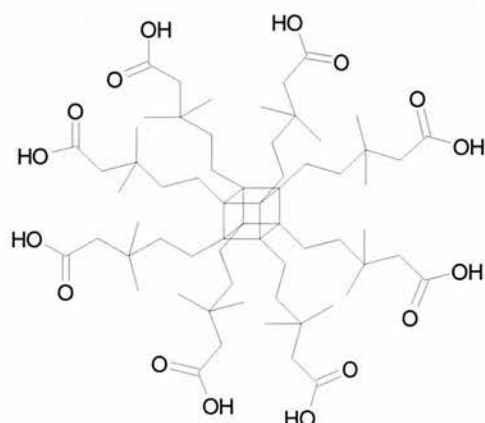
3,3-dimethyl-4-pentenoic acid chloride



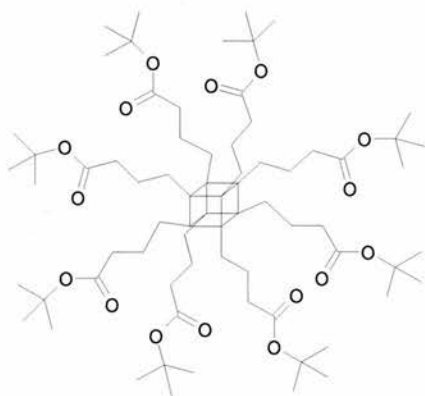
t-butyl-3,3-dimethyl-4-pentenoate



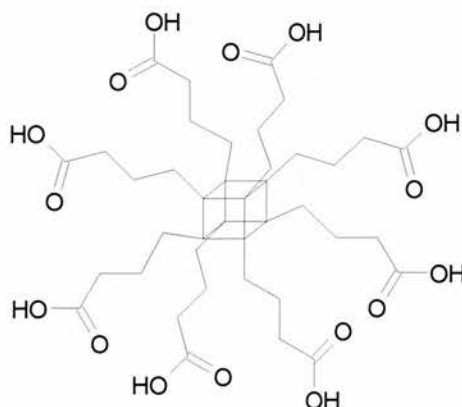
octakis[t-butyl-3,3-dimethylpentanoate]
octasiloxane



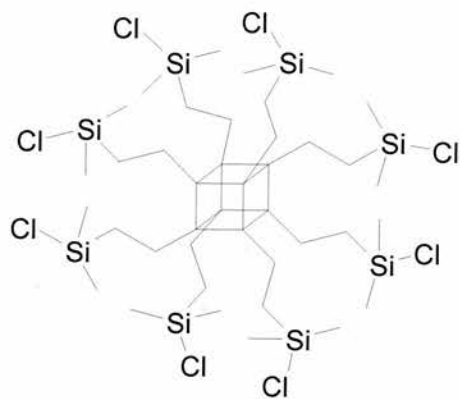
octakis[3,3-dimethylpentanoic
acid]octasiloxane



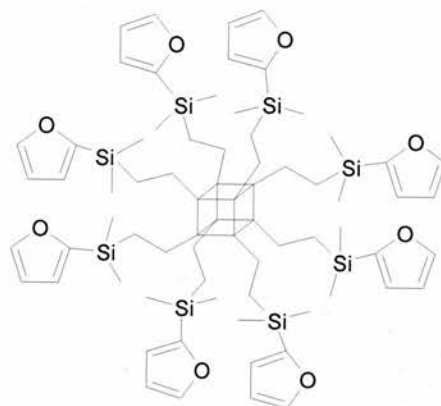
octakis[t-butylbutanoate]octasiloxane



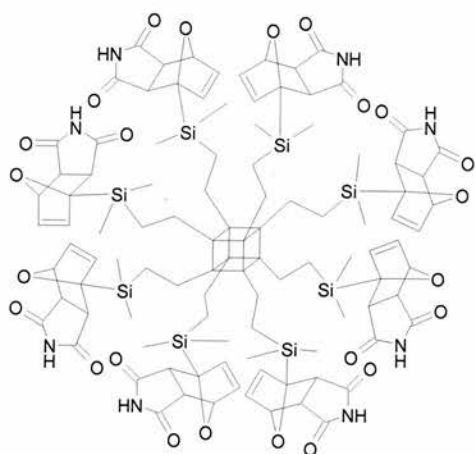
octakis[t-butylbutanoic acid]octasiloxane



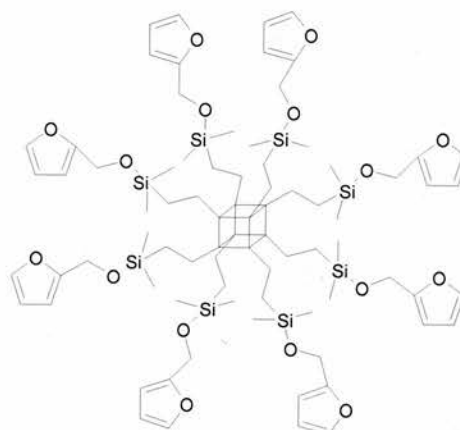
octakis[chlorodimethylsilylethane]
octasiloxane



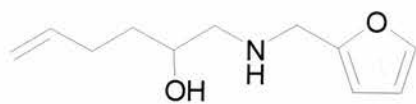
Furyl POSS 1 (FP1)



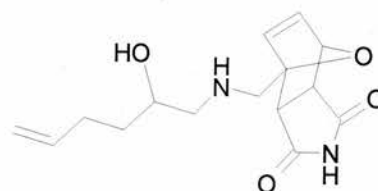
FP1 Diels-Alder Adduct



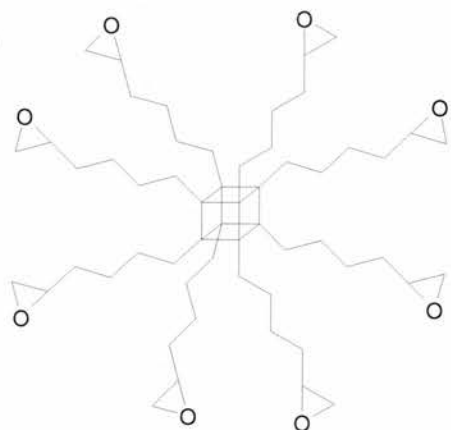
Furyl POSS 2 (FP2)



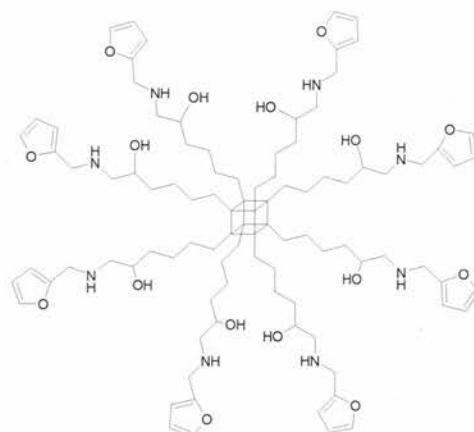
Furyl Alkene (FA)



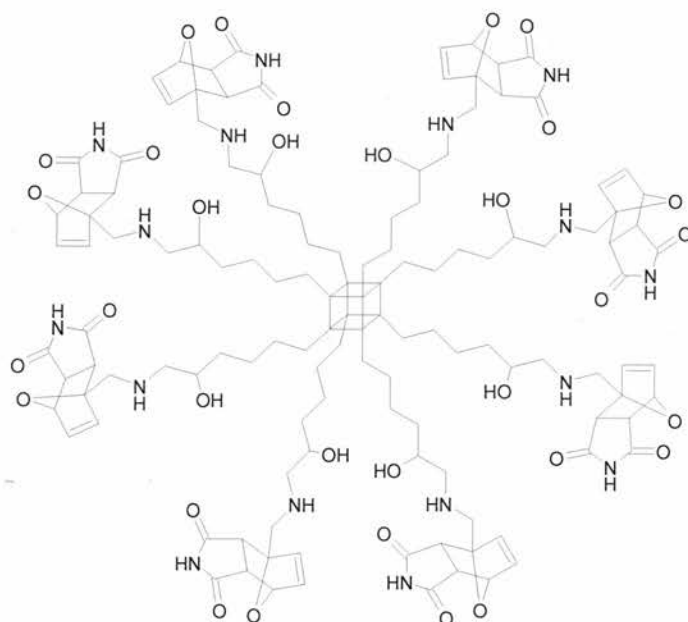
Furyl Alkene Diels-Alder Adduct



octakis[epoxyhexane]octasiloxane



Furyl POSS 3 (FP3)



FP3 Diels-Alder Adduct